9-19-2017

Structural Surface Mapping for Shape Analysis

Muhammad Razib
mrazi003@fiu.edu

DOI: 10.25148/etd.FIDC004045

FLORIDA INTERNATIONAL UNIVERSITY

Miami, Florida

STRUCTURAL SURFACE MAPPING FOR SHAPE ANALYSIS

A dissertation submitted in partial fulfillment of the

requirements for the degree of

DOCTOR OF PHILOSOPHY

in

COMPUTER SCIENCE

by

Muhammad Razib

2017

To: Dean John Volakis
College of Engineering and Computing

This dissertation, written by Muhammad Razib, and entitled Structural Surface Mapping for Shape Analysis, having been approved in respect to style and intellectual content, is referred to you for judgment.

We have read this dissertation and recommend that it be approved.

S. S. Iyengar

Niki Pissinou

Leonardo Bobadilla

Yuanchang Sun

Wei Zeng, Major Professor

Date of Defense: September 19, 2017

The dissertation of Muhammad Razib is approved.

Dean John Volakis
College of Engineering and Computing

Andrés G. Gil
Vice President for Research and Economic Development
and Dean of the University Graduate School

Florida International University, 2017

DEDICATION

To my parents, Muhammad Abdul Hakim and Mursheda Begum,

and my wife, Jebun Nahar.

Without your love and support, none of my success would be possible.

ACKNOWLEDGMENTS

First, I would like to thank my parents and my wife for showing extreme patience and support throughout this hard but successful journey of Ph.D. I also thank them for understanding the value of my time and effort for achieving this highest level of academic excellence.

Ph.D. was not only an academic degree for me but also a life-changing experience in many ways. I would like to express my heartfelt gratitude to my adviser, Professor Wei Zeng for providing me the opportunity to go through this experience. I am also grateful for her constant guidance through proper scientific discussions, asking insightful questions and giving me the freedom to explore different ways to find the best solutions to the research problems.

Also, I would like to thank the committee members, Professor S. S. Iyengar, Professor Niki Pissinou, Professor Leonardo Bobadilla and Professor Yuanchang Sun, for their valuable suggestions and insightful comments about the research in this dissertation. I am also grateful to our collaborators, Professor Zhong-Lin Lu and his group from The Ohio State University, and Professor Yi-Jun Yang from Shandong University. Professor Lu helped us with providing data and personality questionnaire, and Professor Yang helped us with concept discussion and reviewing paper writing.

Part of the work in this dissertation has been supported by NSF CCF-1544267 and Dissertation Year Fellowship (DYF), 2017 provided by the University Graduate School of FIU.

ABSTRACT OF THE DISSERTATION

STRUCTURAL SURFACE MAPPING FOR SHAPE ANALYSIS

by

Muhammad Razib

Florida International University, 2017

Miami, Florida

Professor Wei Zeng, Major Professor

Natural surfaces are usually associated with feature graphs, such as the cortical surface with anatomical atlas structure. Such a feature graph subdivides the whole surface into meaningful sub-regions. Existing brain mapping and registration methods did not integrate anatomical atlas structures. As a result, with existing brain mappings, it is difficult to visualize and compare the atlas structures. And also existing brain registration methods can not guarantee the best possible alignment of the cortical regions which can help computing more accurate shape similarity metrics for neurodegenerative disease analysis, e.g., Alzheimer's disease (AD) classification. Also, not much attention has been paid to tackle surface parameterization and registration with graph constraints in a rigorous way which have many applications in graphics, e.g., surface and image morphing.

This dissertation explores structural mappings for shape analysis of surfaces using the feature graphs as constraints. (1) First, we propose structural brain mapping which maps the brain cortical surface onto a planar convex domain using Tutte embedding of a novel atlas graph and harmonic map with atlas graph constraints to facilitate visualization and comparison between the atlas structures. (2) Next, we propose a novel brain registration technique based on an intrinsic atlas-constrained harmonic map which provides the best possible alignment of the cortical regions. (3) After that, the proposed brain registration technique has been applied to compute

shape similarity metrics for AD classification. (4) Finally, we propose techniques to compute intrinsic graph-constrained parameterization and registration for general genus-0 surfaces which have been used in surface and image morphing applications.

TABLE OF CONTENTS

LIST OF TABLES

LIST OF FIGURES

FIGURE PAGE

CHAPTER 1

INTRODUCTION

1.1 Background and Motivation

Surface mapping is the process of flattening a 3-dimensional (3D) surface to a unit sphere or to a 2-dimensional (2D) planar canonical domain such as a unit disk or a rectangle. The primary objective of the mapping is to create a simpler representation of the complex 3D surface to a more regular and less complex domain to carry further geometric analysis tasks. It is a fundamental task in computer graphics, computer vision and medical imaging fields which facilitates many other applications including visualization, texture mapping, surface modeling, matching, registration, morphing, and so on. In medical imaging fields especially in neuroscience, brain surface mapping is used to map the convoluted 3D brain surface to a unit disk or a unit sphere for anatomy visualization and comparison of the brain structures. In computer graphics field, the mapping, commonly known as parameterization, usually maps the surface to a planar canonical domain. Parameterization provides a way to map surfaces with different coordinate systems to a common coordinate system which can be used to establish one-to-one correspondence between two surfaces. The process of establishing the correspondence between the surfaces is known as surface registration. For human brains, surface registration is typically used for computing shape similarity metrics for group analysis purposes; the method is particularly useful in brain morphometry analysis to identify or classify different psychological or neurodegenerative diseases, e.g., Alzheimers disease (AD), where the brain structure or geometry is highly affected and changed. The registration process helps to quantify the similarity and differences among the brains by mapping similar portions of different brains to the similar position in the mappings. Surface

registration also plays key role for many other geometry processing applications. One such important application is surface morphing which shows the transition of transforming one geometric shape or surface to another; morphing is widely used in animation and motion picture industries.

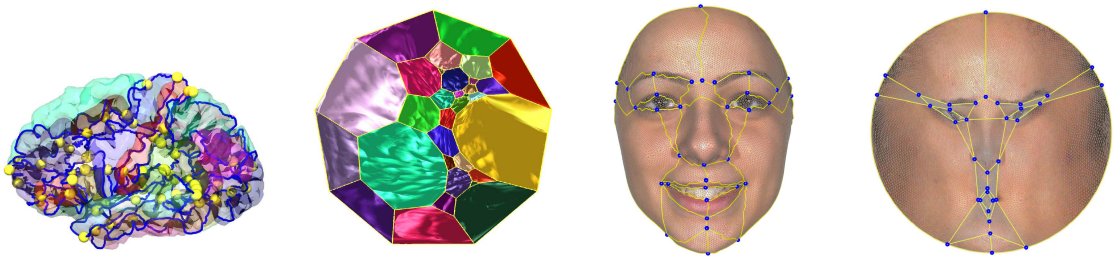

(a) graph on brain surface (b) structural brain mapping (c) graph on facial surface (d) graph-constrained parameterization

Figure 1.1: Feature graphs, and mappings of the surfaces. (a) and (c) show brain surface and human facial surface; (b) and (d) show the structural brain mapping and graph-constrained parameterization of the facial surface respectively. The anatomical regions of the brain surface are color coded.

This dissertation explores structural mapping for shape analysis of surfaces using the novel feature graphs naturally embedded in the brain and other surfaces. The feature graph subdivides the whole surface into meaningful sub-regions that can be used as constraints in the mapping. For example, the human brain is divided into several anatomical regions based on their functionality, and geometric structures which can be used combinedly to define a topological graph, each of these regions is inter-connected to several other regions; together they create the brain atlas. The curvy connection among these regions can be used as the edges of the graph, and the junctions of these anatomical regions can be used as the nodes of this graph; together they create the atlas graph (see Fig. 1.1(a)).

A crucial step of brain analysis is the visualization of the brain atlas, and comparing the connecting patterns of the regions and geometry between the brain surfaces. But due to the highly convoluted structures of the brain, 3D brain surface is not

useful for the exploration, visualization, and comparison of the brain structures. So effective visualization technique is required for easy exploration and visualization of the whole brain; brain mapping was introduced for this purpose. But in existing brain mappings atlas boundaries (connecting curves between the regions) appear highly curvy as they did not integrate the anatomical atlas structures into the mapping, which makes the visualization and comparison tasks very difficult. In this dissertation, we present a novel brain mapping method using the anatomical atlas graph to provide a well-structured view for straightforward visualization and comparison among the brain structures (see 1.1(b)). The method maps the brain cortical surface onto a planar convex domain using the classical Tutte embedding [137] and minimizing harmonic energy where the anatomical regions are mapped to convex subdivisions.

One important aspect of the proposed brain mapping is that it can be applied to compute the registration between the brain surfaces. Moreover, the straight lines and the convex faces from the mapping can be used to map similar faces of the two surfaces to similar positions in the registration process. However, for good registration result, the mapping should consider the original geometry of the 3D surface efficiently. Otherwise, the registration may suffer from stretches and fold over triangles. So, a rigorous method is required to compute the mapping which can preserve the intrinsic property of the surface as much as possible; then the mapping can be used efficiently to compute the atlas-constrained brain registration. It is required to map similar faces of the atlas graphs to similar convex faces on the map to register brains with optimal shape similarity. It would be a trivial task if the atlas graphs of the brains were consistent (with same nodes and connectivity). But the atlas graphs among the brain surfaces are not guaranteed to be consistent which have been verified experimentally in this dissertation. To solve this problem,

we propose graph-refinement procedure to make the atlas graphs consistent in the registration process. The proposed graph refinement procedure performs minimal changes to the atlas-graphs to register different regions of the brains as much as possible.

The brain registration method provides a powerful way to analyze the structural difference or similarity among the brains. The idea is to co-register the brains and then define the similarity metric using the registered brains to find out the difference between the normal brains and brains with diseases. The proposed brain registration method guarantees optimal alignment of the cortical regions which can be used to compute optimal shape similarity metrics to classify brains. In this dissertation, we have presented a framework using this registration technique to classify patients with Alzheimer's disease (AD). The method uses the supervised learning techniques to build models from the training dataset using the geometric attributes of the brain surfaces as features, which is used to predict whether the input brains have AD or not.

The graphs are also found on other natural surfaces. For example, in human or animal facial surfaces the graphs can be extracted from the surfaces using the prominent feature points, e.g., eye and mouth corners, nose tips, etc., as the nodes, and the landmark contours and curves, e.g., eye and mouth contours, etc., as the edges (see Fig. 1.1(c)). Moreover, similar objects may have similar feature graphs, e.g., two different human facial surfaces may have similar feature graphs which can be used to compute the registration between them. These graphs can be used as constraints to parameterize similar surfaces onto similar canonical convex domains. Like brain mapping, these parameterized surfaces then can be used to compute registration between the two surfaces. But most of the existing methods either use points or curves in the parameterization and registration process. However, for

surfaces with consistent feature graphs, it is worthy to deal with the graph as a whole rather than split the graph into separate points and curves as the graph is equipped with both global and local information, which serves as a skeleton structure of the surface. But to date, not much attention has been paid to tackle surface parameterization and registration with graph constraints in a rigorous way. So, at the end of this dissertation, we have presented methods to compute intrinsic graph-constrained parameterization (see Fig. 1.1(d)) for genus zero surfaces with graph structures to map them onto planar convex domain which considers the intrinsic geometric structures of the surface as much possible. The curvy edges are mapped to straight lines and the closed regions consisting with the curvy edges (which form the faces of the graphs) are mapped to the convex subdivisions in the parameter domain. The method is a generalization of the intrinsic atlas-constrained harmonic map for the brain surfaces. After that, the parameterization is used to compute the registration between two surfaces. We have applied the proposed graph-constrained parameterization and registration methods to generate surface and image morphing sequences, which show the usefulness and effectiveness of the proposed methods.

1.2 Research Questions

The main research questions that this dissertation aims to answer are as follows:

1. How to generate brain surface mapping with atlas constraints?
2. How to compute brain registration with atlas constraints?
3. How to apply brain registration to large-scale brain classification?
4. How to compute parameterization and registration with graph constraints?

1.3 Solutions and Contributions

In this dissertation, we provide computational solutions to the questions mentioned above. We divide this dissertation into four main chapters which contain the solutions to these four questions. (1) First, we present structural brain mapping using a novel atlas graph to map the brain cortical surface onto planar convex domain using Tutte graph embedding and harmonic map to create a well-structured view for efficient visualization and comparison between the atlas structures. (2) Next, we present a novel brain registration method using atlas-constrained harmonic map with graph refinement strategy to create consistent atlas graphs among the brain surfaces which guarantees the best possible alignment of the anatomical regions of the brains. (3) After that, we present a framework for classifying AD patients from normal patients using the proposed brain registration method to compute the similarity metric by co-registering the brains. (4) Finally, we present a graph-constrained registration method for general genus zero surfaces using the intrinsic graph-constrained parameterization technique which is applied to surface and image morphing.

As this dissertation is based on the human brain and 3D surface representation, below we provide an overview of the basic construction of the human brain modeling and 3D surface representation.

Human brain. The human brain consists of the three major parts, i.e., the cerebrum, the brainstem and the cerebellum. The cerebrum is the largest part among them, which is divided into two parts known as the left hemisphere and right hemisphere. Various parts of both the left and right hemisphere perform and contribute to different neurological functions, e.g., cognition, reasoning, learning, memory, etc. Based on these functionality and geometric structures, these two hemispheres can

be divided into several inter-connected regions. The labeling and mapping of these regions are performed on the images of the brains captured with brain imaging techniques. One of these imaging techniques is Structural Magnetic Resonance Imaging (sMRI or simply MRI) which is widely used for capturing the image of static anatomical structures of the brain. These images are used by the physicians to diagnose the patients having brain-related diseases or disorders. The labeling and mapping of the regions can be performed manually or by some advanced automatic pipelines on the MRI image. Automating this process requires a considerable amount of research, but techniques have been developed to automatically label the regions of the brain with high accuracy. MRI normally provides volume image data which is a series of 2D slice images that captures the picture of the whole 3D space of the brain. The images are captured at a regular interval, e.g., one slice image in every one millimeter and each of the slice images has the same resolution, e.g., 1024x1024 pixels (pixel on the slice image is known as voxel which has x, y, z position and one intensity value). After some cleaning operations, the volume image can be used directly in the analysis and is called volume-based analysis in literature. Another way is to use the cortical, i.e., the outer layer of the brain, or sub-cortical surface extracted from the 3D volume image (hence, the brain surface is often termed as cortical surface) for the analysis. This kind of analysis technique is known as surface-based analysis. Several automatic methods and mapping techniques have been proposed to automatically label the brain regions and extract surface from the volume image, among which Freesurfer [36], Brainsuite [113], etc., are widely used. In the literature, both volume-based [5, 6, 27, 32, 50] and surface-based [37, 59] analysis have been proved to be very effective for different brain analysis purposes. This dissertation proposes methods and performs surface-based analysis of the human brain.

3D surface. The surface is a 2-dimensional manifold embedded in 3D ($\mathbb{R}^3$) space. In computer graphics, the 3D surface is discretized with a set of planar polygons each consisting of discrete points. The set of points are known as vertex set, and the set of polygons are known as face set; such a discretization of the surface is known as a mesh. Typically, triangles are used as faces to discretize the surface known as a triangular mesh (in some cases tetrahedrons or other polygons are also used). The surfaces used in this dissertation have been discretized with points and triangles.

In the following sections, we provide overviews of our presented solutions and our key contributions to each of the methods.

1.3.1 Structural Brain Mapping

Brain mapping is the process of flattening the 3D convoluted brain cortical surface onto a canonical domain, e.g., disk conformal map, so that the hidden details of the brain surface is fully exposed onto that domain. It generates better visualization for the convoluted brain geometry, and the whole brain surface can be explored more easily. But in existing brain mapping methods, e.g., conformal mapping onto a disk, the anatomical atlas boundaries appear highly curvy on the mapping. It is hard to compare the anatomical atlas structures between the brains from such mapping. Therefore, a canonical map with canonical atlas structure is highly desired, which can be used directly for atlas visualization and comparison, and further for brain registration and brain morphometry analysis. So, we propose structural brain mapping which maps the brain cortical surface with atlas division (i.e., brain regions) to a convex subdivision domain. The method takes into consideration the whole anatomical atlas structure and defines a novel graph based on the connectivity of the cortical regions which we call brain net graph. This graph is different from the

existing brain graph in [19]. In our definition, the nodes are the junctions of the anatomical regions and the edges are the common boundaries of the neighboring regions (see Fig. 1.1(a)). The method first extracts the brain-net graph from the 3D brain surface and then embeds the graph onto a 2D convex domain using Tutte embedding where each face of the graph is also mapped as a convex polygon inside the convex domain. In the second step, the whole brain surface is mapped inside the 2D convex domain using harmonic map with the convex subdivision constraint.

Contributions. The major contributions of our brain mapping method have been summarized below:

1. Our proposed brain mapping is first to use the whole anatomical atlas structure as a graph in the mapping. As a result, the method can capture the global topology and local geometry of the whole cortical surface. The proposed graph is a novel graph different than the existing ones.

2. The method provides a better visualization tool to compare the local and global relationship among the regions of the two brains. The important properties of the proposed graph are that its a planar and 3-connected graph (after minor filtering). So according to Tutte embedding theorem [137], the graph can be embedded onto the plane without crossing edges, and every face of the graph is convex. Also, the computation of the graph embedding is linear. One important property of the proposed mapping is that it is theoretically guaranteed to be diffeomorphic and the computation of the mapping is also linear.

3. The method has been verified on a total of 290 brains from two brain databases; one is our own captured 250 MRI brain scans processed by Freesurfer, and the

other one is 40 manually labeled brain scans from publicly available LPBA40 dataset.

1.3.2 Atlas-Constrained Brain Registration

In brain study, the dense registration between cortical surfaces is highly desirable in neuroscience, medical imaging, cognitive neuroscience, and psychology fields which finds out one-to-one correspondence between the source and the target cortical surface. The process aims to generate the optimal diffeomorphism between the surfaces. Diffeomorphic cortical surface registration can give a detailed guidance for locating the deformation areas for progression measurement and morphology analysis of the brain structure. The registration process is designed to map the similar structures of the brains to the closest position so that their overall similarity measurement is maximized. After that, one can define the shape similarity metrics globally for brain comparison, classification and for finding patterns among the brains of different subjects. Therefore, it has broad applications for brain disease diagnosis and treatment, such as brain tumor/abnormality growth tracking, radiotherapy monitoring, surgery outcome evaluation, personal health monitoring, etc.

Although there are some brain registration techniques in literature, but none of the existing methods consider the whole anatomical atlas structure into the computation. As a result, none of the methods can guarantee the best possible alignment of the cortical regions which can help computing more accurate shape metrics. In this dissertation, we propose a novel cortical surface registration method by fully considering the anatomical atlas structure by using the atlas graph proposed in structural brain mapping. For the registration, atlas graphs between the source and the target need to be consistent to map the source and the target to the same 2D domain. But it has been verified experimentally on the manually labeled brain dataset

that the atlas graphs may not be consistent among the brains. So, we propose a graph refinement method on the triangular mesh to make the graphs consistent while keeping the modification as low as possible. The method then generates 3D to 2D canonical parameterization of the source and the target using the intrinsic atlas-constrained harmonic map. The mapping minimizes the harmonic energy with atlas-graph constraints by considering the intrinsic geometric structures of the surface. The positions of the graph nodes and graph edges are determined intrinsically by their local graph neighborhood instead of the mesh vertex neighborhood, thus removing the use of graph embedding step. Finally, we register the source to the target surface using the harmonic map with graph constraint. To minimize the distortion due to the graph modification we propose a relaxation procedure after the registration. The proposed method can more accurately align the cortical regions and the region boundaries, and perform better than the existing registration method in terms of the overlap of the regions, i.e., Freesurfer [36], as measured by the Dice coefficient.

Contributions. The major contributions of our brain registration method have been summarized below:

1. We provide a novel brain registration framework using the atlas graph considering the whole anatomical atlas structure. None of the previous methods consider the whole atlas structure for registration.
2. We provide a novel graph refinement procedure to make the atlas graphs consistent among the brains. The modification is done on the very few triangles of the cortical surface and is kept as few as possible. As a result, the method can generate registration with the best possible alignment of the cortical regions.

3. We also provide a novel atlas-constrained map minimizing the quadratic convex harmonic energy considering the local graph neighborhood for the vertices of the graph nodes and graph edges. The method respects the intrinsic geometric structures of the surface and does not require any initial graph embedding (Tutte embedding) which is heuristic and not intrinsic. The proposed mapping has been proved to be unique, globally optimal and diffeomorphic.

4. The proposed registration with consistent feature graphs (if not consistent, then the graphs are made consistent with graph refinement strategy) has been proved to be globally optimal, unique and diffeomorphic. The registration method has been tested on the manually labeled brain databases, LPBA40 [114] and Mindboggle [72]. Registration results show significant improvement with our method over Freesurfer's registration method as measured by the Dice coefficient which is used to measure the overlap of the cortical regions of the cortical surfaces.

1.3.3 AD Classification using Atlas-Constrained Brain Registration

The human brain is the center of the nervous system which functions as the bridge or signal provider behind all of our neurological and psychological activities. Any change or abnormality in any part of the brain may result in a different psychological behavior, or the extreme case may result in neurological or neurodegenerative diseases, e.g., Alzheimers disease (AD) and Parkinsons disease, or psychological disorders, e.g., schizophrenia, epilepsy, acute depression, etc. So, these diseases have a direct relation to the underlying biological structures of the brain. Biological structures can be affected due to the changes of the biological fluid of the brain, e.g., gray matter and white matter volume, or neural cell loss. In most cases, if the biological structure of the brain is changed, this change is also reflected on

the geometric structures of the brain, which in turn changes the structure of the cortex of the brain, i.e., cortical surface. Detecting and analyzing these structural changes in the brain can help early detection and prevention of many of these diseases or disorders. Many researches, especially in neuroscience and medical imaging fields, have given tremendous efforts to find and establish a rigorous relationship between the geometric structures of the brain and neurological diseases. Many different geometric analysis methods have been proposed which have been found to be very effective for identifying these geometric changes and classifying brains having these diseases, e.g, AD [42, 87, 140, 151, 161], schizophrenia [14, 43, 94, 98, 99], epilepsy [88, 106, 138, 146, 147, 147], acute depression [78, 117], etc.

Brain morphometry analysis refers to the study of the size and shape of the brain structures and functions and their relations to the development and evolution of the brain due to aging, learning, diseases, etc. Analysis method also studies the best suited geometric attributes and features to find out the optimal structural differences between the two brain surfaces. The process typically uses brain mapping and registration methods to establish the relationship between the brains. Once the registration is computed, some shape similarity metrics can be used for finding the shape difference between the cortical surfaces. Different geometric attributes or features can be used as the metrics, e.g., normal, curvature, area, gray/white matter thickness, volume, etc., using the one-to-once correspondence between the vertices to compute the metric similarity and difference between the surfaces. This difference of the measurement can be used to investigate the abnormality in the diseased brain different from the normal brain.

Alzheimers disease is a premier example of a disease where the atrophy of the gray matter or white matter fluids in the brain cortex is significant, and it alters the geometric structure of the brain. Registering the brains help us to define

some shape similarity metric to analyze the difference between the brains. As the atlas-constrained brain registration considers more regional geometry of the brain, it can be used to compute the optimal shape metrics. In this dissertation, we have presented a framework using atlas-constrained brain registration for Alzheimers disease classification. The process takes one brain as the source and deforms that to all other brains using atlas-constrained brain registration. After that, we use supervised learning methods to classify the brains into two categories, normal brains, and brains with the AD. In the process, we show the use of various types of geometric measurements that can be used as the shape metric. We also show the detailed use of different machine learning classifiers. Among the methods, K-NN shows the best results with 88.0% accuracy with 10-fold cross-validation.

Contributions. The major contributions of the proposed brain analysis framework for AD have been summarized below:

1. We provide a framework based on the co-registration of brain cortical surfaces using the atlas-constrained brain registration process for AD classification. As the atlas-constrained brain registration technique can guarantee registration with the best possible alignment of the cortical regions, the proposed analysis framework can provide optimal alignment of the two brain surfaces so that their similarity measurement is maximized; as a result, similar brains can be grouped more accurately.

2. We show the use of several types of features for AD classification using supervised learning based classification algorithms, e.g., K-NN and SVM with k-fold Cross-verification. We compute the best combination of features by feature selection algorithm for AD classification. We also show the detailed analysis of the best models for the classification.

1.3.4 Intrinsic Graph-Constrained Surface Parameterization and Registration

Many natural surfaces have similar anatomical structures represented as graphs, e.g., two human facial surfaces have same topological graphs consisting with the similar prominent feature points, e.g., eye, nose tip, mouth corners, etc. This similar or isomorphic graphs between the two surfaces can be used as constraints to register the surfaces. The idea is to compute the graph-constrained parameterization that maps the surface to a canonical convex domain, and then register the surfaces on this domain. But to obtain good registration results, the graph-constrained parameterization need to retain the original geometry as much as possible. The registered surfaces can be used for many applications in computer graphics; one such important application is morphing used to deform one geometric shape to another.

In this part of the dissertation, we generalize the atlas-constrained mapping of the cortical surfaces to compute the quasiconformal mapping of the graph constrained surface (genus-0 surface with single boundary) intrinsically by the adaptive harmonic map which we call intrinsic graph-constrained parameterization. After that, we compute the graph-constrained registration based on this parameterization to register two surfaces. The proposed registration method has been applied to generate morphing sequence by interpolating the shapes between the source and the deformed source surface (generated from the target).

Contributions. The major contributions of the proposed parametrization and registration method have been summarized below:

1. We provide a graph-constrained registration technique based on the intrinsic graph-constrained parameterization method for general genus-0 surfaces with a single boundary. The method can be used for surfaces having isomorphic

graph structures embedded on the surface. Like the atlas-constrained mapping and registration of the cortical surfaces, the proposed mapping in the proposed parameterization and registration method for genus-0 surfaces are unique, globally optimal and diffeomorphic.

2. We have applied the proposed parameterization and registration methods on various surfaces and images, and also applied the registration to surface and image morphing. Experiments show that the morphing method based on the graph-constrained parameterization and registration can generate high-quality morphing sequences for surfaces with complicated geometry, and also for images having single and multiple objects.

1.4 Related Publications

This dissertation has been written based on the following list of publications:

1. Wei Zeng, Yi-Jun Yang, and Muhammad Razib. Graph-Constrained Surface Registration Based on Tutte Embedding. In *The IEEE Conference on Computer Vision and Pattern Recognition (CVPR) Workshops*, June 2016
2. Muhammad Razib, Zhong-Lin Lu, and Wei Zeng. Structural Brain Mapping. In *Medical Image Computing and Computer-Assisted Intervention–MICCAI 2015*, pages 760–767. Springer, 2015
3. Wei Zeng, Muhammad Razib, and Abdur Bin Shahid. Diffeomorphism Spline. *Axioms*, 4(2):156–176, 2015

The following two manuscripts are currently under review:

1. Muhammad Razib, Yi-Jun Yang, Zhong-Lin Lu, and Wei Zeng. A Novel Brain Registration Framework by Atlas-Constrained Mappings. In *IEEE Conference on Computer Vision and Pattern Recognition (CVPR)*, 2018.

2. Muhammad Razib, Yi-Jun Yang, and Wei Zeng. Intrinsic Parameterization and Registration of Graph Constrained Surfaces. In *Graphical Models*, 2018.

1.5 Organization of the Dissertation

This dissertation involved research in the areas of brain mapping, brain registration, brain morphometry analysis, and surface parameterization, registration, and morphing. We discuss a comprehensive list of the related works involving all of these topics in chapter 2. Section 2.1 discusses the related works of brain mapping, section 2.2 discusses the related works of brain registration, section 2.3 discusses the related works of brain morphometry analysis, and section 2.4 discusses the related works of surface parameterization, registration, and morphing. We also discuss the novelty, and key difference of our works form the existing works with each of these sections.

In chapter 3, we present structural brain mapping. Section 3.1 provides an introduction, section 3.2 discusses the background information and motivation, section 3.3 provides an overview of our approach, section 3.4 discusses some theoretic background, section 3.5 elaborates the computational algorithm, section 3.6 shows the experimental results with some discussion and provides comparison with other approaches, and section 3.7 provides a summary of the method.

In chapter 4, we present atlas-constrained brain registration method. Section 4.1 provides an introduction, section 4.2 discusses the background information and motivation, section 4.3 provides an overview of our approach, section 4.4 elaborates the computational algorithm, section 4.5 shows the experimental results with some discussions, and section 4.6 provides a summary of the method.

In chapter 5, we present the method for AD classification using atlas-constrained brain registration. Section 4.1 provides an introduction, section 4.2 discusses the background information and motivation, section 4.3 provides an overview of our

approach, section 4.4 elaborates the computational algorithm, section 4.5 shows the experimental results, and section 4.6 provides a summary of the method.

In chapter 6, we present graph-constrained parameterization, registration and its application to surface and image morphing. Section 6.1 provides an introduction, section 6.2 discusses the background information and motivation, section 6.3 provides an overview of our approach, section 6.4 elaborates the computational algorithm, section 6.5 shows the experimental results with discussion, and section 6.6 provides a summary of the method.

Finally, we present a summary of this dissertation and future research directions in chapter 7.

CHAPTER 2

RELATED WORK

This dissertation proposes novel solutions for brain mapping, brain registration and brain morphometry analysis, and graph-constrained surface parameterization, registration and their applications to morphing. Below we discuss the related works of each of these topics; we also provide the key differences of our methods with existing methods.

2.1 Brain Mapping

Brain mapping was introduced to map the genus zero 3D brains cortical surface (usually brain hemisphere) onto a unit sphere [12, 39, 53, 54] or a planar canonical domain (e.g., a unit disk [144], a rectangle domain [55, 67]), so that the convoluted and invisible cortical folds are flattened, and the geometric details are fully exposed onto the canonical domain. For the genus-0 closed surface, the surface is mapped to the sphere. For mapping the brain surface to disk or rectangular domain, one region (normally the region named unknown region) of the brain is cut open to create the boundary. A plausible category of the methods is conformal mapping, which preserves angles (local geometric shapes) and therefore, is highly desired for brain morphometry study in neuroscience and medical imaging fields. Several methods have been proposed to conformally map the brain cortical surface onto a canonical domain. Angenent et al. [3] summarized earlier works on conformal mapping of the brain cortical surface. In recent years several methods also have been proposed for computing conformal brain mapping. Spherical harmonic mapping [53] conformally maps the cortical surface onto the sphere. Ricci curvature flow [144] conformally maps the cortical surface onto the unit disk with cutting brain regions

mapped to holes inside the disk. Riemann surface structure [143] divides the whole cortical surface into several patches and then conformally maps each patch separately to a rectangle. Hacker et al. [54] presented finite element approximation of the Laplace-Beltrami operator for computing parameterization of the cortical surface conformally to a spherical domain. Hurdal and Stephenson used circle packing method [61] which flattens the cortical surface conformally onto the sphere, disk or a rectangular domain by an iterative approach. They also proposed some metrics, e.g., extremal length metrics, calculated based on the circle packing for computing anatomical differences for cortical regions of different subjects. Ju et al. [69] presented a solution for computing conformal mapping of the cortical surface based on the so-called least squares method [69]. The method can conformally flattens the cortical regions by fixing two points onto a planar domain where other vertices on the boundary of the regions can move freely. The method can also generate a conformal map of the cortical regions onto the disk or the whole cortical surface onto the sphere. The method is comparatively faster than the circle packing method [61] as it solves the linear system of equations. Another interesting method is conformal slit mapping [142] which maps the cortical surface onto the disk or rectangle domain while mapping the landmark curves as straight lines or concentric arcs inside the domain.

In some cases, the conformal mapping may introduce high area distortions in the mapping which creates difficulty in shape analysis for the cortical surface, so area-preserving mapping is required. Some methods have been proposed based on the optimal mass transportation theory [55,126] for computing area-preserving brain mapping. However, it is well known that such mappings cannot be both conformal and area preserving.

There are other methods which try to minimize a combination of metric(linear), angular and areal distortions by adding the distortion terms to the energy functional, e.g., Fischl et al. [38] proposes an energy functional combining geodesic distance term and area distortion term in the energy function. Another interesting method is p-harmonic energy minimization method [66] where the energy function is defined with the p^{th} norm of the harmonic energy function.

Brain anatomical landmarks including gyri and sulci curves are used to help brain surface matching, shape registration, and analysis applications. Surface matching is used to map corresponding cortical regions of two brains to a similar location of a canonical domain to visualize and compare the geometry. Typically brain mapping is first used to map the surfaces to a canonical domain and selected landmark curves, e.g., gyri and sulci curves, are placed to the similar location in the mapping by minimizing their Euclidean distance in the domains. For example, spherical harmonic mapping [53] was applied to brain cortical surface matching applications using these landmark curves. The method first maps the brain cortical surfaces onto the spheres, and then the Euclidean distance between the corresponding landmark curves (discretized with points) of the two brains is minimized by an optimal Möbius transformation for optimal matching between the two surfaces for visualizing the differences. Another approach [144] is to slice the brain surface open along these curves, and map the new surface to a unit disk with circular holes or a hyperbolic polygon; the curves are mapped to circular holes or hyperbolic lines for generating intrinsic shape signatures and then to use in brain matching. The other method [162] maps the whole brain surface with interior curve straightening constraints based on the holomorphic 1-form method, without changing surface topology; the interior curves are mapped to canonically-shaped segments, e.g., straight lines in a rectangle or circular arcs in a unit disk.

Our method. Although there are some existing brain mapping methods, in existing mappings anatomical atlas boundaries appear highly curvy as they did not consider the anatomical atlas graphs which is not useful for straightforward visualization and comparison of the atlas structures. Our brain mapping method integrates the whole anatomical atlas graph into mapping by defining a novel atlas-graph based on the connectivity of the cortical regions to map the cortical surface onto the planar convex domain with convex subdivisions. The method provides a very useful and efficient way to visualize and compare the atlas structures. The mapping is guaranteed to be unique, globally optimal, and diffeomorphic.

2.2 Brain Registration

Brain registration is an important step for shape analysis of the brains. The process can be used for registering one brain to another directly. In some group analysis, often the brains are registered to a template brain. The template is created by creating an average brain by an iterative process of a number of brains from the study. Klein et al. [71] suggested to use the same algorithm for creating this average pattern which is used for brain registration in brain analysis. There are two types of registration used for the analysis, (i) volume image registration and (ii) cortical surface registration. In literature, both volume-based and surface-based analysis has been proved to be very effective for different analysis purposes. Below we review both of these techniques, but we focus more on the surface registration methods as our proposed registration is also a cortical surface registration method. A comparison between the volume-based and surface-based brain registration can be found in [71].

Volume image registration. Volume based registration method tries to align the whole brain volume images. Normally in volume image registration procedure, both source and the target volumes are considered to be of the same resolution,

i.e., same number of 2D images in the volume with each 2D image having the same dimension of pixels (typically known as voxel for volume image) resolution; if not, interpolation is used to make the volumes as same resolution. In 1973, Talairach [130] first proposed a volumetric alignment method based on the piecewise linear transformation. But it results in relatively poor alignment [2] due to the use of a limited set of landmark constraints and linear transformation which ignores complex geometry of the cortical folds and only use the rigid transformation. So non-rigid transformation with nonlinear deformation is required for registering very folded anatomical brain structures. In recent years, it has been well established that linear registration process of any kind may suffer from such poor alignment of the brain structures, so some nonlinear image registration methods have been proposed. Typically in these methods, a linear transformation is used as an initial or starting position for further nonlinear alignment procedure, e.g., ART [4]. To improve the alignment between the anatomical structures, manual labeling of the similar anatomical structures on the brain images can be performed by the neurologists to establish correspondence manually. But the method requires a considerable amount of efforts and time, and also it is not practical for large set of data, so automatic methods are required. Several intensity based automatic alignment methods [7, 149] have been proposed which allow non-rigid transformation with nonlinear deformation technique. Johnson and Christensen [64] proposed an image registration method combining both landmarks and intensity. The corresponding landmarks are identified manually and then used as constraints combining with the intensity; the correspondence is computed using the landmarks near the areas of the landmarks and intensity is used for the areas away from the landmarks. Shen et al. [118] proposed a method based on mass-preserving and hierarchical attribute-based deformation mechanism.

One important but challenging property of the registration is diffeomorphism. Some recent methods can ensure diffeomorphic mapping which can handle large deformations and can improve the alignment accuracy, e.g., SyN [11] ensures diffeomorphic mapping where the cross-correlation is maximized within the space of diffeomorphic maps. Diffeomorphic Demons [139] can also handle large deformation with faster computation while ensuring diffeomorphism. But as the volumetric registration methods do not constrain to align cortical features, they often suffer from poor alignment of cortical features in the registered volumes. To better align the brain structures and geometry, methods have been proposed [68] to use cortical surface registration as constraints for computing brain image registration. Klein et al. [70] provided detailed comparison among 14 non-linear volumetric registration methods. The accuracy is measured by comparing the overlapping and the distance measures of the anatomical regions. According to their study, ART [4] and SyN [11] provide the best result for volumetric brain image registration.

Cortical surface registration. Cortical surface registration method aligns the geometric features on the cortical surfaces. In past, some studies [8,38,105,131] indicated the usefulness of the cortical surface registration. Some recent studies [37, 59] also show the effectiveness of the surface registration methods. The methods can be broadly divided into two categories: (i) curvature or convexity based optimization method in which shape metrics or geometric attributes like cortical convexity, curvature, and conformal factor computed over the whole surface are best aligned. For example, Fischl et al. [39] proposed a curvature alignment method which first maps the brain surfaces onto the spheres with curvature pattern mapped onto it and then uses a $2D$ warping on the source sphere so that the curvature patterns of the two brain surfaces are best aligned. The mapping process on the sphere is constrained by adding a distance and an areal term to the energy functional to minimize the

total distortion. The distance term gives the surface some local stiffness to prevent excessive shear, and the areal term prevents folds and significant compression or expansion. The method is widely used with Freesurfer [36] package. BrainVoyager's method [49] also uses a similar curvature alignment approach implemented with the iterative gradient-descent method.

Another category is, (ii) landmark-based or constrained brain registration methods in which cortical landmarks or features such as sulci or gyri curves or points are used as constraints in the registration process [15, 22, 74, 121, 135, 162]. Again, constrained brain registration can be categorized as follows: 1) Point-constrained methods. The challenge here is to guarantee diffeomorphism. Recently, progress has been made to ensure diffeomorphism. A recent work [135] generates the exact landmark alignment and guarantees diffeomorphism based on hyperbolic orbifold model. The LDDMM [15] and diffeomorphism geodesic [74] methods compute the registration while generating the deformation. 2) Curve-constrained methods [22]. Most common works discretize curves to points for registration, but cannot guarantee the point interval alignment. Rigorous methods to handle curve constraints have been presented based on the hyperbolic harmonic mapping model [121] and the curve constrained quasi-conformal mapping model [162]. They can guarantee the exact alignment of curves with harmonic energy (stretches) minimized in the meanwhile. Recently, spectral methods have been applied [89, 90] for registration which can register brain surfaces very fast while achieving good accuracy.

Automatic curvature based methods are suitable for large-scale studies, as no manual help from an expert is required for labeling, but they can suffer from inaccurate alignment. On the other hand, landmark-based methods can use automatic or semi-automatic methods which require some user interactions for landmark detection or selection, but it can provide better alignment of the landmarks. Joshi et

al. [67] proposed a method which first parameterizes the brain surfaces to the square domain and then aligns the manually traced sulcal landmarks in the registration by minimizing an elastic energy function using the sulcal curves as constraints. The method employs a parameter to control the amount of alignment of the sulcal curves, but the method is not bijective. Although manual labeling can produce accurate labeling of landmarks, but are often time-consuming and sometimes may suffer from inter-rater variability. To minimize the effort for manual labeling, a minimal set of sulci curves (6 curves instead of 26) [65] have been proposed to use in the registration which can also achieve high accuracy. Pantazis et al. [100] provided comparisons between manual landmark-based methods using 26 consistent landmarks curves, and automatic methods of the Freesurfer and BrainVoyager for brain registration. Their comparison is based on the curvature overlap measure and curve alignment measure using Hausdorff distance [33] which calculates the distance between two curves. They concluded that although automatic method tries to best align the curvature, but still sometimes landmark-based method performs well in curvature alignment. Also, they find find few cases, where the landmark curves do not align perfectly in the landmark-based methods.

Our method. Existing brain registration methods do not consider the connectivity between the regions of the surfaces. As a result, the methods can not guarantee the best alignment of the cortical regions in the registration. Our proposed brain registration method uses a novel intrinsic atlas-constrained mapping technique with minimal graph refinement strategy to align the cortical regions among the brain surfaces as much as possible. The proposed registration framework is based on the automatic computation of landmark curves. Instead of using the landmark curves separately we employ the whole atlas graph as constraints in the registration. To make the atlas graphs consistent among the brains, we have proposed strategy which

guarantees minimal changes in both graphs to match them completely and also ensures that the 3-connected property of the graph is maintained. The mapping and registration is guaranteed to be unique, globally optimal and diffeomorphic.

2.3 Brain Morphometry Analysis

Brain morphometry analysis from brain MRI is a well known and widely used procedure for the physicians. Physicians normally look for any abnormality in the brain image or surface manually. But the task is heavy time consuming for even an expert physicians, and in some cases, an expert physician is not even available. Also, it is not practical to depend on the manual procedure of the physicians for a large volume of data analysis, so computer-aided automatic morphometry analysis is required. To automate the process, researchers use both volume based and surface-based analysis approach. Volume-based approach normally uses 2D image processing techniques on individual images (the images contain the inside picture of the brain) and then combine the results on the whole volume image. On the other hand, surface-based analysis usually looks for the changes in the geometric shape of the brain in the 3D surface. The analysis often develops or finds the appropriate geometric attributes useful for identifying abnormalities on the brain cortical surface. Both approaches have been used for different morphpmetry analysis tasks. Volume-based analysis have been found very effective for identifying and classifying scizophrenia [32], autism [62], depression [18], etc. Surface-based analysis also has significant importance for morphometry analysis as indicated by earlier researchers [38, 131] and recently have been used successfully for many other applications such as AD classification [161], schizophrenia [28], brain growth trajectories in childhood [9], identifying developmental disorder [133], etc. Ashburner et al. [8] showed that in many cases surface-based analysis might be more useful than

volume-based analysis. As this dissertation is based on the surface-based analysis, we focus the discussion on the surface based morphometry analysis. Although our work is on AD classification, we also discuss some other surface based brain analysis works using geometric attributes of the cortical surfaces.

For brain surface analysis, some approaches propose different types of shape measurement strategies using various surface mapping approaches. Some other approaches compute the shape metrics by mapping the genus-0 closed brain surface to a sphere or a region (normally unknown or black region) is removed to make the surface open and mapped to a disk. For example, Zeng et al. [161] proposed a method which uses the contours around the brain regions to compute the features for shape analysis. Their method computes the 3D shape signatures by mapping the contours as holes inside a disk domain using Ricci curvature flow. Gerig et al. [48] proposed ventricular shape descriptor via spherical harmonics for brain analysis of twins. Chung et al. [24] proposed tensor-based morphometry analysis via weighted spherical harmonics which is a generalization of the previous method. Tosun et al. [133] proposed a combined shape measures using cortical gyrification index, curvedness, and L_2 norm of mean curvature to analyze the folding pattern of a developmental disorder called Williams syndrome, and to quantify the difference with normal brains. Liu et al. [85] proposed shape spaces for general topological space, and used the cost to interpolate between the shapes as shape metrics; they show the use of the shape metrics for brain surfaces. Qiu et al. proposed [104] momentum maps to analyze the difference in the brain's hippocampusamygdala network of the elders and young adults. Other shape analysis approaches include metamorphosis through Lie group [134], conformal invariants [141] for AD classification, etc.

For some diseases, it is identified by the expert physicians which regions of the brain are most affected due to the disease, e.g., for the AD, cortical regions like

entorhinal, hippocampal, supramarginal, etc., are most affected and different geometric statistics on these regions are used for the classification. Other approaches use the statistics on the whole cortical surface, often try to find out experimentally which kinds of feature or features of which regions are the most significant discriminators for the classification. Davies et al. [28] proposed a method by computing the parameterization of the hippocampal region and aligning the surfaces onto the parameter domain minimizing the distance between them. They find out a subset of shape parameters from the correspondence by using minimal description length principle and use that as shape descriptor in the linear discriminant analysis for classifying schizophrenia patients.

Different types of approaches have been presented for AD classification. Desikan et al. [30] proposed a method for MCI (mild cognitive impairment, which is considered to be the earlier stage of AD) and AD classification using the ROI (region of interest) based comparison of some measurements, e.g., entorhinal cortex thickness, hippocampal volume, and supramarginal gyrus thickness. The approach uses the measurements over the whole regions and uses those measurements in the classification with logistic regression. Marcus et al. [95] proposed a similar approach based on the region based statistics using the regression analysis. In their study, the best discriminatory features were the entorhinal cortex thickness, the supramarginal gyrus thickness, and the hippocampal volume. Also, several methods have been proposed based on hippocampal region's shape measurement to classify MCI and AD. For example, the coefficient of spherical harmonics was used as the shape measurement feature of the hippocampal in [47], and volume of the hippocampal was used in [25]. Cuingnet et al. [26] provided detailed comparisons among the ten methods for AD classification. Cortical network-based analysis has also been used recently for AD

classification. For example, Yao et al. [151] finds the presence of abnormal cortical networks in the patients with mild cognitive impairment (MCI) and AD.

Our method. Our approach uses the atlas-constrained brain registration method proposed in this dissertation to co-register the brains which guarantees the best possible alignment of the cortical regions. As a result, the method can generate more optimal shape similarity metrics. The method uses the attributes of the whole cortical surface or parts of the surface to compute the similarity metrics. The method uses the feature selection strategy to find out the best set of features to classify brains.

2.4 Surface Parameterization, Registration and Morphing

2.4.1 Surface Parameterization

Surface parameterization was first introduced to computer graphics as a method for mapping texture onto the surface [17, 93] and has gradually become a useful tool for many geometry processing applications, such as detail mapping, synthesis and transfer, mesh editing and compression, remeshing, fitting, morphing, and so on [29, 116]. Surface conformal mapping as the most popular surface parameterization method has its nice property, angle preserving, and has been widely used for various shape analysis applications [112]. It has been intensively studied over the last two decades, including the harmonic energy minimization [41], least square conformal maps [79], holomorphic differentials [51], discrete curvature flows [16, 63, 124], and so on [34, 44, 81, 83, 84, 97, 109, 110]. As a general mapping, quasiconformal mapping has been arousing more and more attention recently [145, 162]. The auxiliary metric method was presented with the 1-form and curvature flow methods [154, 158]. The holomorphic Beltrami flow method [92] was introduced using a variational principle.

2.4.2 Surface Registration

3D surface registration is a fundamental task in Computer Graphics which has a broad range of applications including shape matching and recognition, shape modeling, morphological study and animations. In the past decade, surface registration methods have been intensively explored [45,60,76,125,129,150]. Most existing methods directly deal with non-rigid deformations, but always stop at a local optima and hardly get a global solution. Recently, a lot of research focuses on surface conformal and quasiconformal mapping based methods [91, 128, 156, 157, 162]. According to surface uniformization theorem [35], any arbitrary surface can be conformally mapped to one of three canonical domains, the unit sphere, the Euclidean plane or the hyperbolic disk. By mapping surfaces to 2D canonical domains, the problems of 3D surface registration is reduced to a 2D image registration problem. In real applications, landmark constraints are usually prescribed to guide the surface registration, which may introduce fold singularities in the resultant mapping. Among the various feature landmarks (points, curves, and graphs), the feature graph plays an important role in the constrained surface registration. For the surfaces with feature graph, it will introduce more benefits to treat the feature graph as a whole rather than split it into separate curves, and apply the traditional curve based methods [155, 162]. Zeng [163] presented a method to parameterize and register surfaces with graph constraints. However, it determined the weights of the tutte embedding by a heuristic method.

2.4.3 Surface Morphing

There have been a lot of research on image morphing in the past (e.g., see survey paper [148]). Some methods automatically find the correspondence between the images for morphing, e.g., optimal mass preserving mapping [164] and other optimization

technique [115]. Recently, Liao et al. [82] presented a semi-automatic method which provides some artistic control in morphing. The method uses the structural similarity, and user-provided points similarities as constraints. With the advance of 3D graphics in recent years, morphing between 3D surfaces have also been used extensively in animation and motion picture industries. Some patch-based methods have been proposed [13, 77] earlier which use harmonic maps on the patches separately, but merging the patches are hard. Recently, Zaharescu et al. [153] presented a surface evolution method for high genus surfaces which is applied to surface morphing, but the method does not match feature points or curves between the surfaces.

Our method. Most existing constrained parameterization method only uses points or curves which is later used as constraints in the surface registration process. Recently, Zeng [163] presented a method to parameterize and register surfaces with graph constraints. But the parameterization method first computes the planar graph embedding using Tutte embedding, and then in the next step computes a harmonic map which tries to fit the map inside the canonical domain obtained from the graph embedding. Therefore, the final parameterization and registration highly depend on the chosen weights during the Tutte embedding computation, which is heuristic and not intrinsic. On the other hand, our graph-constrained parameterization method computes the quasiconformal mapping of the graph constrained surfaces intrinsically by an adaptive harmonic map, which can be formulated by sparse linear systems. The method is general, easy to implement and the entire process is automatic, which straightens the graph curves, and preserves the local and global shape of the original surface as much as possible. The proposed graph-constrained parameterization and registration method has been applied to generate morphing sequence of surfaces and images.

CHAPTER 3

STRUCTURAL BRAIN MAPPING

3.1 Introduction

Brain mapping plays an important role in neuroscience and medical imaging fields, which flattens the convoluted brain cortical surface and exposes the hidden geometry details onto a canonical domain. In this work, we present a novel brain mapping method to efficiently visualize the convoluted and partially invisible cortical surface through a well-structured view, called the structural brain mapping. In computation, the brain atlas network (node - the junction of anatomical cortical regions, edge - the connecting curve between cortical regions) is first mapped to a planar straight line graph based on Tutte graph embedding, where all the edges are crossing-free and all the faces are convex polygons; the brain surface is then mapped to the convex shape domain based on harmonic map with linear constraints. Experiments on two brain MRI databases, including 250 scans with automatic atlases processed by FreeSurfer and 40 scans with manual atlases from LPBA40, demonstrate the efficiency and efficacy of the algorithm and the practicability for visualizing and comparing brain cortical anatomical structures.

3.2 Background and Motivation

Brain networks, the so-called brain graphs [19], have been intensively studied in neuroscience field. Bullmore et al. [19] gave thorough reviews and methodological guide on both structural and functional brain network analysis. In this work, we focus on brain structural network on cortical surface, i.e., cortical network. It has been used to discover the relation of its disorganization to diseases such as Alzheimers disease [58]. One important task within this is brain network visualiza-

tion and comparison. Existing methods such as conformal mappings didnt consider the anatomical atlas network structure, and the anatomical landmarks, e.g., gyri curves, appear highly curvy on the canonical domains. Using such maps, it is difficult to recognize the connecting pattern and compare the atlases. To date, it still needs a lot of efforts to explore a more perceptively straightforward and visually plausible graph drawing. In summary, the motivation of this work is to provide a well-structured convex shape view for convoluted atlas structure, which is more accessible for reading than pure surface mapping (e.g. conformal) views with curvy landmarks and more efficient for anatomical visualization and comparison.

3.3 Approach overview

This work presents a novel method for brain cortical anatomical structure mapping using the cortical network. But the cortical network studied in this work is different from the definition of structural brain graph in [19], where the node denotes the cortical region, the edge denotes the connectivity between two cortical regions, and it is completely a topological graph. In this work, we define the node as the junction of anatomical cortical regions and the edge as the common curvy boundary of two neighboring cortical regions. This anatomical graph (see Fig. 3.1(b)) is embedded on the 3D genus zero cortical surface, has physically positioned nodes and crossing-free curvy edges, and therefore is planar in theory [75]. For simplicity and differentiation, we call it brain net. In terms of topology, it is the dual graph of the brain graph in [19]. We have verified this in our experiments. In this work, brain net is used to drive a canonical surface mapping (the regions and the whole domain are convex). We call this technique brain-net mapper. The mapping employs the special properties of the anatomical brain net: 1) planar and 2) 3-connected (after testing and minor filtering). The computational strategy is to employ the planar

graph embedding as guidance for structural brain surface mapping using constrained harmonic map. In detail, first, the 3-connected planar brain net graph is embedded onto the Euclidean plane without crossing graph edges and every face is convex based on Tutte embedding theorem [137]; then, using the obtained convex target domain with convex subdivision as constraints, a harmonic map of the brain surface is computed. The mapping is unique and diffeomorphic, which can be proved by generalizing Radó theorem [111]. The algorithm solves sparse linear systems, therefore is efficient and robust to topology and geometry noises. The resulting mapping exposes invisible topological connectivity and also details cortical surface geometry.

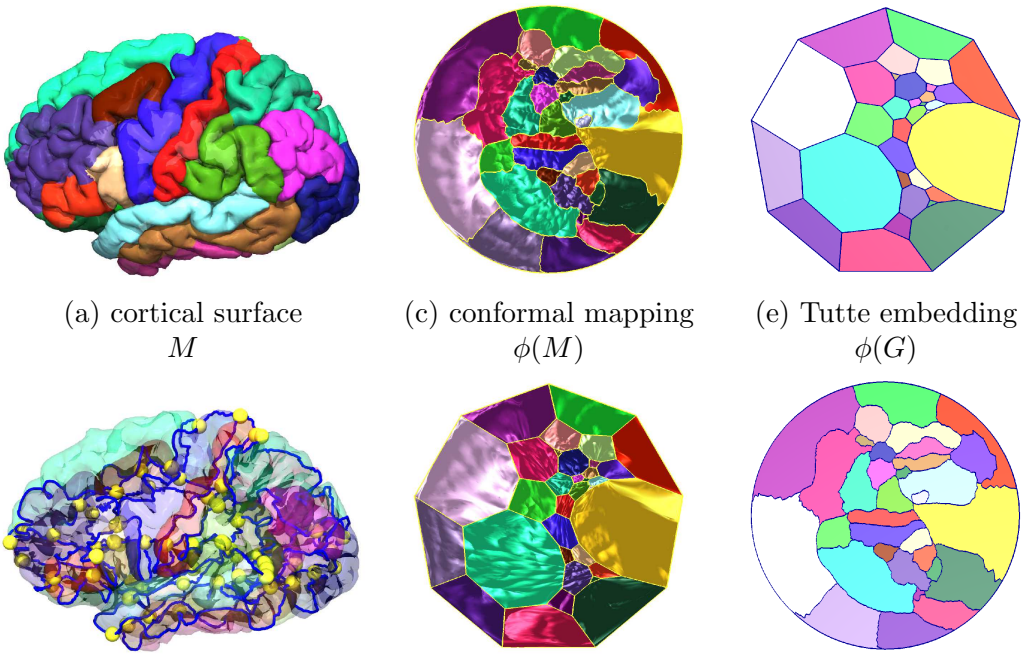

(a) cortical surface M (c) conformal mapping $\phi(M)$ (e) Tutte embedding $\phi(G)$

(b) cortical net G (d) structural mapping $h(M, G)$ (f) conformal embedding $\eta(G)$

Figure 3.1: Brain net embeddings for brain A_1 (left hemisphere).

Figure 3.1 gives an example where regions are denoted in different colors (a). The brain net G (b) is mapped to a planar polygonal mesh (e), where each face is convex and assigned with the corresponding regions color. The planar representation

(f) is the final map guided by (e), with visually plausible structure, i.e., planar straight lines and convex faces with interior surface harmonically flattened (stretches minimized). It illustrates the cortical anatomical structure (a). We call this mapping structural brain mapping. In contrast, conformal map (c) generates the planar graph embedding but with curvy graph edges (d).

To our best knowledge, this is the first work to present a structural view of brain cortical surface associated with anatomical atlas by making all anatomical regions in convex polygonal shapes and minimizing stretches. Experiments were performed on 250 brains with automatic parcellations and 40 brains with manual atlas labels to verify the 3-connected property of brain nets (anatomical connectivity) and test the efficiency and efficacy of our algorithm for brain cortical anatomical atlas visualization and further cortical structure comparison.

3.4 Theoretic Background

This section briefly introduces the theoretic background.

Graph embedding. In graph theory, a graph G is k-connected if it requires at least k vertices to be removed to disconnect the graph, i.e., the vertex degree of the graph $deg(G) \geq k$. A planar graph is a graph that can be embedded in the plane, i.e., it can be drawn on the plane in such a way that its edges intersect only at their endpoints. Such a drawing is called the planar embedding of a graph, which maps the nodes to points on a plane and the edges to straight lines or curves on that plane without crossings.

A 3-connected planar graph has special property that it has planar crossing-free straight line embedding. Tutte (1963) [137] gave a computational solution, the classical *Tutte embedding*, where the outer face is prescribed to a convex polygon and each interior vertex is at the average (barycenter) of its neighboring positions. Tutte's

spring theorem [137] guarantees that the resulting planar embedding is unique and always crossing-free, and specially, every face is convex.

Harmonic map. Suppose a metric surface $(S, \mathbf{g})$ is a topology disk, a genus zero surface with a single boundary. By Riemann mapping theorem, S can be conformally mapped onto the complex plane, $\mathbb{D} = \{z \in \mathbb{C} || z| < 1\}$, $\phi : S \to \mathbb{D}$, which implies $\mathbf{g} = e^{2\lambda(z)} dz d\bar{z}$, where λ is the conformal factor.

Let $f : (\mathbb{D}, |dz|^2) \to (\mathbb{D}, |dw|^2)$ be a Lipschitz map between two disks, $z = x + iy$ and $w = u + iv$ are complex parameters. The *harmonic energy* of the map is defined as $E(f) = \int_{\mathbb{D}} (|w_z|^2 + |w_{\bar{z}}|^2) dxdy$. A critical point of the harmonic energy is called a *harmonic map*, which satisfies the Laplace equation $w_{z\bar{z}} = 0$. In general, harmonic mapping is unnecessarily diffeomorphic. Radó theorem [111] states that if the restriction on the boundary is a homeomorphism, then the map from a topological disk to a convex domain is a diffeomorphism and unique.

3.5 Computational Algorithms

The computation steps include: 1) compute graph embedding; and 2) compute harmonic map using graph embedding constraints (see Algorithm 3).

The brain cortical surface is represented as a triangular mesh of genus zero with a single boundary (the back-side black unknown region is cut off), denoted as $M = (V, E, F)$, where V, E, F represent vertex, edge and face sets, respectively. Similarly, the brain net is denoted as a graph $G = (V_G, E_G, F_G)$ (3-connected and planar, embedded on M) (see Fig. 3.1(b)). Thus, we use (M, G) as the input.

Step 1: Isomorphic Graph Embedding The first step is to compute a straight line convex graph embedding of G, $\eta : G \to \hat{G}$ by Tutte embedding [137]. We first place the graph nodes on boundary ∂M onto the unit circle uniformly, and then compute the mapping positions $\eta(v_i)$ for interior nodes v_i as the barycenters of

Algorithm 1: Graph Embedding for Surface Mapping

Require: A triangular mesh with decorative graph (M, G)
Ensure: A planar triangular mesh with straight line decorative graph $(\Omega, \hat{G})$
1: Compute Tutte embedding $\eta : G \to \hat{G}$
2: Compute harmonic map $\phi : (M, G) \to (\Omega, \hat{G})$ with constraints $\phi(G) = \hat{G}$

the mapping positions of neighboring nodes v_j, $\{\eta(\hat{v}_i) = \Sigma_{(v_i,v_j)\in E_G}\lambda_{ij}\eta(\hat{v}_j)\}$. We use $\lambda_{ij} = 1/deg(v_i)$, where $deg(v_i)$ denotes the degree of node v_i in G. Solving the sparse linear system, we obtain the Tutte embedding result $\hat{G}$, which defines a convex planar domain Ω (see Fig. 3.1(e)).

Step 2: Constrained Harmonic Mapping The second step is to compute a surface mapping $h : (M, G) \to (\Omega, \hat{G})$ to restrict graph G to the planar Tutte embedding result $\hat{G}$ by a constrained harmonic map (see Fig. 3.1(f)). We map the whole surface M onto the convex planar domain Ω by minimizing the discrete harmonic energy under graph constraints, formulated as $\min\{E(\phi(v_i)) = \Sigma_{[v_i,v_j]\in E} w_{ij}(\phi(v_i) - \phi(v_j))^2, \forall v_i \in V\}$, s.t., $\phi(l_k) = \hat{l}_k, \forall l_k \in G, \hat{l}_k = \eta(l_k)$, i.e., l_k is the curvy edge of graph G, and $\hat{l}_k$ is the corresponding edge on the planar graph embedding $\hat{G}$. The solution to the harmonic energy minimization problem is equivalent to solving the linear system $\Delta\phi = 0$ (Δ is the Laplacian operator), descreterized as the linear equations $\{\Sigma_{[v_i,v_j]\in E} w_{ij}(\phi(v_i) - \phi(v_j)) = 0, \forall v_i \in V\}$.

We only specify the target positions for the two end vertices of l_k. Other interior vertices on l_k are constrained to $\hat{l}_k$ through a linear combination of two neighbors on $\hat{l}_k$. The linear constraints between coordinates x, y on straight line $\hat{l}_k$ can be plugged into the above system. We employ the mean value coordinates to guarantee the edge weight w_{ij} to be positive. Then in our construction, for each vertex there is a convex combination of neighbors. According to Tutte's spring theorem [137], Radó theorem [111] and generalized Tutte embedding [40], the solution achieves a unique and diffeomorphic surface mapping.

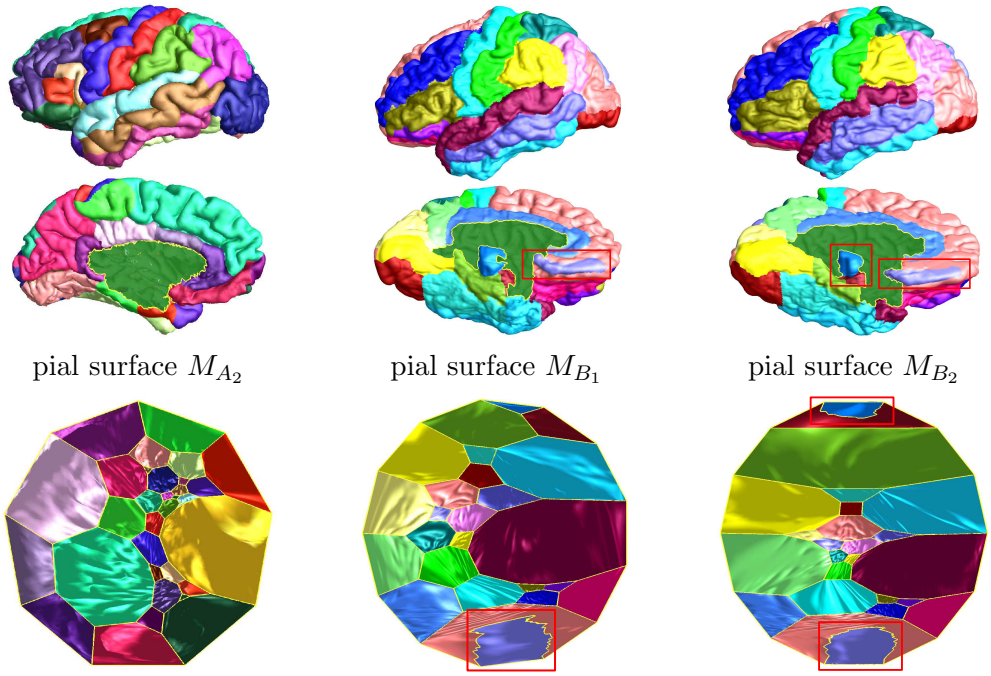

pial surface M_{A_2} pial surface M_{B_1} pial surface M_{B_2}

convex mapping Ω_{A_2} convex mapping Ω_{B_1} weighted convex Ω_{B_2}

(a) brain A_2 (lh) (b) brain B_1 (lh) (c) brain B_2 (lh)

Figure 3.2: Structural brain mappings driven by graph embedding.

3.6 Experiments

The proposed algorithms were validated on two databases with different atlas types: 1) the own captured 250 brain MRI scans, we use FreeSurfer to automatically extract triangular cortical surfaces and anatomical atlas (see Figs. 3.1, 3.2(a)); and 2) the public 40 brains with manual atlas labels provided by LPBA40 [114] (see Fig. 3.2(b-c)), we use BrainSuite to correlate the triangular cortical surface with manual labels. All the brains come from human volunteers.

3.6.1 Brain Net Extraction

We extract the brain nets from cortical surface using anatomical region id or color assigned. To employ Tutte embedding, we then test the 3-connected property of all

Table 3.1: Statistics on brain nets, meshes and time. lh (rh) - left (right) hemisphere.

Data	FreeSurfer (lh)	FreeSurfer (rh)	LPBA40 (lh)	LPBA40 (rh)
#region,#node	33~35, 62~70	33~35, 64~72	24~28, 41~52	20~22, 39~55
#triangle,time	$277k$, 20 secs	$279k$, 20 secs	$131k$, 10 secs	$131k$, 10 secs
#good (a-b)	57	250	5	33
#bad (i/ii/iii)	193/0/0	0/0/0	24/10/1	7/0/0

the brain nets using two conditions: (a) every node has ≥ 3 neighboring regions; (b) every region has ≥ 3 boundary nodes. If both are satisfied, then the brain net is 3-connected, a "good" one.

Our tests show that all brain nets satisfy condition (a). All the "bad" regions detected contain 2 nodes, i.e., 2 boundary edges, which contradicts (b). There may be (i) 1, (ii) 2, or (iii) 3 bad regions. Table 4.1 gives the number of brains for each above case. We use (lh, rh) to denote the percentage of left and right hemisphere brain nets satisfying both (a-b): FreeSurfer $(22.8\%, 100\%)$, LPBA40 $(12.5\%, 82.5\%)$, both $(21.4\%, 97.6\%)$. The tests give that most exception cases are with $1 \sim 2$ "bad" regions, for which we only map one boundary edge to straight line and ignore the other in next structural brain mapping procedure. If the region is totally interior, we randomly select one; if it is adjacent to the brain surface boundary, then we select the boundary one, as shown in Fig. 3.2(b-c).

3.6.2 Structural Brain Mapping

The algorithms were tested on a desktop with 3.7GHz CPU and 16GB RAM. The whole pipeline is automatic, stable and robust for all the tests. Table 4.1 gives the averaged running time. Figures 3.1-3.2 show various results, by which it is visually straightforward to figure out local topology (adjacency of regions) and tell whether two atlases are isomorphic (or topologically same); in contrast, it is hard to do so in

a 3D view. Note that the polygonal shape is solely determined by the combinatorial structure of the brain net. Brains with consistent atlases are mapped to the same convex shape (see brains A_1, A_2), which fosters direct comparison. Brains B_1, B_2 from LPBA40 are with different brain nets, especially around the exception regions. Even though the unselected edges of the bad regions appear irregular, the mapping results are visually acceptable and functionally enough for discovering local and global structures and other visualization applications, such brain atlas comparison.

3.6.3 Discussion

This work focuses to present a novel brain mapping framework based on Tutte embedding and harmonic map with convex planar graph constraint. For better understanding the method and its potentials, we have the discussions as follows.

Convex shape mapping. The cortical surface can be directly mapped to canonical domains such as conformal map to a disk [144] (Fig. 3.1(c)) and harmonic map to a convex domain [53] (Fig. 3.3(b)). Each map can define a planar straight line graph embedding (Fig. 3.3(a,c)) by simply connecting the nodes on the planar domain, but it may generate concave and skinny faces and cannot guarantee "crossing-free" and further the diffeomorphic brain mapping. Our method can solve these, and the diffeomorphism property has been verified in all the tests. If the graph is not 3-connected, we use valid subgraph for guiding the mapping. The unselected part is ignored and won't affect the diffeomorphism.

Topology and geometric meanings. This work studies "graph on surface" and its influence to surface mapping. The convex map preserves the topology of the graph on the canonical domain and minimizes the constrained harmonic energy (preserving angles as much as possible under constraints), therefore is more accessible and perceptually easy to capture global and local structures.

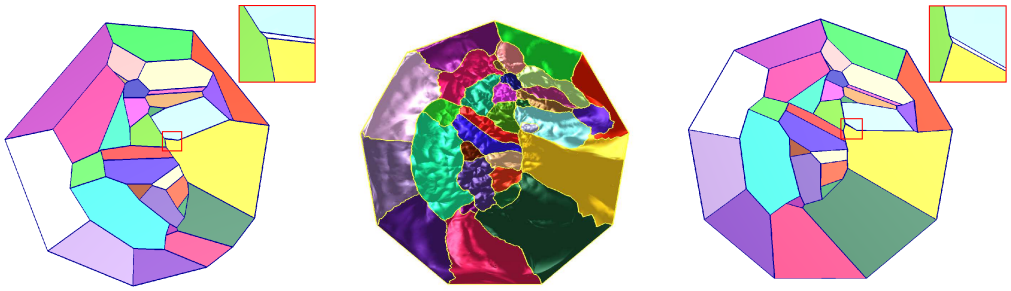

(a) straight line drawing of Fig. 3.1(c) (b) convex harmonic mapping of Fig. 3.1(a) (c) straight line drawing of (b)

Figure 3.3: Straight line graph drawings induced by conformal and harmonic mappings.

Advantages. *In theory*, the method is rigorous, based on the classical Tutte graph embedding for 3-connected planar graphs (Tutte's spring theorem [137]), and the harmonic map with linear convex constraints with uniqueness and diffeomorphism guarantee (Radó theorem [111], generalized Tutte embedding [40]). *In practice*, all the algorithms solve sparse linear systems and are easy to implement, practical and efficient, and robust to geometry or topology noises. The framework is general for surfaces decorated with graphs.

Extensions. This method is able to reflect more original geometry by introducing weighted graph embeddings, and can be extended to handle high genus cases by using advanced graph embeddings.

Potentials for brain mapping and other biomedical research. The structural brain mapping can help understand anatomical structures and monitor anatomy progression, and has potential for brain cortical registration with atlas constraints. This anatomy-aware framework is general for other convoluted natural shapes decorated with feature graphs (e.g., colons), and can be applied for their anatomy visualization, comparison, registration and morphometry analysis.

3.7 Summary

In this chapter, we present a brain cortical surface mapping method considering the whole cortical anatomical structure, such that the complex and convoluted brain cortical surface can be mapped in a well-structured view, i.e., a convex domain with convex subdivision. The algorithms based on Tutte embedding and harmonic map are efficient, practical, and are extensible for other applications where 3-connected feature graphs are associated. In next chapters, we will introduce strategies to reflect more original geometry in the mapping, and show the application of the proposed mapping in brain registration and brain analysis.

CHAPTER 4

ATLAS-CONSTRAINED BRAIN REGISTRATION

4.1 Introduction

In this chapter, we present a novel cortical surface registration method by fully considering the anatomical atlas structure, where the atlas graph (as presented in chap. 3) is extracted as feature constraints. Our experiments on brain databases with manual atlas labels have verified that atlas graphs are not guaranteed to be consistent over brains. In order to align the atlas graphs as much as possible and keep the graphs consistency in registration, we modify the graphs on triangular meshes as local as possible by pruning and splitting operations. We then employ the 3D-to-2D canonical parameterization method to carry out the registration: 1) compute an intrinsic graph-constrained harmonic map for each cortical surface, which maps curvy 3D atlas graph to a 2D planar straight line graph (PSLG) in a 2D *convex subdivision domain*; and 2) compute the alignment over the 2D domains using the PSLG constraints, with a relaxation procedure to minimize the distortions introduced by graph modification. Experiments on various brains demonstrate the efficiency and efficacy of the algorithm and the practicability for registering cortical anatomical structures.

4.2 Background and Motivation

In brain study, the dense registration between cortical surfaces is highly desirable in neuroscience, medical imaging, cognitive neuroscience, psychology, etc. It aims to create an optimal diffeomorphism (one-to-one, onto, bijective mapping) between cortical surfaces. Diffeomorphic cortical surface registration can give a detailed guidance for locating the deformation areas for progression measurement and brain

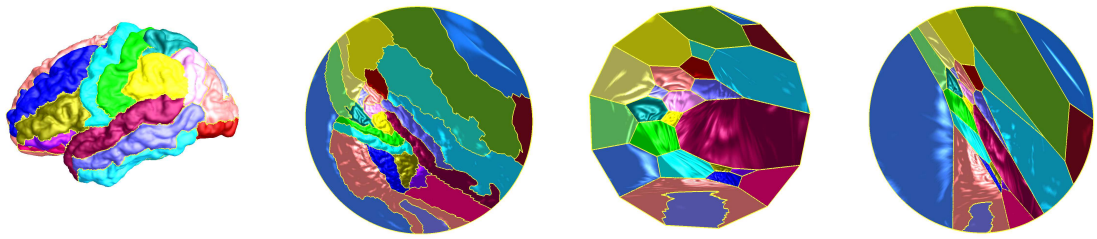

(a) 3D brain (b) harmonic map (c) uniform mapping (d) our mapping

Figure 4.1: Cortical surface mappings, where the atlas labels are color encoded.

structure morphology analysis. In addition, based on the registration, one can define the shape similarity measurements(distance, metric) globally for brain comparison and classification. Therefore, it has broad applications for brain growth development measurement [132], shape-function variability in retinotopy [89], language lateralization analysis [52], and disease diagnosis, e.g., Alzheimer's disease [30, 120], Autism [23], etc.

There have been a lot of research on brain surface registration; some of the methods use geometric mappings and feature constraints. The existing constrained brain registration methods use either sulci/gyri curves or points as constraints. Here, we will introduce a novel method taking into account the whole cortical anatomical atlas graph as constraint. The cortical atlas graph is embedded on the 3D cortical surface and has geometry, i.e., the nodes are the junctions of the anatomical cortical regions, and the edges are the connecting curves of the adjacent regions. The atlas graph, as an anatomical feature, is used to drive the registration to make the anatomical regions well aligned.

This work is motivated by presenting a novel brain registration framework through the alignment of atlases and is inspired by the uniform convex mapping based on graph embedding presented in chap. 3, which generates a convex subdivision domain

(where each face is convex) for a cortical surface with atlas graph. In this work, we use the intrinsic convex subdivision mapping instead of the uniform convex mapping, without using graph embedding, to achieve the atlas-based registration, where 3D curvy graph constraint is converted to linear straight line constraint. Since brains may not have consistent atlases [10] (verified by our experiments), in theory, there is no perfect atlas alignment. One criterion is that we can make the atlas regions registered as much as possible. Therefore, we need to make changes as minor as possible to the graphs to make them isomorphic (having one-to-one corresponding nodes and edges among the graphs). The registration result is evaluated by the comparison to the results using only the common atlas graphs and FreeSurfer registration.

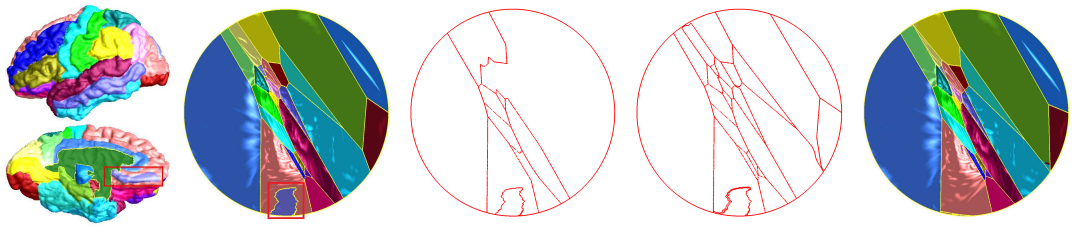

(a) B_0 (b) $\phi_0(B_0, G_0)$ (c) G_0^c (d) G_0' (e) $\phi_0'(B_0, G_0')$

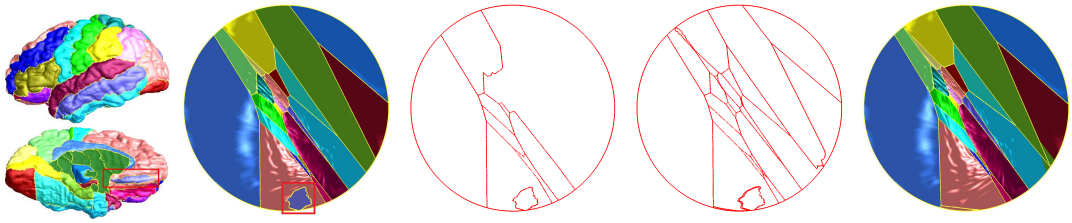

(f) B_1 (g) $\phi_1(B_1, G_1)$ (h) G_1^c (i) G_1' (j) $\phi_1'(B_1, G_1')$

Figure 4.2: Registration of cortical surfaces B_k with atlas graphs G_k. G_k^c: the common subgraphs, G_k': the refined consistent graphs, ϕ: the graph-driven convex mapping, and ϕ': the graph-driven convex mapping with refined graph.

4.3 Approach Overview

The overall solution is based on the intrinsic graph-driven harmonic map along with graph modification and mapping relaxation techniques. Without considering graph constraint, the harmonic map is intrinsic, but the graph appears highly curvy on the planar domain (see Fig. 4.1(b)), which cannot be used directly as constraint in the registration. In our intrinsic convex harmonic map, the positions of the mesh vertices on atlas are computed based on the adjacent mesh edges on the graph. Here we set the boundary vertices onto the unit circle. This ensures that the atlas graph is straightened to be convex (see Fig. 4.1(d)). Importantly, the positions of the graph-nodes are computed automatically, intrinsically determined by the surface and graph geometry. In contrast, in the uniform convex mapping (presented in chap. 3, see Fig. 4.1(c)), the positions of the graph-nodes are given by the uniform Tutte embedding, which are not intrinsic without considering graph geometry; the final embedding is constrained by the initial Tutte embedding [137] which is heuristic and not intrinsic.

Given the source and target cortical surfaces to be registered, first, we perform the atlas graph consistency check and make changes as minimal as possible to make the graphs 3-connected (node degree ≥ 3) and isomorphic (with same nodes and edges connectivity). Then, we construct the registration over the intrinsic convex subdivision domains by the graph-constrained harmonic map with the convex subdivision constraint. This process maps both the source and target surface in the same parameter domain. Finally, we perform a relaxation algorithm to minimize the distortions introduced by graph modification around the unmatched areas. The resulted registration is guaranteed to be unique and diffeomorphic based on the

generalized Radó theorem [111] and Floaters convex combination theorem [41]. The method is linear and implemented by solving sparse linear systems.

Figure 4.2 illustrates the pipeline of the registration for cortical surfaces B_0, B_1. The atlases are denoted by coloring (see Col. 1). From the convex mapping visualization (see Col. 2), it is obvious that the atlas graphs are inconsistent in the two brains but with common subgraphs (see Col. 3). In order to match all the regions as much as possible, the graphs are locally modified around unmatched edges and two-edged regions (as shown in the red rectangles, final graph modification is shown in Col. 4). We can observe that the two-edged regions become three-edged regions and the graphs are mapped to convex subdivisions. Using the modified graphs as constraints, we generate two convex mappings with consistent graphs (see Col. 5). Experiments were performed on LPBA40 and Mindboggle data sets with manual atlas labels to verify atlas inconsistency and to evaluate the algorithm performance.

4.4 Computational Algorithms

The major steps for registration include: 1) check atlas consistency and refine atlas graph if inconsistent; 2) compute intrinsic atlas-constrained harmonic maps; and 3) register the two harmonic map domains and relax the mapping due to atlas modification.

The cortical surface is represented as a triangular mesh of genus zero with a single boundary (the back-side unknown region is cut off), denoted as $M = (V, E, F)$, where V, E, F represent vertex, edge, and face sets, respectively. The atlas graph is denoted as $G = (V_G, E_G, F_G)$, where V_G, E_G, F_G represent graph node, edge and face sets, respectively. Thus, we use (M, G) to denote an atlas-constrained surface.

4.4.1 Graph Consistency Check and Modification

We first check if the two atlas graphs are consistent. Graph consistency is checked by matching the same nodes on both graphs. If two nodes in both graphs have exact same surrounding regions, they are matched. If all the nodes in two graphs are matched, they are consistent, otherwise the graphs we perform refinement operation to create consistent graphs (see Fig. 4.3). For creating the consistent atlas graphs between source and target, we detect the matched and unmatched edges from both the graphs. There are two cases we need to consider to meet the requirements of the framework which is described as follows:

Case 1: Unmatched Edge. The operation to handle this is *edge pruning*. Two graph-edges in both atlases are matched, if they have the same left and right neighboring regions; Otherwise, they are unmatched. We remove the unmatched edge by moving two nodes to the middle. The original graph-edge is then divided into two segments. Each segment is shifted to every side by one triangle away from the original position. Repeat edge pruning until there is no unmatched edge. This operation wont introduce new connectivity between regions. It is equivalent to merging two edge nodes to one. As shown in Fig. 4.3(a), we select the middle vertex v of the graph-edge e as the new node. We then select the closest vertex v_{ik} on each graph-edge e_{ik} rooted at the two nodes v_{ek} of e. Then we perturb the curves connecting v, v_{ik} by one triangle away from the original position towards the interior of the corresponding region of each.

Case 2: Two-Edged Region. The operation to handle this is *edge splitting*. These regions have only two graph nodes and edges (see Fig. 4.2), and need to be refined as 3-connected (degree ≥ 3), required in convex embedding. We first split the interior edge at the middle vertex to segments and then perturb one segment by one triangle away from the original (see Fig. 4.3(b)). Thus the region becomes three

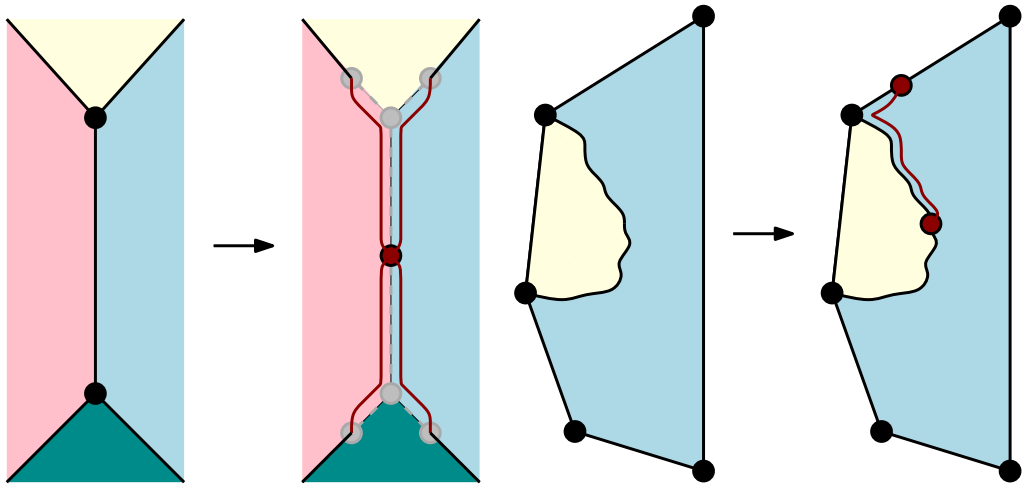

(a) edge pruning (b) edge splitting

Figure 4.3: Graph consistency modification. The nodes and edges in dark red are newly added. The ones in grey are deleted.

sided. The selections of the interior edge for splitting and the segment for perturbing are remembered for consistent operation over atlases. As shown in Fig. 4.3(b), the region f has two nodes v_{f_1}, v_{f_2} and graph-edges e_{f_1}, e_{f_2}. We need to refine these regions to guarantee the 3-connected (node degree ≥ 3) property required in convex graph embedding. We select the middle vertex v of e_{f_1} and select the closest vertex v_1 on the first neighboring edge e_1 of node v_{f_1}. Then similarly, we perturb the graph curve connecting v_1, v_{f_1} to v by one triangle away from the original. The original face f becomes triangular.

We first extract the unmatched graph-edges in both the source and target atlas graphs and run edge pruning operations in Case 1 to get consistent graphs, and then detect consistent two-edged regions and run edge splitting operations in Case 2. This guarantees the graphs are consistent with 3-connected property.

There are some special cases which may arise during the edge pruning: *(i)* If one of the nodes v_{ek} of the edge e is on the boundary and the other is inside, we select the node which is on the boundary (see Fig. 4.4(d)), otherwise some portions of

the boundary may go outside the domain. *(ii)* If both the nodes of the edge e are on the boundary, then for the boundary edges that are connected to the two nodes v_{ek}, instead of perturbing the connection, we just use the original graph-edge path (see Fig. 4.4(e)) as there is no other path outside the boundary. *(iii)* If there are multiple connected edges e_j to prune, an iterative edge pruning can be performed. We can first prune one edge, after that we detect if there is any edge to prune in the newly formed edge $e_j^{'}$. The procedure continues until there is no edge to be pruned. Alternatively, we can also select the middle vertex v of the multiple edges e_j considering all the e_js as one edge and select all v_{ik} for all e_j to connect to the middle vertex v of all e_js. So in the final pruning, node v in the refined graph will have more than 4 edges to connect (see Fig. 4.4(f)). Note, if node v does not have enough degree to connect, another node from the unmatched edge can be chosen or edges around v can be splitted.

4.4.2 Intrinsic Graph-Constrained Harmonic Map

We map the cortical surface M onto the convex subdivision domain Ω, $\phi : (M, G') \rightarrow (\Omega, \hat{G'})$, by minimizing harmonic energy (stretches) with the atlas graph constraints. The critical point of harmonic energy is a harmonic map. The energy is formulated as

$$\min\{E(\phi(v_i)) = \Sigma_{[v_i,v_j]\in E} w_{ij}(\phi(v_i) - \phi(v_j))^2, \forall v_i \in V\}, \tag{4.1}$$

where w_{ij} is the edge weight; in our method, we use the mean value coordinates [107] as edge weights.

We map the outer boundary of the brain surface to the unit circle. The discrete harmonic map in eqn. 4.1 can be computed by the convex combination map with the Dirichlet condition, where each interior vertex v_0 can be expressed as a linear

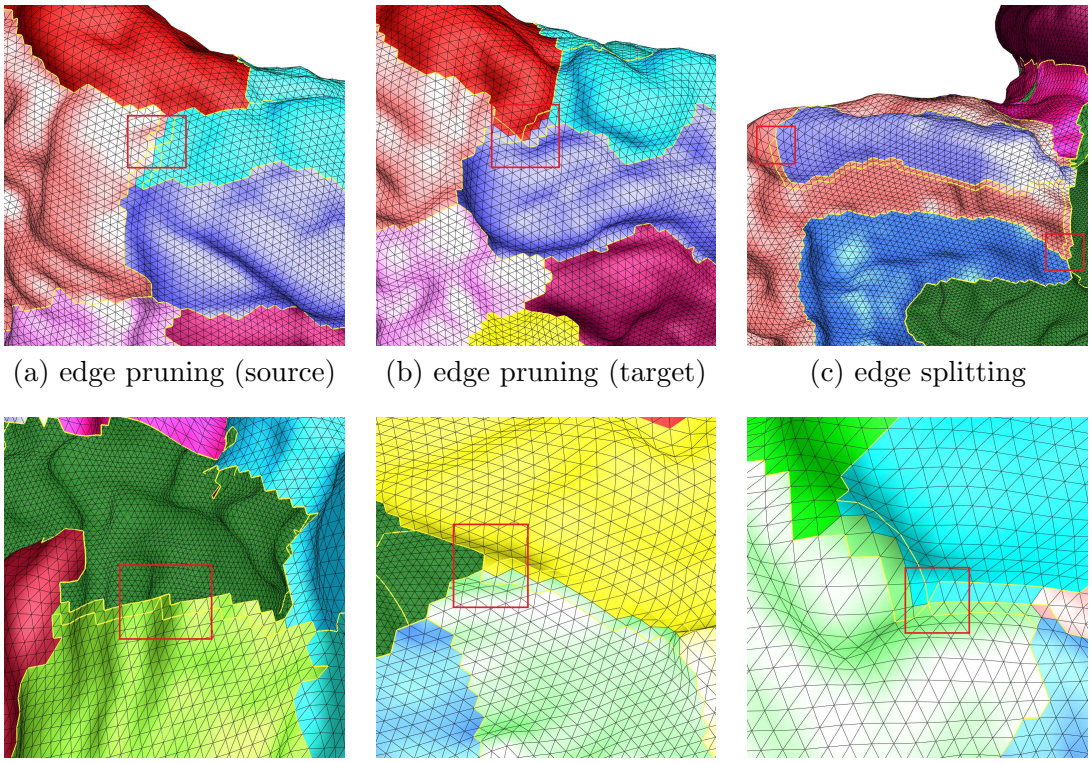

(a) edge pruning (source) (b) edge pruning (target) (c) edge splitting

(d) boundary case (e) boundary case (f) pruning multiple edges

Figure 4.4: Edge pruning, edge splitting, and special cases for graph refinement.

combination of its neighboring vertices v_i as follows

$$\begin{cases} v_0 = \sum_{i=1}^{k} \lambda_i v_i \quad i = 1, \cdots, k \\ \sum_{i=1}^{k} \lambda_i = 1 \\ \lambda_i > 0 \end{cases}, \tag{4.2}$$

where λ_i are the harmonic weights. For the convex combination map, we have the following lemma.

Lemma 1. *(Convex Combination map [136])Given a simply connected triangular mesh M and a convex domain Ω, if the map : $\phi : M \to \Omega$ is a convex combination map, i.e. for every interior vertex, it satisfy the conditions in Equation (4.2), and ϕ maps ∂M to $\partial\Omega$ homeomorphically, then ϕ is one-to-one.*

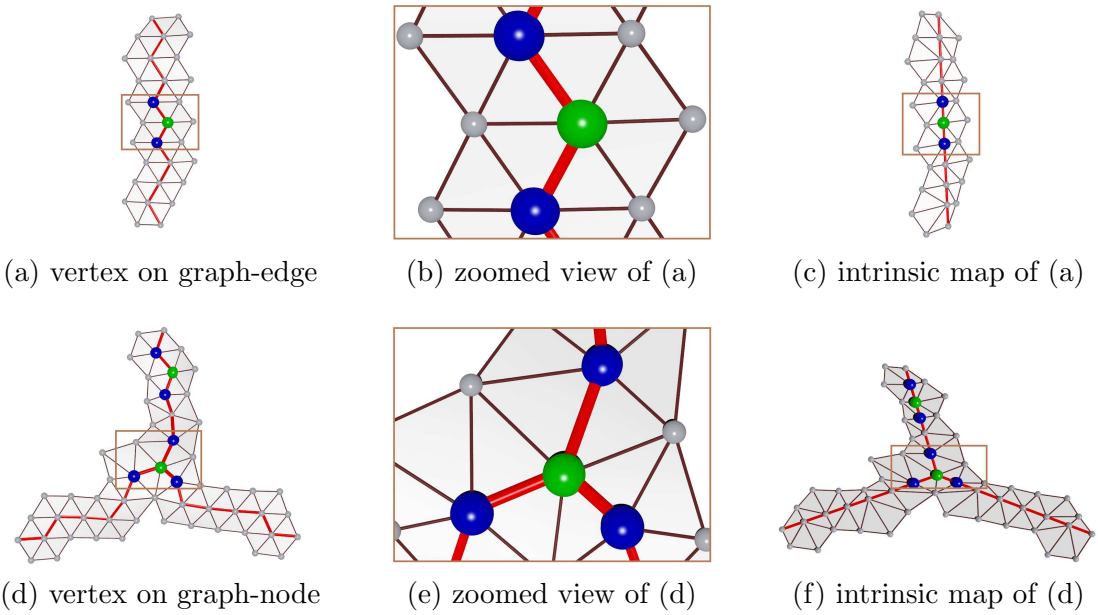

(a) vertex on graph-edge (b) zoomed view of (a) (c) intrinsic map of (a)

(d) vertex on graph-node (e) zoomed view of (d) (f) intrinsic map of (d)

Figure 4.5: Adaptive mean value coordinate. Top row and bottom row show the two cases of the vertex lying inside the interior of the graph-edge and graph-node, respectively. The blue points are the one ring graph neighborhood of the green ones.

For the cases $k = 2, 3$, the weights λ_i can be determined automatically by Equation (4.2); they are the barycentric coordinates. For the general cases $k > 3$, the mean value coordinate can be obtained by approximating the harmonic energy using the Circumferential Mean Value Theorem at each interior vertex [41]

$$\omega_i = \frac{tan(\alpha_{i-1}/2) + tan(\alpha_i/2)}{|v_i - v_0|}, \tag{4.3}$$

where the α_{i-1} and α_i are the adjacent angles in triangles $[v_{i-1}, v_0, v_i]$ and $[v_i, v_0, v_{i+1}]$, respectively.

We employ special handling to automatically and intrinsically map the curvy graph G' as a PSLG on the unit disk which can be used to simplify and improve methods of surface registration. To compute this map, we modify the mean value coordinate adaptively according to the atlas graph such that the convex combination map defined in Eqn. (4.2) satisfies the Circumferential Mean Value Theorem [41] at

every interior vertex, and it straightens the atlas graph to a PSLG in the canonical domain. The key observation is that all vertices move to the weighted barycenter of their one-ring neighbors during the harmonic minimization. For a vertex on the atlas graph, we define its *one-ring graph neighborhood* as its adjacent vertices lying on the graph while the *one-ring neighborhood* includes all adjacent vertices. For the vertices on the atlas graph, we utilize their one-ring graph neighborhood instead of one-ring neighborhood during the computation of the adaptive mean value coordinate, and the interior points of the graph curves will move to the linear interpolation of their two adjacent graph neighbors on the atlas curves instead, which will result in a PSLG in the canonical domain. Furthermore, the PSLG forms a convex subdivision of the 2D canonical domain. In detail, to compute the intrinsic harmonic map of graph constrained surfaces, we compute the harmonic weights adaptively as follows. If the vertex v_0 is

1. not on the graph, we utilize the mean value coordinate as the weight.
2. lying inside the interior of the graph-edge, the barycentric coordinate is applied to its one-ring graph neighborhood instead. Let v_1 and v_2 denote its two adjacent neighboring vertices on the graph. The adaptive harmonic weight is defined as $w_1 = \frac{|v_2 - v_0|}{|v_2 - v_0| + |v_1 - v_0|}$ and $w_2 = \frac{|v_1 - v_0|}{|v_2 - v_0| + |v_1 - v_0|}$.
3. the graph-node, the Circumferential Mean Value Theorem is applied to its one-ring graph neighborhood to compute the adaptive harmonic weight.

For the intrinsic harmonic map, we have the following theorem.

Theorem 1. *The intrinsic harmonic map, which maps the atlas graph to a PSLG in the canonical domain, is unique, globally optimal and diffeomorphic when the target domain is convex. Furthermore, the PSLG forms a convex subdivision of the 2D canonical domain.*

Algorithm 2: Intrinsic Graph-Constrained Harmonic Map

Input: A triangular mesh with graph (M, G)

Output: A mapping $\phi : (M, G') \to (\Omega, \hat{G}')$, such that $\hat{G}'$ is a convex subdivision on convex domain Ω.

1: Set weights w_{ij} of the edges in Eqn. 4.1 using adaptive mean-value weight.
2: Compute mapping using these altered weights of edges using energy minimization Eqn. 4.1.

For the vertices lying outside the atlas graph, according to the adaptive scheme, it is the same as the mean value coordinate defined in [41]. By using the one-ring graph neighborhood during the weight computation for the vertices lying on the atlas graph, and removing the pulling to other directions, the graph curves will be straightened to canonical shapes (straight line segments) in the intrinsic harmonic map, and the atlas graph will become a PSLG in the canonical domain. At the same time, the formulated harmonic energy remains to be convex, and each vertex can be expressed as a convex combination of its one ring neighborhood. According to Lemma 1, the intrinsic harmonic map is a diffeomorphism when the boundary is a convex polygon. Furthermore, it is unique and a global minima of the Dirichlet energy under the graph straightening constraints. Finally, the vertices on the atlas graph are expressed as the convex combinations of the vertices which are only on the graph. Thus, the PSLG is a 2D embedding in the canonical domain, and forms a convex subdivision.

4.4.3 Diffeomorphic Atlas-Constrained Registration

Registration is performed on the two convex domains. Given two cortical surfaces (M_1, G_1), (M_2, G_2) as the source and target to be registered, the goal is to find an optimal diffeomorphism $f : (M_1, G_1) \to (M_2, G_2)$, such that atlases G_1 and G_2 are aligned as constraint. If the graphs G_1, G_2 are not consistent, we modify them as

little as possible to be consistent, i.e., G_1', G_2', and then the registration becomes $f : (M_1, G_1') \to (M_2, G_2')$.

The registration employs the 3D-to-2D mapping strategy, which maps 3D surfaces to 2D canonical domains and then simplifies 3D surface registration problems to 2D ones. We first compute the intrinsic graph-driven harmonic maps $\phi_k : (M_k, G_k') \to (\Omega_k, \hat{G}_k')$, where G_k' are canonicalized to be planar convex subdivisions $\hat{G}_k'$ on the unit disk Ω_k. Then we compute the mapping $h : (\Omega_1, \hat{G}_1') \to (\Omega_2, \hat{G}_2')$ via a constrained harmonic map, followed by an operation η to relax the distortions introduced by atlas modification. Because consistent graphs have the same form of uniform embedding results, the two 2D domains $(\Omega_k, \hat{G}_k)$ can be aligned directly to generate the mapping h. Therefore, the registration $f = \phi_2^{-1} \circ \eta \circ h \circ \phi_1$, as shown in Diagram (4.4).

$$\begin{array}{ccc} (M_1, G_1) & \xrightarrow{f} & (M_2, G_2) \\ {\scriptstyle \phi_1}\downarrow & & \downarrow{\scriptstyle \phi_2} \\ (\Omega_1, \hat{G}_1) & \xrightarrow{h} & (\Omega_2, \hat{G}_2) \end{array} \tag{4.4}$$

With the refined consistent atlas graphs, the source (M_1, G_1') and target (M_2, G_2') are mapped onto the disk domains with interior convex subdivision by the above intrinsic harmonic map. We then register the two planar domains, $h : (\Omega_1, G_1') \to (\Omega_1, G_2')$, by minimizing the harmonic energy. We specify the positions of the boundary vertices (by interpolation) and the graph-nodes as the corresponding ones on the target, and set the combinations for the vertices on graph-edge only using adjacent edges on graph. For the surface registration, we have the following theorem.

Theorem 2. *The surface registration f is unique, globally optimal and diffeomorphic.*

As the registration f can be expressed as a combination of mappings $f = \phi_2^{-1} \circ h \circ \phi_1$, and the intrinsic parameterization ϕ_1 and ϕ_2 are proved to be unique,

Algorithm 3: Atlas-Based Cortical Surface Registration

Require: Two triangular meshes with atlas graphs $(M_1, G_1), (M_2, G_2)$
Ensure: A mapping $f : (M_1, G_1) \to (M_2, G_2)$
1: Check consistency of graphs: if $!(G_1 \sim G_2)$, then modify G_1, G_2 to G_1', G_2' respectively, such that $G_1' \sim G_2'$
2: Compute intrinsic graph-constrained harmonic map $\phi_k : (M_k, G_k') \to (\Omega_k, \hat{G}_k')$ such that $\phi_k(G_k') = \hat{G}_k'$, for $k = 1, 2$ using Algorithm 2
3: Compute $f := \phi_2^{-1} \circ h \circ \phi_1$

globally optimal and diffeomorphic by Theorem 1, we only need to demonstrate that the constrained intrinsic harmonic map h is unique, globally optimal and diffeomorphic. The detailed proof is described as follows. As we adopt the one-ring graph neighborhood during the weight derivation for the vertices on the atlas graph, the map h can be divided into two sequential steps. First, the atlas graphs are exactly aligned by the map h, where the graph-nodes of the source atlas graph $\hat{G}_1$ are mapped to the corresponding ones of the target atlas graph $\hat{G}_2$, and the interior vertices on the graph-edges in the source domain are mapped onto the target graph-edges automatically by constrained harmonic map. The interior vertices of the graph-edges in the source domain can slide along the corresponding graph-edges in the target domain. According to Theorem 1, the PSLG subdivides the canonical domain into convex subregions, which are then registered using the constrained harmonic maps. As the boundary of each convex subregion is a subset of the atlas graph, and the two atlas graphs are already exactly aligned, the problem of registering two corresponding subregion is reduced to the problem of mapping a 2D surface to a convex domain with fixed boundaries by a harmonic map, which is unique, globally optimal and diffeomorphic.

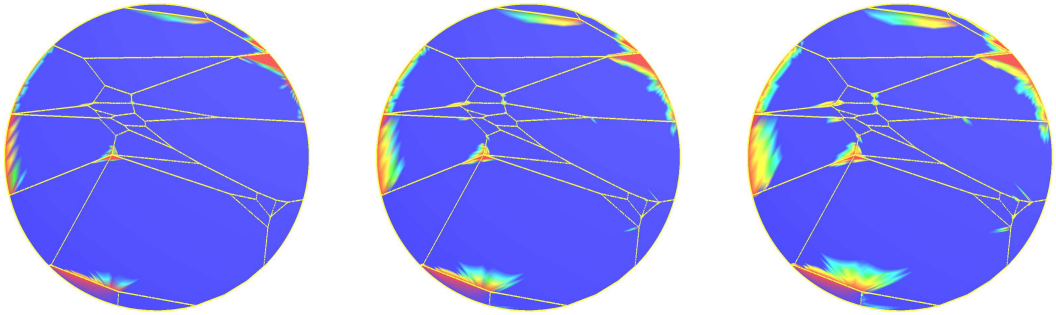

(a) 1-ring (b) 2-ring (c) 3-ring

Figure 4.6: Different levels of neighborhood and relaxation for brain cortical surface. Top row shows the relaxation scalar; the minimum value 0 is color coded with blue and the maximum value 1 is color coded with red.

4.4.4 Relaxation for Virtual Curves.

The virtual curve by atlas refinement may introduce fake alignment. Thus we relax the mapping h to lower the distortions. We first set $\eta = h$. At each step, we compute the gradient of vertex $v_i \in V_1$ as, $\triangle\eta(v_i) = \sum_{v_i,v_j \in E} w_{ij}(\eta(v_i) - \eta(v_j))$, and update the position of vertex $\eta(v_i)$ as,

$$\eta(v_i) \leftarrow \eta(v_i) - \lambda(v_i) \times \triangle\eta(v_i), \tag{4.5}$$

where $\lambda \in [0, 1]$ is a movement scalar function. In detail, (1) for the graph-nodes and the vertices on the graph-edges which are on both original and refined graphs of M_1 and boundary vertices, we set $\lambda = 0$ (i.e., exactly aligned by h and fixed); (2) for the vertices which are on virtual curves, we set $\lambda = 1$. To further smoothen the mapping at the end areas of virtual curves, we set $\lambda = \frac{d}{r}$ for the vertices inside, where d is the distance to endpoint, r is the radius of the range; and (3) for the resting mesh vertices, we set $\lambda = 1$ (i.e., with full movement). The size of local range needs to be carefully selected, depending on the length of the virtual curve. We have flipping check during the relaxation procedure, and reduce movement scalar or stop

moving if the movement produces flip. In this relaxation, each step reduces the constrained harmonic energy, and therefore this iterative process converges. The process stops when the energy minimization reduces to a certain limit or maximum number of iteration is reached. The composed mapping $\eta \circ h$ gives a diffeomorphism. Along with the ϕ_k, we can generate the diffeomorphic registration f between the 3D atlas-constrained cortical surfaces, under the optimality criterion of minimizing stretches.

Different neighborhood vertices (e.g., 1-ring, 2-ring, 3-ring, etc.) will produce different movement results. Figure 4.6 (a-c) shows the color-coded movement scalar, where 0 is the minimum scalar which is colored as blue, and 1 is the maximum scalar which is color coded as blue.

Algorithm 4: Relaxation

Input: A triangular cortical surface mesh with decorative graph (M, G), its parameterized 2D mesh, $\phi(\omega, \hat{G})$, neighborhood size (e.g. 1-ring, 2-ring, 3-ring etc.), V is the vertex set which includes all the mesh vertices, v_i

Output: Modified vertex set, $\eta(V)$

1: $\eta \leftarrow h$
2: $iter \leftarrow 0$
3: $E_{prev}(V) \leftarrow \infty$
4: Compute current energy, $E_{current}(V)$ using Eqn. 4.1
5: **while** $E_{prev}(\eta)$ - $E_{current}(\eta) < \epsilon \parallel iter <$ MAX_ITER **do**
6: **for** all vertices $\phi(v_i)$ of $\phi(\omega, \hat{G})$ **do**
7: Compute movement scalar, λ
8: Compute new position $\eta(v_i)$ using Eqn. 4.5
9: **if** new $\eta(v_i)$ does not generate flipping **then**
10: $\eta(v_i) \leftarrow$ new $\eta(v_i)$
11: **end if**
12: **end for**
13: $E_{prev}(V) \leftarrow E_{current}(V)$
14: Compute $E_{current}(V)$
15: $iter \leftarrow iter + 1$
16: **end while**

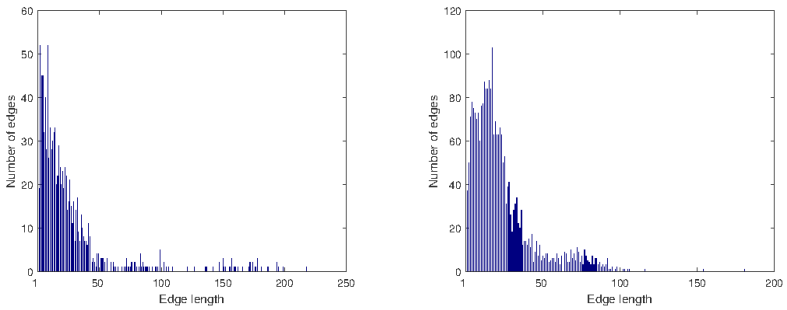

(a) LPBA40 (b) Mindboggle

Figure 4.7: Histograms of unmatched edges.

4.5 Experiments

The proposed algorithms were validated on two publics human brain databases with manual atlas labels: 1) 40 brains from LPBA40 [114] (processed by Brainsuite) and 2) 95 brains from Mindboggle [72]. The two databases have different human cortical labeling protocols and generates different atlases, so we perform registration within each own database. The cortical surfaces are denoted as triangular meshes with colored atlas regions.

4.5.1 Atlas Consistency Analysis and Refinement

With the consistent labeling protocol, each database generates the fixed number of cortical regions with its own anatomical interpolations, but there is no further consideration on the junctions (nodes of atlas graphs) of the neighboring anatomical regions. We extracted the cortical atlas graphs and analyzed them for both databases.

Each database corresponds to a consistent number of cortical regions, but has no further consideration on the junctions (graph-nodes) of anatomical regions. *Topologically*, we have done statistics on the two databases, as follows: 1) all the graphs are embedded on the hemispherical cortical surfaces and are intrinsically planar;

Table 4.1: Statistics on cortical atlas graphs of left hemispheres: G - original graph, G^c - maximum common subgraph, and G' - refined consistent graph over all brains.

Data	Mindboggle (lh)	LPBA40 (lh)
G-#node/edge/face	59-71/89-103/31	46-48/68-72/25
G^c-#node/edge/face	0/0/0	0/0/0
G'-#node/edge/face	25/47/23	19/40/22
#triangle, time	$293k$, 50 secs	$131k$, 20 secs
#avg unmatched edge	25.10	25.85
#avg two-edged face	0	1.175

2) LBPA40 data has at most 2 two-edged regions, violating 3-connected property, and Mindboggle data has none; and 3) atlas graphs are not consistent (isomorphic) among brains, and there is no common subgraphs in each data set, therefore the connection types at junctions are diverse. We further excluded the unmatched edges to find out the common subgraphs.

Geometrically, we analyzed the length of unmatched edges and modified the atlas graph on triangular meshes to solve Cases 1-2. The length here is computed as the number of vertices (hops) along the curvy edge based on the observation that the triangular mesh is relatively uniform. The histogram of the unmatched edge lengths within each database (see Fig. 4.7) shows that in most cases the differences of atlases are restricted in a local range. By edge pruning and splitting operations, the original regions won't disappear. For example, in Fig. 4.2, the consistent refined graph for brain pair $< B_0, B_1 >$ has 45 nodes, 70 edges, and 26 faces (same as the original). Table 4.1 gives the statistics of the numbers of edges, nodes, and regions of the original graph G, and the average numbers of node degree, two-edged regions and unmatched edges over all the brains in each database.

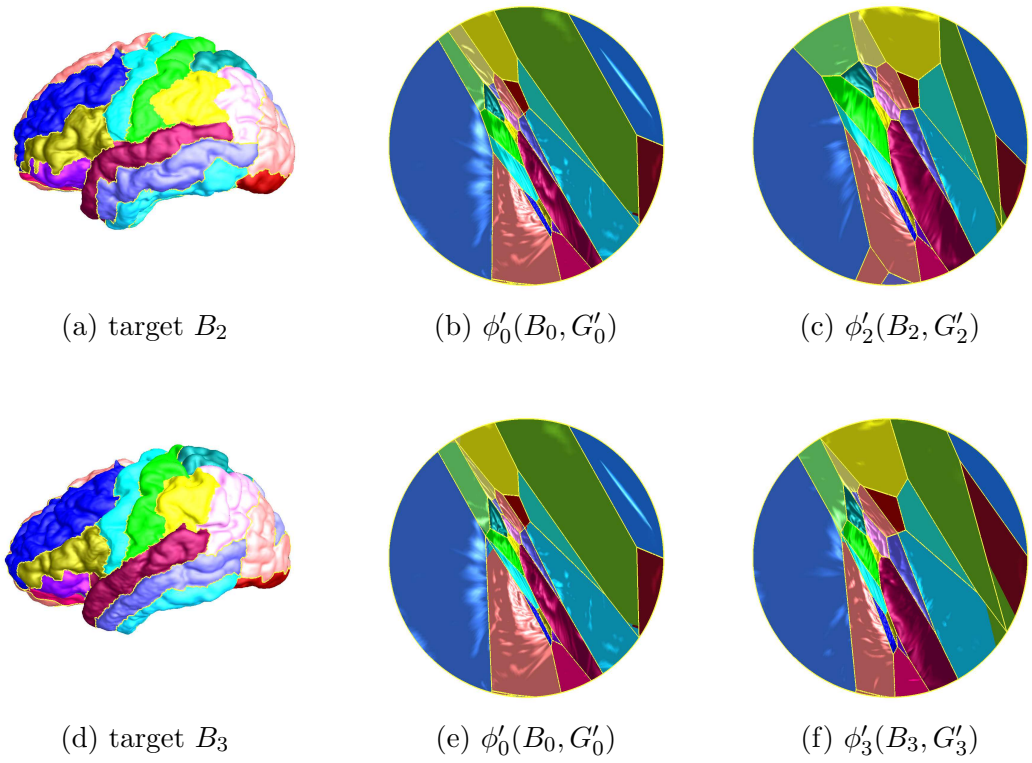

(a) target B_2 (b) $\phi_0'(B_0, G_0')$ (c) $\phi_2'(B_2, G_2')$

(d) target B_3 (e) $\phi_0'(B_0, G_0')$ (f) $\phi_3'(B_3, G_3')$

Figure 4.8: Registration for experiment I of brains B_0 to B_2 and B_3. Note that the parameterizations $\phi_0'(B_0, G_0')$ is different for these two cases as the refined graph is different.

4.5.2 Atlas-Constrained Brain Registration

We implemented the algorithms in C++ and use Matlab as sparse linear system solver. Tests were performed on a desktop with 3.7GHz CPU and 16GB RAM. All the computations are automatic, stable and robust for all the tests without human intervention. The method is efficient and practical. Table 4.1 gives the averaged running time. gives the averaged running time for registering one pair of cortical surfaces. The method is efficient and practical. Here, for illustration, we co-register four brains, (B_0, G_0), (B_1, G_1), (B_2, G_2), (B_3, G_3). We register B_0 (as a reference) to every other brain, to achieve the co-registration among all brains. Two ways

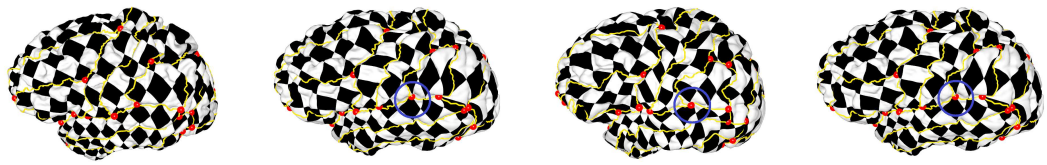

(a) source B_0 (b) target B_1 (c) target B_2 (d) target B_3

Figure 4.9: Visualization of registration for experiment I by refining atlases for each pair $< B_0, B_k >$, $k = 1, 2, 3$ separately. For the visualizations of texture mappings, we transfer the texture coordinates of disk harmonic map of B_0 to all other brains.

of atlas refinement are as follows: **I.** Refine atlases to be consistent for each pair separately. **II.** Refine atlases to be consistent for 4 brains together. We show the results of both the experiments below. We find out the unmatched edges among all atlases and prune them iteratively. By the registration, we can transfer the texture coordinates (e.g., using disk harmonic map parameters in Fig. 4.1) of B_0 to all other brains, then the one-to-one registrations can be visualized by the consistent texture mappings (see pink circle areas in Fig. 5).

Experiment I. We compute the refined atlas graphs between pairs of brains (e.g., (B_0, B_1), (B_0, B_2), (B_0, B_3), etc.) and register one to the other by parameterizing them to a common domain using the intrinsic graph-constrained harmonic map. Figure 4.9 shows the result of the registration for (B_0, B_1) that is used in Fig. 4.2. Figure 4.8 shows registration results between another two pairs,(B_0, B_2) and (B_0, B_3).

Experiment II. We compute the refined atlas graphs among multiple brains (e.g., (B_0, B_1, B_2, B_3)) which we use as a template graph to embed all the brains to a common domain. After that we compute the registration between the pairs in that common domain. For this case, we first find out the unmatched edges among all 4 brains iteratively. We start from (B_0, B_1) and subsequently identify which edges

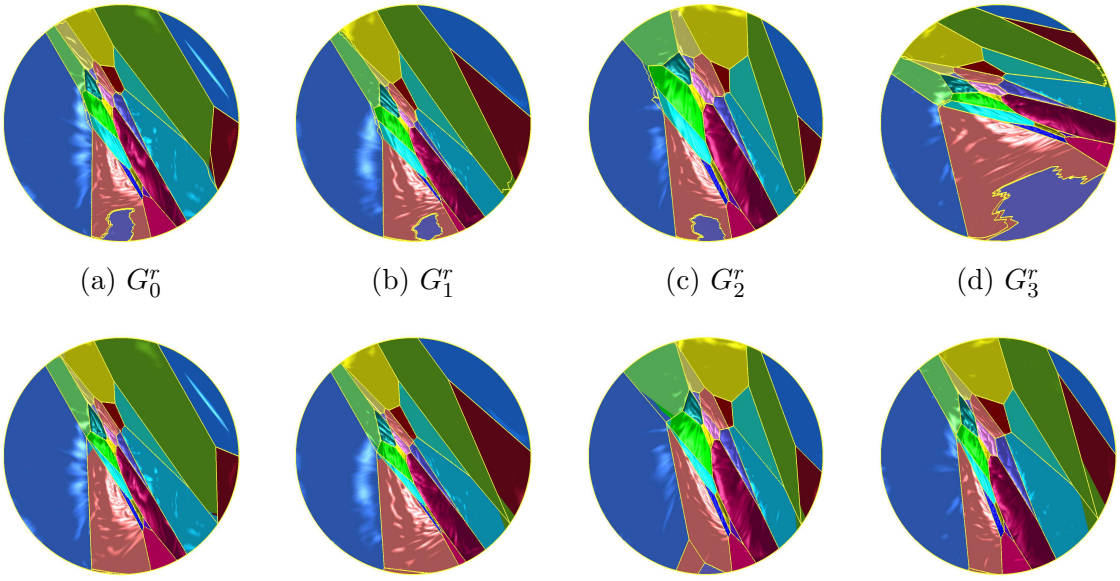

(a) G_0^r (b) G_1^r (c) G_2^r (d) G_3^r

(e) $\phi_0'(B_0, G_0')$ (f) $\phi_1'(B_1, G_1')$ (g) $\phi_2'(B_2, G_2')$ (h) $\phi_3'(B_3, G_3')$

Figure 4.10: Visualization of registration of B_0 to multiple brains, B_1, B_2, B_3 using the common refined graph with $f_i : (B_i, G_i') \rightarrow (B_0, G_0')$ for experiment II. Row 1: common refined graphs; Row 2: mappings with common refined graphs as constraints.

to be pruned for all the brains. The final refined graph is topologically same for all the brains. Figure 4.10 shows the registration results and figure 4.11 shows the visualization of registration by texture mappings.

4.5.3 Registration Accuracy.

Numerically, we compute the registration accuracy metric with the dice coefficient which measures the overlap between the regions M_k^i. It is defined as,

$$D_c(M_1, M_2) = 2 * \frac{\sum_i A(M_1^i) \cap A(M_2^i)}{|A(M_1)| + |A(M_2)|},$$

where A is the area function. The larger value indicates more accurate registration.

1. For the pair $< B_0, B_1 >$, we evaluate the performance under two cases of graph constraints: 1) the maximum common subgraph, and 2) the consistent refined

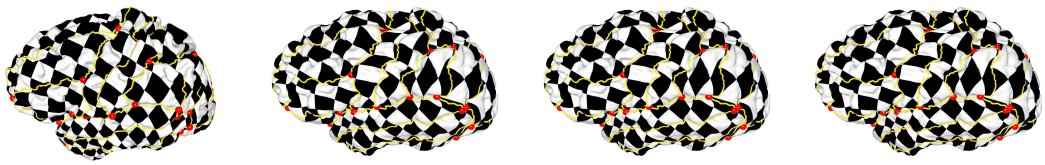

(a) source B_0 (b) target B_1 (c) target B_2 (d) target B_3

Figure 4.11: Visualization of registration by texture mappings for experiment II. We transfer the texture coordinates of disk harmonic map of B_0 to all other brains for the visualizing registration.

Table 4.2: Comparison of registrations with different labels of relaxation.

	Original	Ring 1	Ring 2	Ring 3
B_1	0.9582	0.9590	0.9589	0.9589
B_2	0.9604	0.9611	0.9610	0.9609
B_3	0.9625	0.9628	0.9628	0.9627

graphs, with the registration accuracy D_c = 0.8832,0.9582 (without relaxation), respectively. This shows that the refined graph registration performs better and verifies the intuition.

2. For the three pairs $< B_0, B_k >$, we test different smoothness levels in relaxation by selecting 1-ring (no interior vertices, no control on smoothness), 2-ring and 3-ring local ranges. For example, for the pair $< B_0, B_1 >$, D_c = 0.9590,0.9589,0.9589, for 1, 2, 3-ring respectively. The 1-ring gives the highest result due to less restriction to the movement. Registration with relaxation shows better results than the initial one. We choose the 2-ring one to balance smoothness and accuracy. Table 4.2 shows the registration results without relaxation and with 1-ring, 2-ring, 3-ring movements. Table 4.2 shows the registration accuracy with different relaxation levels.

3. For the three pairs $< B_0, B_k >$, we compare our methods **I**, **II** with 2-ring relaxation with the well-known FreeSurfers method [36]. In all cases, our registration method demonstrates better results (see Tab. 5.6).

Table 4.3: Comparison of registrations.

Brain Pairs	(B_0, B_1)	(B_0, B_2)	(B_0, B_3)
Dice coeff. (Freesurfer)	0.8123	0.8820	0.8838
Dice coeff. (Ours, Exp. **I**)	0.9589	0.9610	0.9628
Dice coeff. (Ours, Exp. **II**)	0.9595	0.9560	0.9612

4.5.4 Discussion

Property of the registration. The proposed registration aligns the common graph-edges as much as possible and at the same time minimizes the harmonic energy, which preserves local shapes as much as possible under the constraints. *Topologically*, if the brains have no consistent atlas graphs, in theory, there will be no solution to atlas-based registration. In our tests, atlas graphs were verified to have partial graphs in common, but most regions are combined together. It is still challenging to find the registration for the common areas for each anatomical region within the combined regions. We introduced the edge pruning and splitting operations to register the brain areas and align the atlas graphs as much as possible. The thin-sliced neighborhoods around unmatched nodes/edges are merged to existing regions or separated as new regions (see Figs. 4.3). *Geometrically*, The introduction of one-triangle wide pieces (the smallest unit in triangular mesh) minimizes the distortions from the original atlas and preserves atlas geometry on cortical surface as much as possible. The relaxation procedure reduces these distortions.

The proposed method is rigorous, based on the classical classical the harmonic map with linear convex subdivision constraints with uniqueness and diffeomorphism guarantee. Compared with other works, it is novel to intrinsically map cortical surface with atlas graph to a convex subdivision domain, and register brains using the whole cortical atlases as constraint. Practically, the algorithms are easy to

implement, practical and efficient, and robust to geometry or topology noises. With this framework, some sophisticated methodology and optimization criteria, e.g., the minimization of angle or area distortions, can be introduced to refine the registration which will be explored in our future work.

Potentials for biomedical research. The graph-driven atlas-based brain registration will help brain morphology study and monitor anatomy progression, and has potential to deal with large-scale dataset to explore the relationship of the brain anatomical structure to diseases, such as Alzheimer's disease which will be discussed in the next chapter. This anatomy-aware framework is general for other biomedical data such as human facial surfaces for their anatomy registration and classification.

4.6 Summary

In this chapter, we present a novel method to register cortical surfaces with atlas constraints. We first perform atlas consistency check and refinement, then map the surfaces to 2D convex subdivision domains by the intrinsic graph-driven harmonic maps, and finally compute the registration over the 2D domains, followed by a relaxation procedure. The mapping is unique and diffeomorphic. The whole process is automatic. Experiments on co-registering brains in two public databases have demonstrated the efficiency and practicality of the algorithms. The registration method has potential to deal with large-scale brain morphometry analysis for medical and cognitive problems, e.g., disease classification, behavioral analysis, etc. In the next chapter, we will show the application of this registration framework for Alzheimer's disease classification.

CHAPTER 5

AD CLASSIFICATION USING ATLAS-CONSTRAINED BRAIN REGISTRATION

5.1 Introduction

Many psychological diseases affect the structure of the brains which can be detected by analyzing the structural or geometric changes of the brain. Brain surface registration provides a robust way to establish a one-to-one correspondence between the brains to measure the changes for finding out any abnormalities in the brain due to the diseases. The registration process is generally used to define shape similarity metrics among the brains for group analysis to identify abnormal groups. Alzheimer's disease (AD) is a well-known disease which shows significant geometric changes in the brain cortical surface. In this chapter, we present a framework for Alzheimer's disease (AD) classification using the atlas-constrained brain registration described in the previous chapter.

First, we apply the atlas constrained brain registration procedure to co-register the brains. We select one brain as the source and register that to all other brains. Then we compute the same kind of geometric attributes for each brain by interpolating the attributes from the target brain to the registered brains. After that, we apply supervised learning algorithms to classify healthy control subjects (CTL) and subjects with AD. For the experiments, we took 50 CTL and 50 patients with AD from the Alzheimer's disease neuroimaging initiative (ADNI) dataset, and apply K-nearest neighbor(K-NN), support vector machine (SVM) and random forest (RF) classifiers for the classification. For K-NN and SVM, the result is cross validated with K-fold cross-validation and for random forest out-of-bag (OOB) prediction er-

ror is used to compute the accuracy. The result shows a classification rate of 88.0% using K-NN algorithm with 10-fold cross-validation.

5.2 Background and Motivation

Human brain goes through many biological changes at different stages of brain development. Changes may occur due to the growth of the brain, tissue loss or gray matter or white matter reduction due to some psychological disorders or diseases, development of tumor inside the brain, synaptic connection loss due to aging or for other diseases. It is well known that biological changes of any kind also changes the geometric structures of the brain which in turn affects the geometric structures or shapes of the cortical surface (outer layer of the brain). Different diseases may affect different parts of the brain, sometimes the changes propagate throughout the whole brain, and result in shape changes for a large portion of the cortical surface or the whole surface.

Although the changes are obvious, due to high complexity and convoluted geometry of the brain, capturing these changes is not a trivial task. In many cases, sophisticated geometric analysis methods are required to calculate the group difference with the most discriminating ability. Among the attributes that are used, the most common attributes are cortical gray matter and white matter thickness, area, volume, surface normal, curvature, sulcal depth, etc. In some cases, several geometric attributes, e.g., normal, curvature, area, etc. are combined to compute an amplified shape measure. Some approaches propose different types of shape measures using different surface mapping approach. Some approaches compute the shape metrics by mapping the genus-0 closed brain surface to a sphere or a region (normally unknown or black region) is removed to make the surface open and mapped to a disk. Region-based approaches to classification have been used previ-

ously by some researchers for AD classification [25, 47] where the similarity metric is computed based on different geometric attributes of some cortical regions, e.g., entorhinal, hippocampal, supramarginal, etc. Other approaches use the statistics on the whole cortical surface, often try to find out experimentally which kinds of attributes or attributes of which regions are the most significant discriminators for the classification.

This work is motivated by the atlas-constrained brain registration work which provides a rigorous way to co-register the brains by the best possible way of aligning the cortical regions and develop similarity metric based on the per-vertex attributes of the cortical surfaces. The advantage of this method is that different geometric attributes can be used for the vertices and shape difference can be computed for the whole brain surface or some specific regions of the brain. The method can also be used to find out which attributes are the most significant discriminator or the attributes of which regions are most affected due to AD. As the atlas-constrained brain registration method can guarantee optimal alignment of the cortical region, the method can be used to define more optimal shape metrics for the classification.

5.3 Approach Overview

The process uses the source to target brain registration technique described in the previous chapter. MRI volume images of the brains are parcellated through automated pipeline to extract cortical surfaces with atlas map. Among the brains, one brain is selected as the source, and it is registered to all other target brains in the dataset. After the registration, all the brains will have one-to-one correspondence. Using the one-to-one correspondence, vertex wise geometric attributes of the target surfaces are interpolated and assigned to the registered surfaces.

After that, we use vertex to vertex attribute distance of the source brain and target (registered) brains to compute the shape similarity metrics for the brains; the distance from source to source is considered 0. We use the distance as features for the brains in learning based classification algorithms to classify brains with K-NN, SVM, and RF algorithms. The models are cross validated with K-fold cross-validation. We apply different strategies to select the best set of features to use in classification.

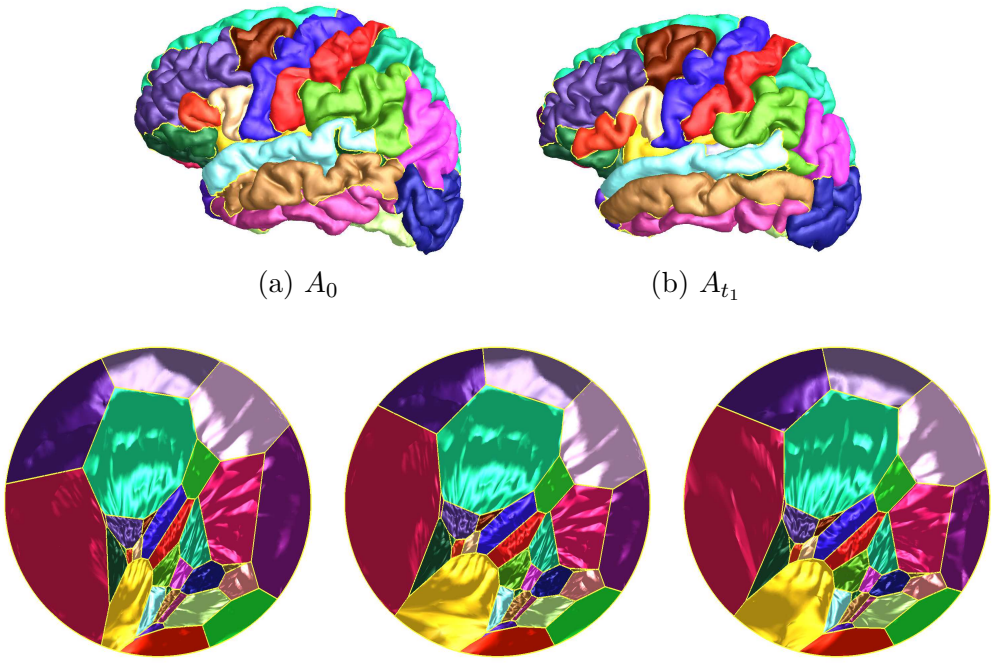

(a) A_0 (b) A_{t_1}

(c) $\phi_0(A_0, G_0')$ (d) $h(A_0, G_0')$ (e) $\phi_{t_1}(A_0, G_0')$

Figure 5.1: Registration of two AD brain surfaces. Top row shows the parcellated source brain surface and a target brain surface. (c) and (e) show atlas-constrained mappings with refined graph of A_0 and A_{t_1} respectively, (e) shows atlas-constrained registration of A_0 to A_{t_1}

.

5.4 Computational Algorithm

The computational algorithm has three main steps, (i) register the source brain surface to all other brain surfaces, (ii) compute and interpolate the attributes of the

target to the registered surface, and (iii) classify brains using supervised learning methods.

5.4.1 Atlas-Constrained Brain Registration

The method uses one brain surface, $A_0 = (V, E, F)$, as the source, and it is registered to all other target brain surfaces, $A_{t_k} = (V, E, F), k = 1, 3...n-1$, where n is the total number of brains using atlas-constrained brain registration described in 4.4.3. The process follows the graph-refinement, computing intrinsic graph-constrained mapping and registration. The registration process generates one-to-one correspondence between the vertices of the brain surface pairs. As the same source is registered to all the brains, the process creates one-to-one correspondence among all the registered brains. Figure 5.1 shows an example of registration between two brains.

5.4.2 Interpolation of the Attributes

After the registration, the deformed source coordinates can be interpolated using the barycentric coordinates from the faces of the target. This process maps each vertex of the source to another vertex in the deformed source (target). The geometric attributes of the target can be interpolated using the same process. For this, same kind of attributes are computed for each vertex of each surface. Attributes may include area, curvature, volume, thickness, sulcal depth, different curvature metrics, etc. After that, the geometric attributes associated with each vertex are interpolated from the target to the registered surface using the same barycentric coordinates.

5.4.3 Classification using Supervised Learning

After computing one-to-one correspondence and interpolation, each brain surface will have the same set of vertices with each vertex having the same set of attributes.

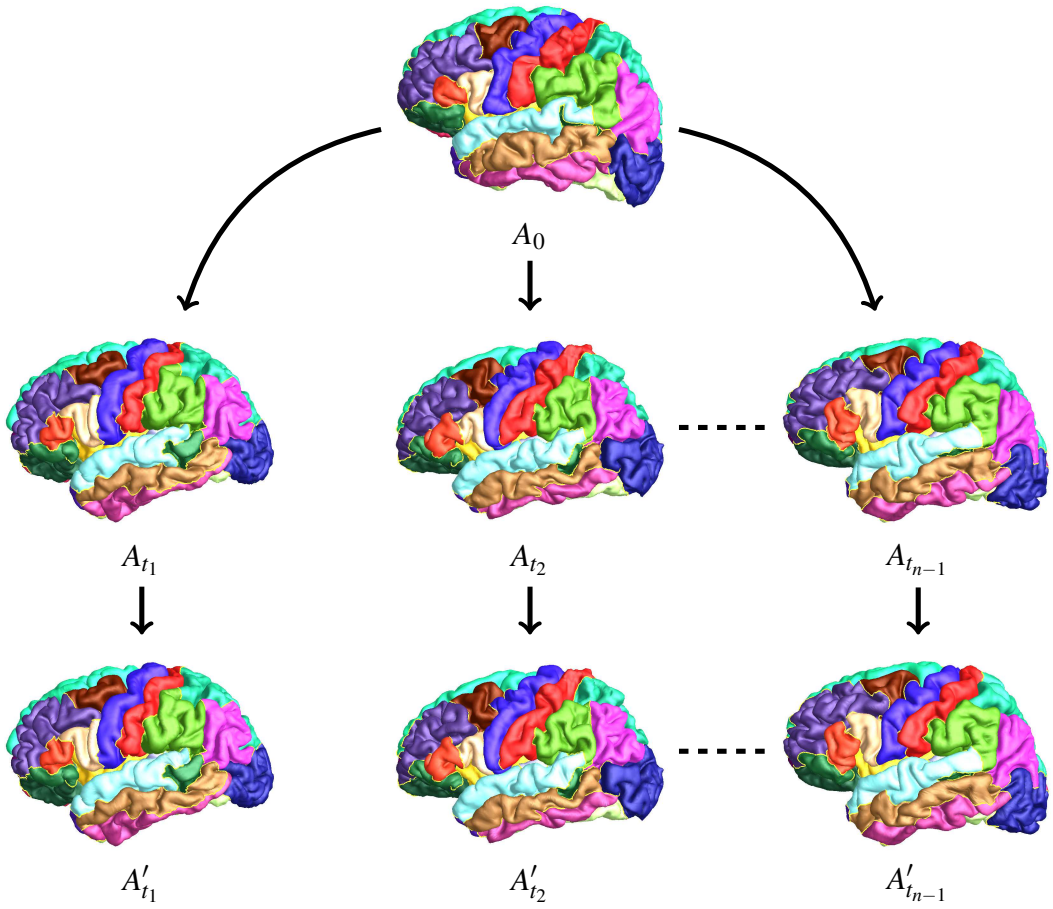

Figure 5.2: AD brain registration pipeline; source brain A_0 is registered to brains, $A_{t_1}, A_{t_2}...A_{t_{n-1}}$. The corresponding deformed surfaces are A'_{t_1}, $A'_{t_2}...A'_{t_{n-1}}$; the attributes of the vertices are interpolated from the target to the deformed surfaces. All the deformed surfaces have the same set of vertices.

Vertex attributes are used to compute features for each brain. We used two strategies to use the features. First, we use all attributes for all vertices as the features for the brain. Another strategy is to compute the region based attribute distance between the source brain and the registered brain, and use this as the features for the registered brain; we used Euclidean distance between the brains. For source, A_0, and target, A_{t_i}, then for region r and attribute $attr$, the distance between them for region r is computed using the following equation,

$$d_r{}^{attr}(A_0, A_{t_i}) = \sum_V ||\text{attr}(v_0) - \text{attr}(v_{t_i})||^2, \tag{5.1}$$

where V is the set of vertices.

After this, supervised learning methods are used to classify the brains. For this, the data is divided into two sets, (1) training set which is used to train the model of the supervised learning algorithm and (2) test set which is used to measure the performance of the model.

5.5 Experiments

We applied the proposed registration method on ADNI dataset to classify AD patients from normal patients. The results are described below.

5.5.1 Brain Processing and Data Preparation

Data source. Data used in the preparation of this article were obtained from the Alzheimer's Disease Neuroimaging Initiative (ADNI) database (adni.loni.usc.edu). The ADNI was launched in 2003 as a public-private partnership, led by Principal Investigator Michael W. Weiner, MD. The primary goal of ADNI has been to test whether serial magnetic resonance imaging (MRI), positron emission tomography (PET), other biological markers, and clinical and neuropsychological assessment can be combined to measure the progression of mild cognitive impairment (MCI) and early Alzheimer's disease (AD). For up-to-date information, see www.adni-info.org.

Data preparation. We processed a total of 100 brains from the ADNI dataset. We processed the same number of brains for both groups to remove any bias during classification. We processed 50 brains with AD and 50 CTL brains (Age: AD: 56.5 - 86.7, CTL: 59.9 - 89.6; MMSE score: AD: 20 - 27, CTL: 26 - 30). All the brains were processed by Freesurfer's [36] automated pipeline to generate parcellated

surfaces. Freesurfer parcellated brains in 36 regions [30], which in our experiment we numbered from 0, 1,...35. We cut off the region named unknown region (numbered 0) for registration, so we have the attributes for 35 regions. For registration, we randomly select one brain as the source, and register that to all other 99 brains (see Fig. 5.2). After the registration, all the brains will have one-to-one vertex correspondence. We used a total of 17 attributes for each vertex. The attributes are, (1) area on the pial surface, (2) area on the mid cortical surface, (3) Gaussian curvature on the white surface, (4) Gaussian curvature on the pial surface, (5) average curvature on the white surface, (6) sulcul depth on the white surface, (7) cortical thickness on the white surface, (8) cortical volume on the white surface, (9) bending energy (BE) on smooth white matter surface (smoothwm), (10) curvedness (C) on smoothwm, (11) folding index (FI) on smoothwm, (12) mean curvature (H) on smoothwm, (13) Gaussian curvature (K) on smoothwm, (14) maximum curvature (K_1) on smoothwm, (15) minimum curvature (K_2) on smoothwm, (16) sharpness (S) on smoothwm, and (17) atlas region. Mean curvature, H is defined as $1/2 \times (K_1 + K_2)$; Gaussian curvature, K is defined as $K_1 \times K_2$; Curvedness, C is defined as, $\sqrt{\frac{K_1^2 + K_2^2}{2}}$; bending energy, BE is defined as $K_1^2 + K_2^2$; folding index, FI is defined as $|K_1| \times (|K_1| - |K_2|)$ [102]. The attributes are interpolated from the target to the registered surfaces using the correspondence from the registration process.

5.5.2 AD Classification

For the classification purpose, we created two types of data, *Type 1* and *Type 2*, and applied classification algorithms separately on both types. For both types, we applied K-NN and SVM for classification. We used Matlab implementation of both the algorithms. The result is cross validated with K-fold cross-validation, where the value of K is chosen to be 5, 7, 9, 10, etc. Other larger folds have not been used as

that creates folds with more training data and less testing data which may introduce bias in prediction. For all tests, the training and testing sets are chosen randomly to prevent bias. The value of K-NN parameter, 'K', and SVM parameters, 'Boxconstraints' and 'Kernelscale' were obtained by using the Bayesian hyper-parameters optimization [123] process. Table 5.4 shows the selected parameters for SVM and K-NN for different experiments. For SVM we used different types of kernel, e.g., 'rbf', 'linear', 'polynomial', etc. As the Type 2 data provides better result, we selected that for further investigations. We applied different feature selection algorithms to select the most significant features for classification using Type 2 data. We also applied random forest algorithm with different feature selection algorithms for Type 2 data.

Type 1 data. In this type, we used each vertex as an independent variable and use all of the above 17 attributes for each vertex. So for each brain, we had a total of $v_n * 17$ attributes, where v_n is the total number of vertices which is same for all surfaces after the registration. The Euclidean distance between the attributes of the surfaces are used to measure similarity between the two surfaces. We noticed that not all of these 17 attributes are positively correlated to classification and may sometimes result in wrong classification. If we use all of the above attributes for the vertices, then the maximum classification rate with K-NN is only 50.0% and 68.18% for SVM algorithm. The reason behind this poor classification rate is that not all the attributes are positively correlated to the classification and some attributes of some regions may differ due to a different reasons other than Alzheimer's effect.

To identify which features are most useful and improves classification rate, we search over these 17 attributes. We experimented by selecting all combinations of 5,6, or 7 attributes from these 17 attributes. Table 5.1 show the summary of the experiments. Among the different number of folds, in general, 10-fold cross

Table 5.1: Classification using type 1 data. Selected attributes have been expressed with the numbers as described in the data preparation section.

No of feat.	Selected attributes	K-NN/SVM(%)			
		5-fold	7-fold	9-fold	10-fold
all	all	45.0/48.0	42.4/68.1	40.9/60.60	50.0/65.0
5	(2,3,5,6,7)	75.5/77.0	80.30/81.5	81.5/75.5	83.0/80.0
6	(2,3,5,6,7,10)	77.0/78.5	80.30/80.30	80.30/75.5	84.0/81.0
7	(1,3,5,6,7,10,12)	72.0/77.0	80.30/78.5	75.75/75.75	80.0 /81.5

validation provides better result in most of the cases. The best result for Type 1 data is 84.84% using K-NN classifier with 10-fold cross-validation.

Type 2 data. We computed the distance between the source and the registered source for all the 17 attributes for each region (total 35 regions excluding the black/unknown region, as obtained by Freesurfer) and used those as the features for the classification. The source brain here is used as the reference and all the distance metrics of the source are 0. For the attribute region, we assign 0 for the similarity and 1 otherwise; for all other attributes, we used the Euclidean distance using eqn. 5.1. Therefore, we get a total of $35 \times 17 = 595$ features for the 35 regions. (ii) For each region, we compute the distance between all the (17) features. First, we run the classification using all these features using K-NN and SVM algorithm. The maximum classification rate that we get is 74.0% for K-NN with 7-fold and 77.0% for SVM with 10-fold validation.

As the type of features is large, we use feature selection strategy for reducing the number of features. To identify which features are most significant for classification, we used three types of feature selection algorithm: (1) forward sequential feature selection (FSFS) algorithm [73] which is a wrapper approach to select important features to improve classification accuracy, (2) correlation based feature selection (CFS) [56] algorithm which selects features that are highly correlated for predicting

the class labels but have low intercorrelation between themselves, and (3) VSurf [46] which selects the important variables based on random forest algorithm. We used Matlab implementation of FSFS, *sequantialfs*, Weka implementation of CFS *cfssubsetEval*, and R implementation of VSurf, *vsurf* package. For FSFS, we selected a total of 200 features out of these 595 features. After that, we searched over the 200 features incrementally to identify the best combination of features for the classification..

Table 5.2 show the result of the classification using K-NN and SVM algorithm with K-fold cross validation, for K = 5,7,9,10. For FSFS, we only show the result for the number of selected features which produce the best result and fig. 5.4 shows the complete graphs of classification result using a different number of features (1-200). Also for FSFS, the number of selected attributes that provide the best result is not the same for different folds. So for this algorithm, we show the number of selected attributes besides the classification rate.

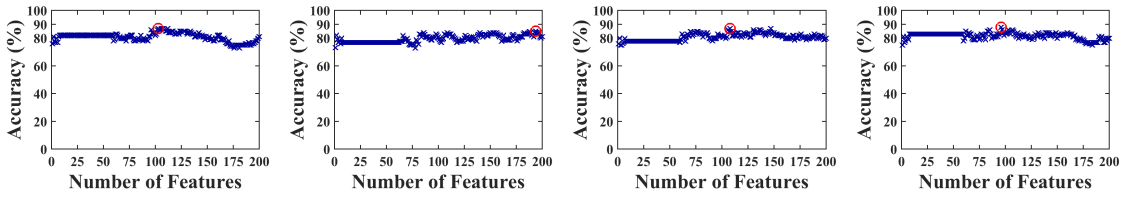

Figure 5.3: Result of feature selection using FSFS with K-NN for 5-fold, 7-fold, 9-fold, and 10-fold cross validation

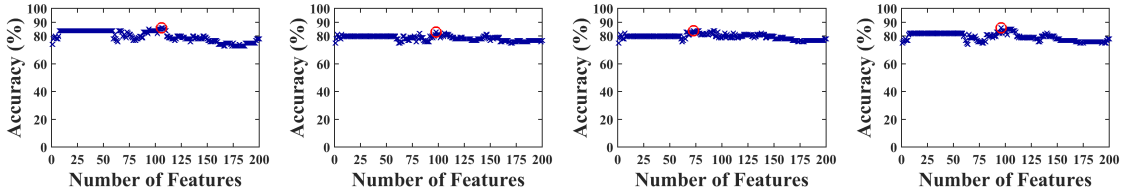

Figure 5.4: Result of feature selection using FSFS with SVM for 5-fold, 7-fold, 9-fold, and 9-fold cross validation.

Table 5.2: Classification using type 2 data.

Feat. selection algo./ Number of feats.	K-NN/SVM(%)			
	5-fold	7-fold	9-fold	10-fold
all	70.0/75.0	74.0/74.0	73.0/75.0	71.0/77.0
FSFS/98 – 194	87.0(103)/ 86.0(106)	85.03(194)/ 83.0(98)	86.95(108)/ 84.0(73)	88.0(98)/ 86.0(98)
CSF/16	78.0/79.0	81.0/81.0	80.30/80.0	81.5/81.0
VSurf/3	80.0/82.0	77.0/79.0	80.97/80.0	81.0/82.0

The classification accuracy for SVM is 86.0%, and accuracy for K-NN is 88.0% with 10-fold cross-validation. Both algorithms achieved the best accuracy with 98 features. We further computed the false positive rate (FPR) and false negative rate (FNR) for the best results for both K-NN and SVM. For K-NN, false positive rate, FPR = 8.0% and FNR = 20.0%, and for SVM, FPR = 8.0% and FNR = 20.0% (see Tab. 5.3). To visualize the trade-off between the true positive rate (TPR) and FNR, we used Receiver Operating Characteristic (ROC). Figure 5.5 shows the ROC curve for SVM and K-NN; area under curve (AUC) value for SVM is 0.856, and for K-NN is 0.882.

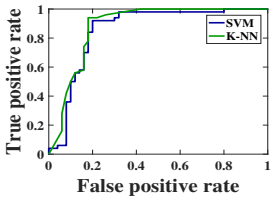

Figure 5.5: ROC curves.

Algorithm	FPR%	FNR%	Accuracy%
K-NN	6.0	18.0	88.0
SVM	8.0	20.0	86.0

Table 5.3: Accuracy with K-NN and SVM.

Table 5.4 shows the selected parameters for K-NN (number of neighbors, and distance metric) and SVM (Kernel Type, BoxConstraints, and KernelScale) for classification using type 1 and type 2 data. The parameters were selected by optimizing the parameters using Bayes optimizer.

Table 5.4: Parameters used for K-NN and SVM with 10-fold cross validation.

		K-NN		SVM		
	Parameters	n	dist	KernelType	BoxConstraints	KernelScale
Type 1	All	3	Euclidnean	rbf	2.11	6.22
	Var Select	3	Euclidnean	rbf	2.11	6.22
Type 2	All	7	Euclidnean	rbf	0.44	34.62
	FSFS	5	Euclidnean	rbf	2.71	3.63
	CFS	5	Euclidnean	rbf	0.89	0.73
	VSurf	5	Euclidnean	rbf	0.69	0.85

We also used random forest algorithm for Type 2 data with feature selection using FSFS, CSF and VSurf algorithm. Instead of using K-fold cross-validation, we used out-of-bag (OOB) error to calculate the prediction error. OOB error is the average estimate of the prediction error for each sample from the original dataset. While predicting OOB error for a sample, RF does not consider the bootstrap datasets which contain that specific sample. Then we calculate the classification error from OOB using (1-OOB)*100.

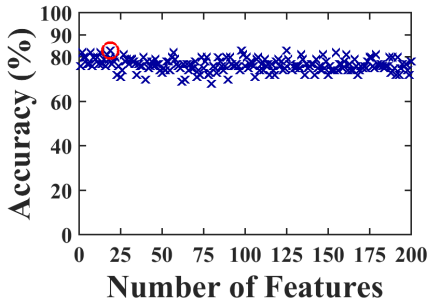

Figure 5.6: RF with FSFS.

Feat. selection algo.	Number of feats.	Accuracy
-	all	78.00
FSFS	19	83.0
CFS	16	79.0
VSurf	3	80.0

Table 5.5: RF accuracy.

Table 5.5 shows the result using random forest classification. Figure 5.6 shows the FSFS results for different number of selected variables. The best accuracy is 89.4% using Vsurf algorithm

Table 5.6: Classification accuracy comparison with Freesurfer registration using same set of features

Reg. method	SVM%	K-NN%%
Freesurfer	82.0	78.0
Ours	86.0	88.0

Comparison We compared the AD classification accuracy using our method with the Freesurfer's registration method. We used the same setting for both SVM and K-NN for which we got the best results, and used the same number of features with the same number of anatomical atlas regions (excluding the black/unknown region as before). Using the same 98 features, classification accuracy using Freesurfer registration is 82.0% with SVM, and 78.0% with K-NN (see Tab. 5.6). For both algorithms, our registration method performs better as it provides better alignment of the similar atlas regions in the registration process.

5.6 Summary

In this chapter, we present a framework for classifying AD patients from normal patients based on atlas-constrained brain registration technique. Per-vertex attributes are used for the surfaces to define the similarity metric by computing the Euclidean distance between the features of the source surface and the registered surface. One surface is selected as the source, and it is registered to all other surfaces. We used different machine learning classifiers and feature selection algorithms for the classification. Among the algorithms, K-NN classifier ($K = 5$) with 10-fold cross validation gives the best result (88.00%). The proposed surface registration based framework is general and can be explored for other disease or psychological behavior classification in future.

Acknowledgment

Data collection and sharing for this project was funded by the Alzheimer's Disease Neuroimaging Initiative (ADNI) (National Institutes of Health Grant U01 AG024904) and DOD ADNI (Department of Defense award number W81XWH-12-2-0012). ADNI is funded by the National Institute on Aging, the National Institute of Biomedical Imaging and Bioengineering, and through generous contributions from the following: AbbVie, Alzheimer's Association; Alzheimer's Drug Discovery Foundation; Araclon Biotech; BioClinica, Inc.; Biogen; Bristol-Myers Squibb Company; CereSpir, Inc.; Cogstate; Eisai Inc.; Elan Pharmaceuticals, Inc.; Eli Lilly and Company; EuroImmun; F. Hoffmann-La Roche Ltd and its affiliated company Genentech, Inc.; Fujirebio; GE Healthcare; IXICO Ltd.; Janssen Alzheimer Immunotherapy Research & Development, LLC.; Johnson & Johnson Pharmaceutical Research & Development LLC.; Lumosity; Lundbeck; Merck & Co., Inc.; Meso Scale Diagnostics, LLC.; NeuroRx Research; Neurotrack Technologies; Novartis Pharmaceuticals Corporation; Pfizer Inc.; Piramal Imaging; Servier; Takeda Pharmaceutical Company; and Transition Therapeutics. The Canadian Institutes of Health Research is providing funds to support ADNI clinical sites in Canada. Private sector contributions are facilitated by the Foundation for the National Institutes of Health (www.fnih.org). The grantee organization is the Northern California Institute for Research and Education, and the study is coordinated by the Alzheimers Therapeutic Research Institute at the University of Southern California. ADNI data are disseminated by the Laboratory for Neuro Imaging at the University of Southern California.

CHAPTER 6

INTRINSIC GRAPH-CONSTRAINED SURFACE PARAMETERIZATION AND REGISTRATION

6.1 Introduction

The natural surfaces are usually associated with feature graphs which can be used as constraints in the process of intra-surface correspondence (registration) computation. In chap. 4, we presented a method to compute brain cortical surface registration using the intrinsic graph-constrained harmonic map. In this chapter, we generalize the method to compute diffeomorphic registration between genus zero surfaces with consistent feature graphs. First, the graph constrained surfaces are mapped to canonical domains by the intrinsic harmonic map, which extends the atlas-constrained harmonic mapping for cortical surfaces to graph constrained surfaces in a rigorous and consistent way. The feature graph on the 3D surface is straightened to a planar straight graph, which forms a convex subdivision of the canonical domain. The parameterization exists, and is unique and intrinsic to the surface and its feature graph. Then the 3D surfaces with consistent feature graphs are registered by matching the straightened graphs and their associated convex regions in the canonical domain by constrained harmonic maps. The method is theoretically rigorous, and computationally efficient and robust. The application of surface morphing on various surfaces and images demonstrates the efficiency and practicality of the proposed methods.

6.2 Background and Motivation

Surface parameterization and registration play important roles in many geometry processing applications such as texture mapping, surface modeling, morphing,

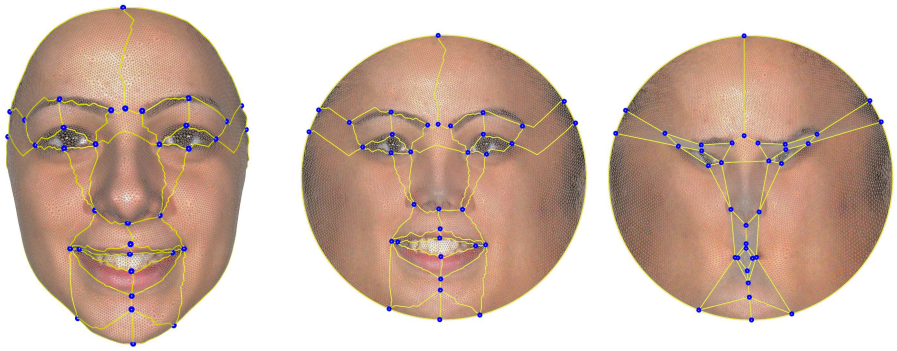

(a) 3D face (b) conformal map (c) intrinsic map

Figure 6.1: Parameterization of 3D facial surfaces with feature graphs. Given a happy facial surface decorated with a 3-connected feature graph in (a), (b) and (c) shows the conformal parameterization and the intrinsic parameterization, respectively.

matching, and so on. In practice, feature landmarks are widely used, and play an important role in the above applications. Anatomical landmarks are used in medical image analysis applications, for example, facial symmetry curves in adolescent idiopathic scoliosis and autism diagnosis, and brain sulci landmarks in Alzheimer' disease diagnosis and brain morphometry analysis. The anatomical landmarks on the surfaces usually form a 3-connected graph with nodes and curvy edges (see Fig. 6.1), where the nodes are the feature points (e.g., eye and mouth corners, nose tips), and the curvy edges are the landmark contours and curves connecting the nodes (e.g., eye and mouth contours). The primary goal of our paper is to compute the intrinsic parameterization and registration of graph constrained surfaces.

Most methods only focus on surface parameterization and registration with feature point constraints [22, 103, 159] and curve constraints [155, 162]. For a surface with feature graph, it is worthy to deal with the graph as a whole rather than split the graph into separate points and curves as the graph has both global and local information, and serves as a skeleton structure of the surface. To our best knowledge, not much attention has been paid to tackle surface parameterization and registra-

tion of surfaces with graph constraints. Recently, Zeng [163] presented a method to parameterize surfaces with graph constraints, and register two 3D surfaces with consistent graphs. The parameterization method first compute the planar embedding of the feature graphs using the Tutte embedding, and then tries to compute a harmonic mapping to fit the graph embedding in the canonical domain. As a result, the final parameterization and registration highly depend on the chosen weights during the Tutte embedding computation, which is heuristic and not intrinsic.

In this chapter, we present intrinsic parameterization and registration methods for graph constrained surfaces by extending the mean value coordinate adaptively according to the associated feature graphs. The parameterization provides an intrinsic representation for surfaces with feature graphs, where the curvy feature graph is straightened to a planar straight line graph (PSLG) in the canonical domain, and its shape is determined intrinsically by the surface geometry and its feature graphs. The parameterization is globally optimal, and has the guarantee of existence and uniqueness, based on which the canonical domains are registered by aligning the two consistent PSLGs using the constrained harmonic map, which is diffeomorphic. For two surfaces with same topological graphs, these graphs serve as guidance for the correspondence computation between them. The nodes of the source graph are mapped to the corresponding ones of the target graph while the interior points of the source graph can slide on the corresponding target graph curves, and their positions are computed automatically by the intrinsic registration method.

6.3 Approach Overview

As before, 3D surface is represented as a triangular mesh denoted as $M = (V, E, F)$, where V, E, F represent vertex, edge, and face sets, respectively. The method uses the intrinsic graph-constrained parameterization method which is used to compute

registration between surfaces with isomorphic feature graphs. The graphs can be extracted from natural surfaces automatically or manually [152], which are defined as 3-connected (i.e., each vertex connectivity ≥ 3) graphs. The nodes of these graphs are the dominant feature points of the surface, and the edges of the graphs are the curves between them. To distinguish with the vertex and edge of the mesh, we use *graph-node* and *graph-edge* to denote the node and edge of the graph in the remainder of the paper, respectively.

In this chapter, we present method to compute the intrinsic harmonic map of graph constrained surfaces, which maps the feature graph on the surface to a PSLG in the parameter domain, and maintains the geometry of the original surface as much as possible (see Fig. 6.1). The harmonic weights are computed by applying the Circumferential Mean Value Theorem adaptively according to the associated feature graph as described in chap. 4. Like the cortical surfaces, for vertices lying on the graph-edges, we adopt the *one-ring graph neighborhood* instead of the traditional *one-ring neighborhood* to derive the harmonic weights, which extends the mean value coordinate to graph constrained surfaces. The intrinsic parameterization is diffeomorphic, globally optimal, and respects the feature graph constraints. To register two surfaces with consistent feature landmarks, the PSLGs and their associated convex subregions in the canonical domain are exactly aligned by a constrained harmonic map, which is unique, globally optimal, and diffeomorphic. The registration method presented in this chapter can be applied to generate morphing sequences between surfaces and images with consistent feature graphs, which demonstrate the efficiency and practicality of the proposed methods.

6.4 Computational Algorithms

In this section, we first present a method to compute the intrinsic harmonic map of graph constrained surfaces, and then describe how to obtain the diffeomorphic registration based on the intrinsic maps.

6.4.1 Intrinsic Parameterization of Graph Constrained Surfaces

From the triangulated surface $M = (V, E, F)$, we extract the graph $G = (V_G, E_G, F_G)$ which is a 3-connected graph (node degree ≥ 3). The graph-nodes V_G are the dominant feature points on the surface. Each graph-edge is embedded on the surface, and therefore is a curve, denoted as a chain of surface vertices which connect the graph-nodes. For the simply connected surface (surface with a single boundary), we parameterize the surface to a canonical domain using graph-constrained parameterization. The algorithm is similar to the one as described in 2 where we adapt the weights of the harmonic energy function in eqn. 4.1. The 3D surface is parameterized to a disk domain and the surface generated from image is parameterized to a rectangular domain. The harmonic map used in the parameterization is unique, globally optimal and diffeomorphic, which can be proved similarly as described in 1.

6.4.2 Diffeomorphic Registration of Graph Constrained Surfaces

The goal is to find a diffeomorphic registration between two 3D surfaces with consistent feature graphs such that the curvy graphs are exactly aligned. The main strategy is to employ the above intrinsic harmonic map to convert 3D surfaces with irregular shaped decorative graphs to PSLGs in the canonical domain. Thus the desired registration can be efficiently obtained by minimizing constrained harmonic energies to align the two PSLGs in the canonical domain.

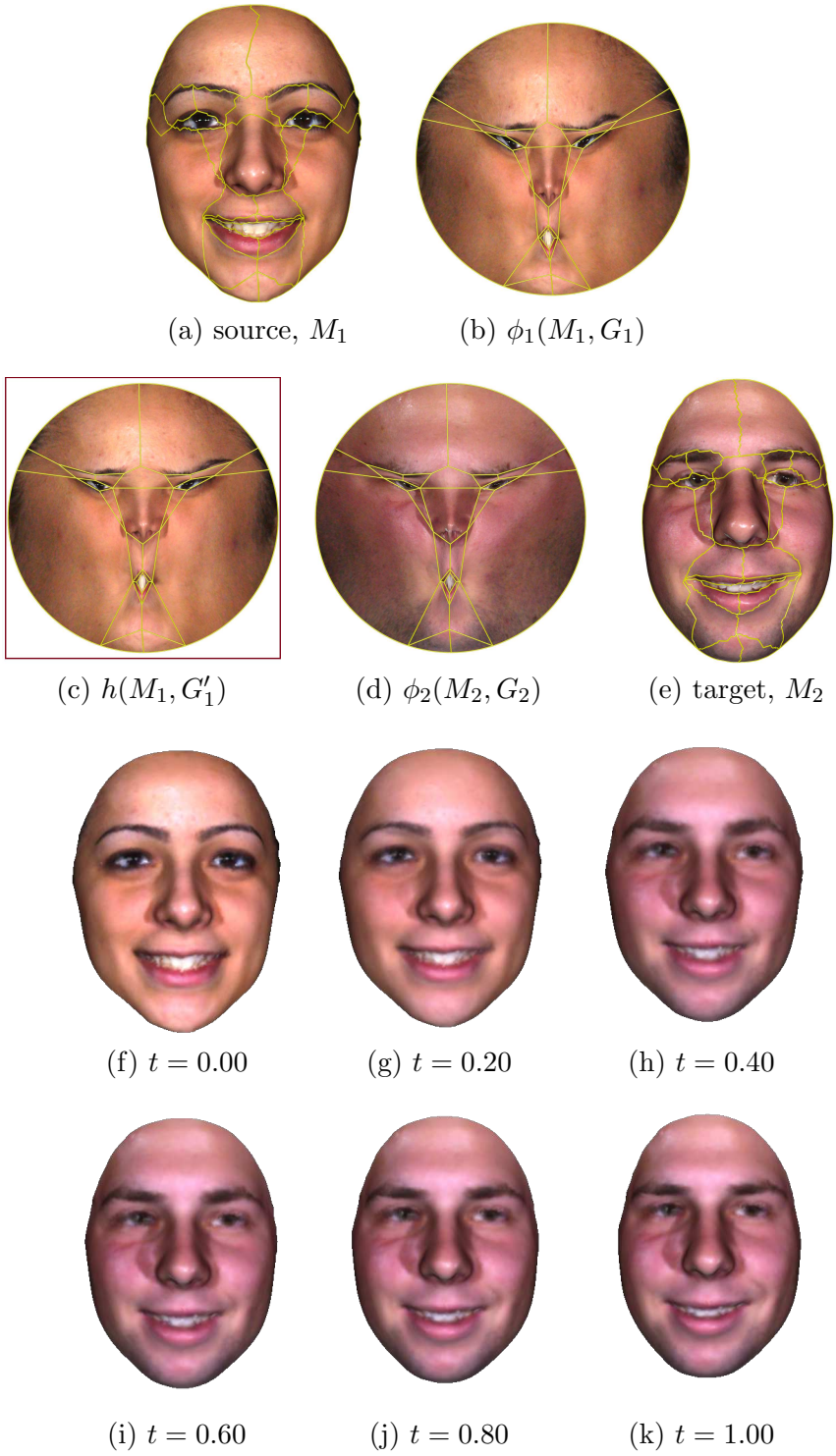

(a) source, M_1 (b) $\phi_1(M_1, G_1)$

(c) $h(M_1, G_1')$ (d) $\phi_2(M_2, G_2)$ (e) target, M_2

(f) $t = 0.00$ (g) $t = 0.20$ (h) $t = 0.40$

(i) $t = 0.60$ (j) $t = 0.80$ (k) $t = 1.00$

Figure 6.2: Human facial surface parameterization, registration and morphing. Row 1 and 2 show the surface registration between the female face surface and the male face surface. Row 3 and 4 illustrate the morphing results, where parameter t shows the progress of morphing.

Given two graph-constrained surfaces, (M_1, G_1) and (M_2, G_2), where $M_1 = (V_1, E_1, F_1)$ and $M_2 = (V_2, E_2, F_2)$, with isomorphic 3-connected graphs as the source and target, our goal is to find an optimal diffeomorphism $f : (M_1, G_1) \rightarrow (M_2, G_2)$ such that graphs G_1 and G_2 are strictly aligned. The registration is computed similarly as the cortical brain surfaces as described in the section 4.4.3. The difference is that no graph-refinement is required as the graphs G_1 and G_2 are isomorphic by construction. The surface registration f is unique, globally optimal and diffeomorphic, which can be proved similarly as 2.

After the graph constrained surfaces are registered, we can obtain the deformed source $M_1^{'} = (V_1^{'}, E_1, F_1)$ by computing the vertex positions $V_1^{'}$ on the target surface M_2. Note that the edge set and face set of M_1 remain the same, only the positions of the vertices are changed. The above registration can be applied to surface morphing between two different surfaces with consistent feature graphs. The idea is to create intrinsic registration of the graph-constrained surfaces, and generate the deformed source 3D surface, $M_1^{'}$. After that, morphing sequence is computed by interpolation between the source M_1 and the deformed source $M_1^{'}$. The morphed surface $M_t^{'} = (V_t^{'}, E_1, F_1)$ is computed using the following equation:

$$V_t^{'} = V_1 \times (1 - t) + V_1^{'} \times t, \text{where } 0 \leq t \leq 1, \text{ and } M_0^{'} = M_1.$$

The parameter t controls the progress of morphing. If $t = 0$, it generates the source surface M_1, and it generates the deformed source surface $M_1^{'}$ when $t = 1$.

6.5 Experiments

We tested the proposed intrinsic parameterization and registration algorithms on morphing of various surfaces and images. Experiments demonstrate that the intrinsic parameterization provides a rigorous shape representation for graph constrained

Algorithm 5: Graph-Constrained Surface Morphing

Input: Two triangular meshes with isomorphic graphs (M_1, G_1), (M_2, G_2)
Output: Morphed triangular mesh $M_t^{'} = (V_t^{'}, E_1, F_1), 0 \leq t \leq 1$
1: Compute parameterization ϕ_k:$(M_k, G_k) \rightarrow (\Omega_k, \hat{G}_k), k = 1, 2$
2: Compute the registration, $f = \phi_2^{-1} \circ h \circ \phi_1$ and generate deformed surface $M_1^{'} = (V_1^{'}, E_1, F_1)$
3: Compute morphed mesh $M_t^{'} = (V_t^{'}, E_1, F_1)$ using Eqn. 6.4.2

surfaces, and the intrinsic registration method is efficient and effective, and therefore is promising for morphing applications.

6.5.1 Applications to Morphing

Graph Design and Generation. For human facial surfaces, we employ the prominent features including the points, curves and contours around the eyes, mouth, nose and eye brows, and geometric features such as the symmetry axis and boundaries to form the graph. These features can be either extracted automatically or manually labeled (e.g., BU3DFE [152]). The graph is constructed by connecting the prominent and geometric features using the shortest paths. Various graphs can be constructed using different connecting patterns. The key idea here is to build 3-connected isomorphic graphs for the source and the target. For facial surface in our experiments, we refer to the natural muscle group of facial surfaces to divide the whole human facial surfaces (see Fig. 6.2(a,e)) and animal's facial surfaces (see Fig. 6.3(a,e)).

Parameterization and Registration. Fig. 6.2 shows the intrinsic parameterization and registration of the source and target face surfaces of two different persons. We can see that the intrinsic parameterization in Fig. 6.2(b,d) well keeps the shape and geometry of the feature graph, and maps the 3D curvy graphs to PSLGs, which form convex subdivisions of the canonical domain. Fig. 6.2(c) illus-

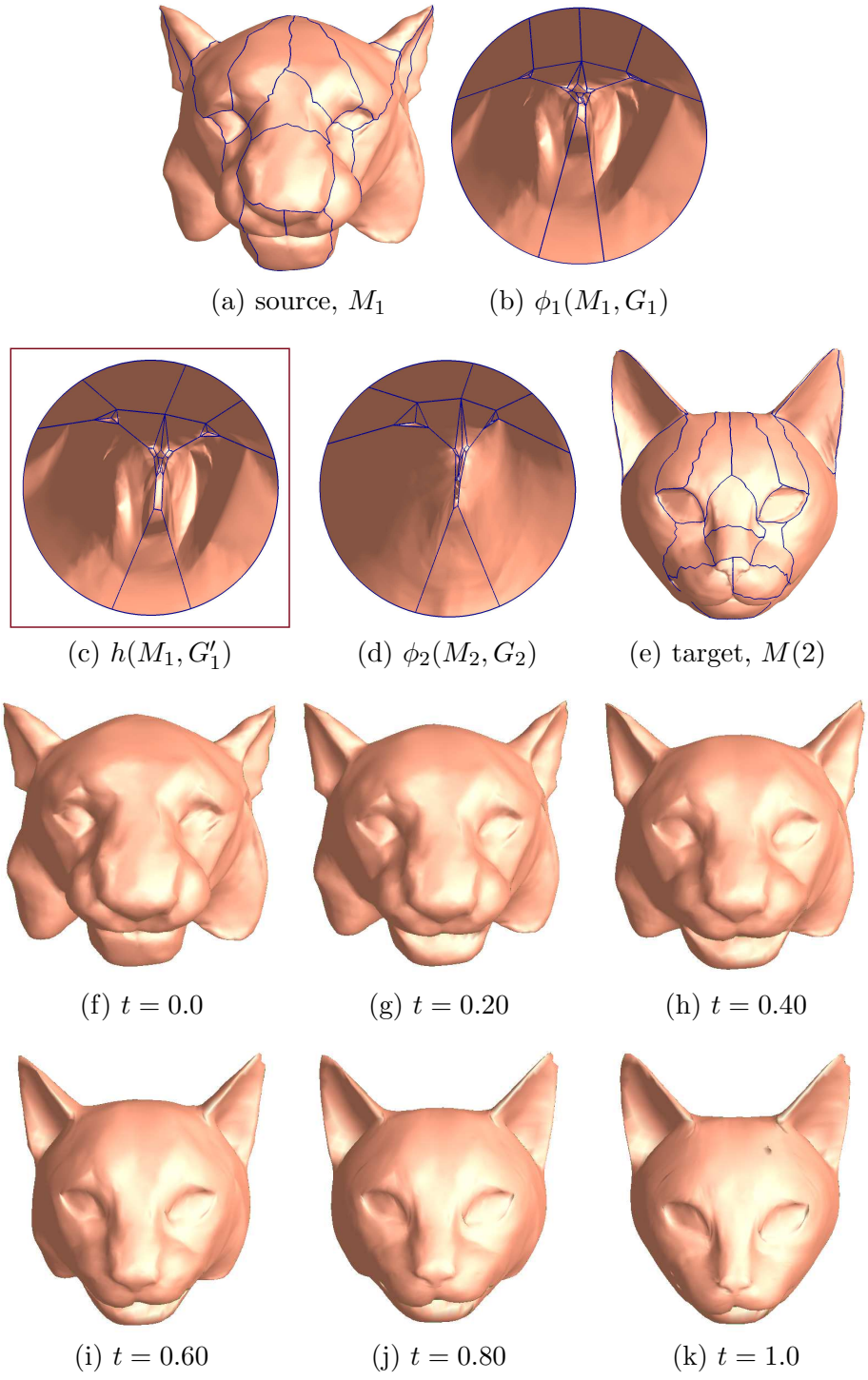

(a) source, M_1 (b) $\phi_1(M_1, G_1)$

(c) $h(M_1, G_1')$ (d) $\phi_2(M_2, G_2)$ (e) target, $M(2)$

(f) $t = 0.0$ (g) $t = 0.20$ (h) $t = 0.40$

(i) $t = 0.60$ (j) $t = 0.80$ (k) $t = 1.0$

Figure 6.3: Surface parameterization, registration and morphing of the lion and cat facial surfaces. Row 1 and 2 show the registration between the lion's facial surface and the cat's facial surface. Row 3 and 4 illustrate the morphing results, where parameter t shows the progress of morphing.

trates the deformed source domain after the surface registration, and the deformed 3D surface is shown in Fig. 6.2(k), which is visually the same as the target surface in Fig. 6.2(e). Based on the intrinsic registration of the human facial surfaces, we compute the morphing sequence shown in Fig. 6.2(f-k), which generates a smooth transition between the source and target surfaces, and demonstrates the efficacy of our intrinsic registration method. Both geometry and texture are blended during the surface morphing. Our method can also work for surfaces with significantly different shapes. Fig. 6.3 gives another example for the registration and morphing between a lion's facial surface and a cat's facial surface. Both the two examples generate satisfying surface registration and morphing sequences, which visually demonstrate the efficiency and practicality of the proposed methods. To further verify the superiority of our presented method, experiments on 2D images are performed, and described as follows.

We apply our intrinsic parameterization and registration for image morphing in Fig. 6.4-6.6. The graph is first extracted from the images as a 3-connected graph using the dominant features, e.g., segment, edge, corner, which can be computed automatically using the detection algorithms [20, 31, 57, 101, 108, 122]. After that, the image is then triangulated [119] to generate the surface, and our proposed registration method is applied to the graph constrained surfaces. An example of image morphing between a star and a maple image is given in Fig. 6.4. For the image with single object in Fig. 6.4, image corners are used as the graph vertices, and the segmented star/maple portions form the faces of the graph. Another morphing example between cows is given in Fig. 6.5. Furthermore, our intrinsic registration method can be applied to handle morphing of images with multiple objects shown in Fig. 6.6. From the above examples, we can see that our intrinsic registration method provides a general framework to deal with the correspondence computation

between graph constrained surfaces, and is promising for the morphing of surfaces and images.

6.5.2 Algorithm Performance

We measure the time cost of the registration and morphing for all the examples presented in this paper. For morphing, we show the average time for 20 morphing sequences from $t = 0.05$ to $t = 1.0$ with a step size of 0.05. Table 6.1 shows the statistics, where V_n, F_n, E_n denote the number of vertex, edge, and face set in the mesh; and V_n^G, F_n^G, E_n^G denote the vertex, edge, face set of the graph, respectively. From Table 6.1, we can see that both the registration and the morphing methods are fast, and the registration takes less than 2 seconds for surfaces with 16k vertices and 35 graph-nodes.

Table 6.1: Algorithm Performance

Model	Mesh			Graph			Time (s)	
	V_n	F_n	E_n	V_n^G	F_n^G	E_n^G	Regi.	Morph
female, male	16k	33k	50k	35	28	61	1.5	2.2
lion, cat	11k	23k	34k	35	27	60	1.0	2.0
brazil_1, brazil_2	3k	6k	9k	17	11	26	0.5	1.1
cow_1, cow_2	2.6k	5k	7.7k	23	13	34	0.5	1.1
star, maple	3k	6k	9k	12	7	17	0.5	1.1

6.5.3 Comparison

3D surfaces can be mapped to the planar domain using other parameterization techniques, such as conformal mapping and harmonic maps. However the feature graph becomes irregular planar graphs in the canonical domain (see Fig. 6.1(b)),

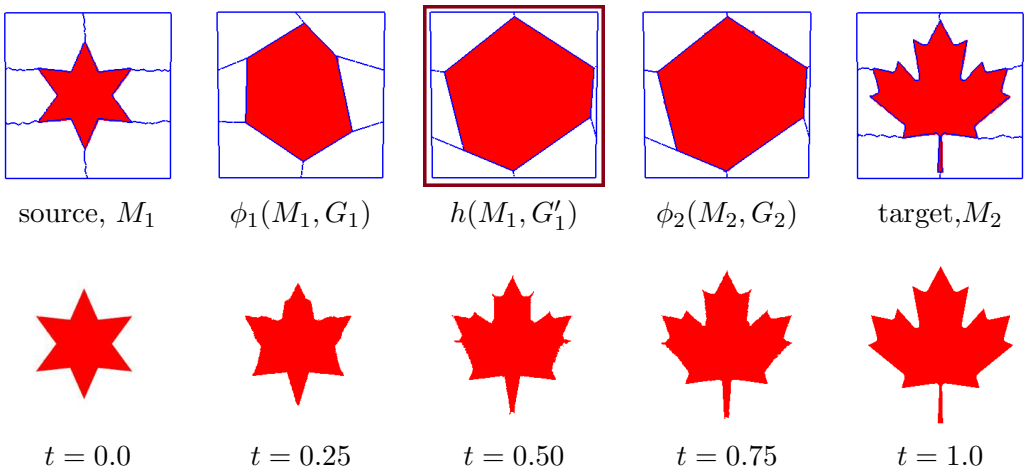

Figure 6.4: Image morphing between star and maple images.

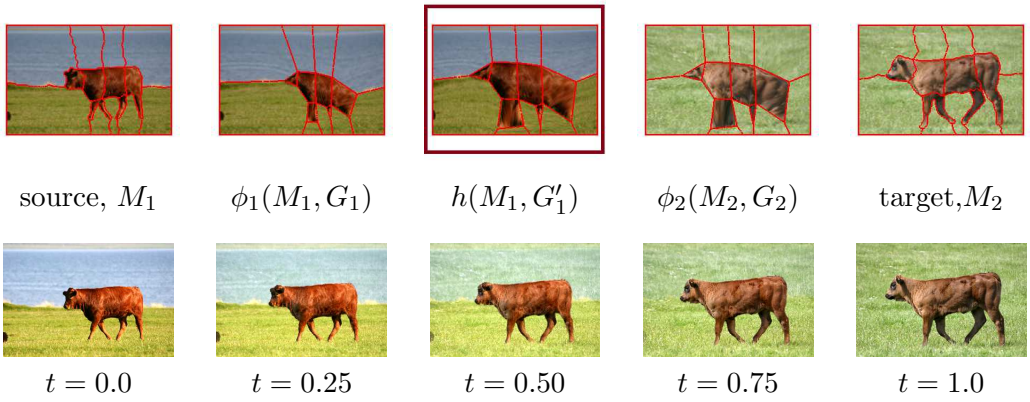

Figure 6.5: Image morphing between two images of cow, cow_1 and cow_2. Image is collected from Microsoft image understanding database [1].

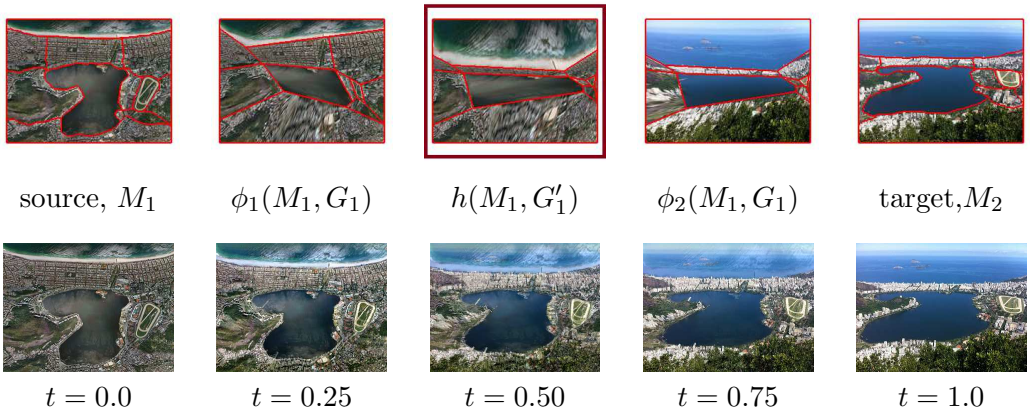

Figure 6.6: Image morphing between two images of Brazil, brazil_1 and brazil_1, which is collected from [82].

which makes the 2D registration difficult. Intuitively, these maps can define a planar straight line graph embedding by simply connecting the nodes on the planar domain, but cannot guarantee crossing-free (with self-flipping) property and may generate concave faces, and skinny faces (not perceptively pleasing). Therefore there is no guarantee of generating a diffeomorphic surface mapping using such straight line graphs. The convex combination map using Tutte embedding [163] maps the feature graphs to a PLSG in the canonical domain, which is a two step procedure, and determines the weights of vertices on the graph using a heuristic method. As a result, the final parameterization and registration are not globally optimal, and highly depend on the chosen weights during the Tutte embedding computation, which may introduce additional distortions. Numerically, we compute the registration accuracy metric as $d(M_1, M_2) = \frac{1}{n}\sum_i^n ||\mathbf{g}(v_i) - \mathbf{g}(f(v_i))||^2)$, where $f(v_i)$ is the corresponding vertex in the deformed source mesh and $\mathbf{g}$ denotes the gauss curvature. Table 6.2 shows the comparison between our method and the convex combination map using Tutte embedding [163], which demonstrates the superiority of our intrinsic registration method. Compared with the Tutte embedding based method, our intrinsic registration method generates better results for the 3D surfaces in Fig. 6.2 and 6.3. The lion and cat faces in Fig. 6.3 have more different shape than the faces in Fig. 6.2, which introduces larger registration accuracy metric as shown in Table 6.2.

Table 6.2: Comparison with Tutte embedding based method [163]

Model	$d(M_1, M_2)$	
	our intrinsic method	Tutte based method
faces in Fig. 6.2	0.00327	0.00371
lion and cat in Fig. 6.3	0.014396	0.016253

6.5.4 Discussion

This work proposes an efficient and flexible way to generate graph-constrained surface parameterization and registration while achieving minimal distortion in the process and apply that for morphing.

Novelty. This work solves the problem of graph-constrained surface parameterization in one step with flexible uses of energy functions. The parameterization process creates straight line graph embedding in the parameter domain. The method does not depend on any initial parameterization which may severely distorts the mapping. Positive edge weights can be used for all the edges to generate flipping free parameterization. If the mesh is good, cotangent weights w_{ij}, can be all positive, otherwise some mesh refinement can be employed to make all the weights positive. Also using mean value coordinates [41], weights can be made all positive. Using positive weights results in a mapping where each vertex is a convex combination of its surrounding vertices. This guarantees uniqueness and diffeomorphism of our parameterization.

Energy modification. Different energy functions can be used in our method which maintains different intrinsic properties of the surface, e.g., conformal parameterization [80, 96], discrete area preserving parameterization (DAP) [29], harmonic map, etc. The energy function in Eqn. 4.1 can be replaced with other energy functions by altering the weights of the edges; special care may need need to be taken to generate flipping free parameterization.

Efficiency. The method is efficient in the sense that it does not depend on any initial embedding for computing graph-constrained parameterization. Also in the computation, it makes minimal changes to the edge weights used in the energy function. The method minimizes the harmonic energy under constraints and the resulted map is as smooth as possible.

Flexibility. The proposed framework is general and highly flexible. Based on the application need, different energy functional can be adapted to the method without making much modification in the process. In this work, we used two different types of energy functions in the parameterization and used the one which show visually better parameterization.

Application and extension. Graph-constrained parameterization can be used in many applications where correspondence between surfaces with graph constraints are desired, e.g., surface and image animation and morphing, matching, etc. The idea is to parameterize the surfaces to convex domains using harmonic map with graph constraints and then compute a constrained harmonic map between the parameterizations of the source and the target which generates the registration. After the registration, animation and morphing can be done easily. Also, the method can be used in biomedical research where the surfaces are naturally associated with graphs, e.g., facial surface analysis for autism.

6.6 Summary

In this chapter, we present an intrinsic method to compute the parameterization of graph constrained surfaces by substituting the one-ring neighborhood with the one-ring graph neighborhood for vertices on the feature graph during the computation of harmonic weights, which extends the mean value coordinate to graph constrained surfaces, and straightens the feature graph to a PSLG in the canonical domain. Based on the intrinsic harmonic map, we provide a general framework to register surfaces with consistent feature graphs, which exactly aligns the guided feature graphs, and is globally optimal and diffeomorphic. The application of surface morphing on various surfaces and images demonstrates the efficiency and practicality of our parameterization and registration methods.

CHAPTER 7

CONCLUSION

This chapter provides a brief summary of the dissertation and discusses possible future research directions based on this dissertation.

7.1 Summary

In this dissertation, we have presented methods for brain mapping, brain registration, brain morphometry analysis, and graph-constrained surface parameterization, registration and their application to surface and image morphing using the feature graph naturally embedded on the surface. First, a novel brain-net graph was defined using the connectivity of the brain regions which was then used as constraints to generate a convex-shaped mapping for brain cortical surface using Tutte embedding and harmonic map that maps each cortical region to a convex subdivision. The method minimizes convex energy function which is guaranteed to be unique and diffeomorphic. The method solves the sparse linear system, and all the computations used in the process are linear. Our experiments on a total of 290 brains have demonstrated the efficiency and efficacy of the proposed method.

Next, we have presented an atlas-constrained brain cortical surface registration technique based on a novel atlas-constrained harmonic map using adaptive mean value weight considering the local graph neighborhood for the vertices on the atlas-graph. As the atlas graphs among brain surfaces are not consistent (not isomorphic), we proposed a graph-refinement process to make the graphs consistent among the brain surfaces by performing minimal changes to the brain surfaces; the registration process was followed by a relaxation process to minimize the distortions introduced by the graph refinement. As the method considers internal structures or regions of

the brain surfaces, it can produce more accurate alignment of the brain regions as verified by the Dice coefficient and comparing the results with existing Freesurfers [36] method.

The proposed registration method was then applied for Alzheimer's disease classification by co-registering the brain surfaces to compute shape similarity metrics using per-vertex attributes of the surfaces. The method used one cortical surface as the source, and it is registered to all other target cortical surfaces so that all the surfaces have one-to-one correspondence among them. The method then interpolated the attributes from the target surfaces using this registration, and assigned them to the corresponding registered surfaces. After that, we used supervised machine learning technique, e.g., K-NN, SVM and Random forest algorithms to classify normal brains from the brains with AD. The accuracy of the method was 88.0% using K-NN classifier (K=5) with 10-fold cross validation for a dataset of 50 normal subjects and 50 subjects with AD.

In the end, we have presented methods to compute intrinsic graph-constrained parameterization and registration for general genus-0 surfaces by extracting isomorphic feature graphs from the source and the target surface. The harmonic map in the parameterization and registration process are unique, globally optimal and diffeomorphic. Finally, the parameterization and registration process was applied to generate morphing sequences between the source and the target shape. Experiments on various surfaces with complicated geometry, and images having single and multiple objects show the effectiveness of the proposed parameterization and registration method and practicability in generating morphing sequences.

7.2 Future Works

The proposed brain mapping method provides a useful way for the brain structures and anatomy visualization. It will be interesting to see how the abnormalities of the brains induced by the diseases are mapped on the domain; other color-coded geometric attributes along with normal information can be assigned to the vertices of the brain surface to facilitate the visualization. Another future work will be to check if the method can be used for other anatomical organs visualization, e.g., hearts, colon, etc.

The proposed method may also help visualization and shape analysis of the 3D volume image of the brain. In future, brain graph can be explored for facilitating visualization of such volume image. For graph extraction, the local neighborhood of the voxels can be used, or the volume image can be tetrahedralized to build the local relationship. Brain surface registration may also be used as constraints for volume image registration of the brains which can improve the Dice coefficient.

The proposed brain analysis framework has been applied to AD classification in this dissertation. However, the geometry of the brain cortical surface is also changed for many other psychological diseases, e.g., autism disorder, schizophrenia, etc. In future, the use of this brain analysis framework can also be explored for other disease classification as well. Also, other advanced machine learning algorithm, e.g., deep learning, can be used for improving the classification accuracy with a large amount of brain data.

One very interesting work will be to explore the use of this brain analysis framework for human behavioral analysis, e.g., IQ, creative talents, etc. There are existing evidence that human behaviors including intelligence (IQ) [127] as measured by

Ravens Progressive Matrices and artistic talents [21] have strong relations with the morphometrics measures of the brain.

The proposed parameterization method uses the harmonic energy minimization approach. Different energy functions have been proposed in the literature which are used to maintain different intrinsic properties (e.g., area, angle, length, etc.) of the surface in the parameterization process. These energy functions can be used in future to generate parameterization with less distortions of these properties; special cares have to be taken to ensure bijective and flipping free mapping as the weights used in many of these energy functions are not all positives. An exciting exploration will be the use of ARAP [86] energy function which can generate area-preserving mapping and also considers angle preservation.

The proposed surface registration has been applied to surface morphing application in this dissertation. In future, the use of the proposed registration can be explored for other geometry processing applications such as animation and modeling. The proposed registration method may also help in other biomedical research such as symmetry curves analysis in adolescent idiopathic scoliosis and facial surface analysis for autism diagnosis.

The proposed methods in this dissertation have been applied to genus-0 surfaces with single boundary. For the genus-0 closed surfaces spherical domains can be used, but unlike disk domains, it will generate geodesics instead of straight lines. An exciting future work will be to compute graph-constrained parameterization and registration for such closed surfaces. Also, it can be further explored how to adapt the proposed methods for high genus surfaces.

BIBLIOGRAPHY

[1] Microsoft image understanding. `https://www.microsoft.com/en-us/research/project/image-understanding/`.

[2] Katrin Amunts, Aleksandar Malikovic, Hartmut Mohlberg, Thorsten Schormann, and Karl Zilles. Brodmann's areas 17 and 18 brought into stereotaxic spacexwhere and how variable? *Neuroimage*, 11(1):66–84, 2000.

[3] Sigurd Angenent, Steven Haker, Allen Tannenbaum, and Ron Kikinis. Conformal geometry and brain flattening. In *Medical Image Computing and Computer-Assisted Intervention–MICCAI99*, pages 271–278. Springer, 1999.

[4] Babak A Ardekani, Stephen Guckemus, Alvin Bachman, Matthew J Hoptman, Michelle Wojtaszek, and Jay Nierenberg. Quantitative comparison of algorithms for inter-subject registration of 3D volumetric brain mri scans. *Journal of neuroscience methods*, 142(1):67–76, 2005.

[5] John Ashburner and Karl J Friston. Voxel-based morphometry–the methods. *Neuroimage*, 11(6):805–821, 2000.

[6] John Ashburner and Karl J Friston. Unified segmentation. *Neuroimage*, 26(3):839–851, 2005.

[7] John Ashburner, Karl J Friston, et al. Nonlinear spatial normalization using basis functions. *Human brain mapping*, 7(4):254–266, 1999.

[8] John Ashburner, Chloe Hutton, Richard Frackowiak, Ingrid Johnsrude, Cathy Price, Karl Friston, et al. Identifying global anatomical differences: deformation-based morphometry. *Human brain mapping*, 6(5-6):348–357, 1998.

[9] Bérengère Aubert-Broche, VS Fonov, Daniel García-Lorenzo, Abderazzak Mouiha, Nicolas Guizard, Pierrick Coupé, Simon F Eskildsen, and D Louis Collins. A new method for structural volume analysis of longitudinal brain mri data and its application in studying the growth trajectories of anatomical brain structures in childhood. *Neuroimage*, 82:393–402, 2013.

[10] Guillaume Auzias, Julien Lefèvre, Arnaud Le Troter, Clara Fischer, Matthieu Perrot, Jean Régis, and Olivier Coulon. Model-driven harmonic parameterization of the cortical surface: Hip-hop. *IEEE transactions on medical imaging*, 32(5):873–887, 2013.

[11] Brian B Avants, Charles L Epstein, Murray Grossman, and James C Gee. Symmetric diffeomorphic image registration with cross-correlation: evaluating automated labeling of elderly and neurodegenerative brain. *Medical image analysis*, 12(1):26–41, 2008.

[12] Muge M Bakircioglu, Sarang C Joshi, and Michael I Miller. Landmark matching on brain surfaces via large deformation diffeomorphisms on the sphere. In *Medical Imaging'99*, pages 710–715. International Society for Optics and Photonics, 1999.

[13] Hujun Bao and Qunsheng Peng. Interactive 3D morphing. In *Computer Graphics Forum*, volume 17, pages 23–30. Wiley Online Library, 1998.

[14] Danielle S Bassett, Edward Bullmore, Beth A Verchinski, Venkata S Mattay, Daniel R Weinberger, and Andreas Meyer-Lindenberg. Hierarchical organization of human cortical networks in health and schizophrenia. *The Journal of Neuroscience*, 28(37):9239–9248, 2008.

[15] M Faisal Beg, Michael I Miller, Alain Trouvé, and Laurent Younes. Computing large deformation metric mappings via geodesic flows of diffeomorphisms. *International journal of computer vision*, 61(2):139–157, 2005.

[16] M. Ben-Chen, C. Gotsman, and G. Bunin. Conformal flattening by curvature prescription and metric scaling. *Computer Graphics Forum (Proc. Eurographics 2008)*, 27(2), 2008.

[17] Chakib Bennis, Jean-Marc Vézien, and Gérard Iglésias. Piecewise surface flattening for non-distorted texture mapping. In *Proceedings of the 18th annual conference on Computer graphics and interactive techniques*, SIGGRAPH '91, pages 237–246, New York, NY, USA, 1991. ACM.

[18] Emre Bora, Alex Fornito, Christos Pantelis, and Murat Yücel. Gray matter abnormalities in major depressive disorder: a meta-analysis of voxel based morphometry studies. *Journal of affective disorders*, 138(1):9–18, 2012.

[19] Edward T Bullmore and Danielle S Bassett. Brain graphs: graphical models of the human brain connectome. *Annual review of clinical psychology*, 7:113–140, 2011.

[20] John Canny. A computational approach to edge detection. *IEEE Transactions on pattern analysis and machine intelligence*, (6):679–698, 1986.

[21] Rebecca Chamberlain, I Chris McManus, Nicola Brunswick, Qona Rankin, Howard Riley, and Ryota Kanai. Drawing on the right side of the brain: a voxel-based morphometry analysis of observational drawing. *NeuroImage*, 96:167–173, 2014.

[22] Pui Tung Choi, Ka Chun Lam, and Lok Ming Lui. FLASH: Fast landmark aligned spherical harmonic parameterization for genus-0 closed brain surfaces. *SIAM Journal on Imaging Sciences*, 8(1):67–94, 2015.

[23] Moo K Chung, Kim M Dalton, and Richard J Davidson. Tensor-based cortical surface morphometry via weighted spherical harmonic representation. *IEEE Trans Med Imag*, 27(8):1143–1151, 2008.

[24] Moo K Chung, Steven M Robbins, Kim M Dalton, Richard J Davidson, Andrew L Alexander, and Alan C Evans. Cortical thickness analysis in autism with heat kernel smoothing. *NeuroImage*, 25(4):1256–1265, 2005.

[25] Marie Chupin, Alexander Hammers, Rebecca SN Liu, Olivier Colliot, J Burdett, Eric Bardinet, John S Duncan, Line Garnero, and Louis Lemieux. Automatic segmentation of the hippocampus and the amygdala driven by hybrid constraints: method and validation. *Neuroimage*, 46(3):749–761, 2009.

[26] Rémi Cuingnet, Emilie Gerardin, Jérôme Tessieras, Guillaume Auzias, Stéphane Lehéricy, Marie-Odile Habert, Marie Chupin, Habib Benali, Olivier Colliot, Alzheimer's Disease Neuroimaging Initiative, et al. Automatic classification of patients with alzheimer's disease from structural mri: a comparison of ten methods using the adni database. *neuroimage*, 56(2):766–781, 2011.

[27] Christos Davatzikos, Ahmet Genc, Dongrong Xu, and Susan M Resnick. Voxel-based morphometry using the ravens maps: methods and validation using simulated longitudinal atrophy. *NeuroImage*, 14(6):1361–1369, 2001.

[28] Rhodri H Davies, Carole J Twining, P Daniel Allen, Timothy F Cootes, and Christopher J Taylor. Shape discrimination in the hippocampus using an mdl model. In *IPMI*, pages 38–50. Springer, 2003.

[29] Mathieu Desbrun, Mark Meyer, and Pierre Alliez. Intrinsic Parameterizations of Surface Meshes. *Computer Graphics Forum*, 21(3):209–218, 2002.

[30] Rahul S Desikan, Florent Ségonne, Bruce Fischl, Brian T Quinn, Bradford C Dickerson, Deborah Blacker, Randy L Buckner, Anders M Dale, R Paul

Maguire, Bradley T Hyman, et al. An automated labeling system for subdividing the human cerebral cortex on mri scans into gyral based regions of interest. *Neuroimage*, 31(3):968–980, 2006.

[31] Piotr Dollár and C Lawrence Zitnick. Fast edge detection using structured forests. *IEEE transactions on pattern analysis and machine intelligence*, 37(8):1558–1570, 2015.

[32] Gwenaëlle Douaud, Stephen Smith, Mark Jenkinson, Timothy Behrens, Heidi Johansen-Berg, John Vickers, Susan James, Natalie Voets, Kate Watkins, Paul M Matthews, et al. Anatomically related grey and white matter abnormalities in adolescent-onset schizophrenia. *Brain*, 130(9):2375–2386, 2007.

[33] Marie-Pierre Dubuisson and Anil K Jain. A modified hausdorff distance for object matching. In *Pattern Recognition, 1994. Vol. 1-Conference A: Computer Vision & Image Processing., Proceedings of the 12th IAPR International Conference on*, volume 1, pages 566–568. IEEE, 1994.

[34] Zhang Eugene, Mischaikow Konstantin, and Turk Greg. Feature-based Surface Parameterization. *ACM Transactions on Graphics*, 24(1):1–27, 2005.

[35] Hershel M. Farkas and Irwin Kra. *Riemann Surfaces*. Springer, 2004.

[36] Bruce Fischl. Freesurfer. *Neuroimage*, 62(2):774–781, 2012.

[37] Bruce Fischl, Niranjini Rajendran, Evelina Busa, Jean Augustinack, Oliver Hinds, BT Thomas Yeo, Hartmut Mohlberg, Katrin Amunts, and Karl Zilles. Cortical folding patterns and predicting cytoarchitecture. *Cerebral Cortex*, 18(8):1973–1980, 2008.

[38] Bruce Fischl, Martin I Sereno, and Anders M Dale. Cortical surface-based analysis: Ii: inflation, flattening, and a surface-based coordinate system. *Neuroimage*, 9(2):195–207, 1999.

[39] Bruce Fischl, Martin I Sereno, Roger BH Tootell, Anders M Dale, et al. High-resolution intersubject averaging and a coordinate system for the cortical surface. *Human brain mapping*, 8(4):272–284, 1999.

[40] Michael Floater. One-to-one piecewise linear mappings over triangulations. *Mathematics of Computation*, 72(242):685–696, 2003.

[41] Michael S Floater. Mean value coordinates. *Computer aided geometric design*, 20(1):19–27, 2003.

[42] Giovanni B Frisoni, Nick C Fox, Clifford R Jack, Philip Scheltens, and Paul M Thompson. The clinical use of structural mri in Alzheimer disease. *Nature Reviews Neurology*, 6(2):67–77, 2010.

[43] Karl J Friston and Christopher D Frith. Schizophrenia: a disconnection syndrome. *Clin Neurosci*, 3(2):89–97, 1995.

[44] XiaoMing Fu, Yang Liu, and Baining Guo. Computing locally injective mappings by advanced mips. *ACM Transactions on Graphics*, 34(4):71:1–71:12, 2015.

[45] T. Funkhouser, P. Min, M. Kazhdan, J. Chen, A. Halderman, D. Dobkin, and D. Jacobs. A search engine for 3D models. *ACM TOG*, 22(1):83–105, 2003.

[46] Robin Genuer, Jean-Michel Poggi, and Christine Tuleau-Malot. Vsurf: An r package for variable selection using random forests. *The R Journal*, 7(2):19–33, 2015.

[47] Emilie Gerardin, Gaël Chételat, Marie Chupin, Rémi Cuingnet, Béatrice Desgranges, Ho-Sung Kim, Marc Niethammer, Bruno Dubois, Stéphane Lehéricy, Line Garnero, et al. Multidimensional classification of hippocampal shape features discriminates alzheimer's disease and mild cognitive impairment from normal aging. *Neuroimage*, 47(4):1476–1486, 2009.

[48] Guido Gerig, Martin Styner, D Jones, Daniel Weinberger, and Jeffrey Lieberman. Shape analysis of brain ventricles using spharm. In *Mathematical Methods in Biomedical Image Analysis, 2001. MMBIA 2001. IEEE Workshop on*, pages 171–178. IEEE, 2001.

[49] Rainer Goebel, Fabrizio Esposito, and Elia Formisano. Analysis of functional image analysis contest (fiac) data with brainvoyager qx: From single-subject to cortically aligned group general linear model analysis and self-organizing group independent component analysis. *Human brain mapping*, 27(5):392–401, 2006.

[50] Catriona D Good, Ingrid Johnsrude, John Ashburner, Richard NA Henson, Karl J Friston, and Richard SJ Frackowiak. Cerebral asymmetry and the effects of sex and handedness on brain structure: a voxel-based morphometric analysis of 465 normal adult human brains. *Neuroimage*, 14(3):685–700, 2001.

[51] Steven J. Gortler, Craig Gotsman, and Dylan Thurston. Discrete one-forms on meshes and applications to 3D mesh parameterization. *Computer Aided Geometric Design*, 23(2):83–112, 2005.

[52] Douglas N Greve, Lise Van der Haegen, Qing Cai, Steven Stufflebeam, Mert R Sabuncu, Bruce Fischl, and Marc Brysbaert. A surface-based analysis of language lateralization and cortical asymmetry. *Journal of cognitive neuroscience*, 25(9):1477–1492, 2013.

[53] Xianfeng Gu, Yalin Wang, Tony F Chan, Paul M Thompson, and Shing-Tung Yau. Genus zero surface conformal mapping and its application to brain surface mapping. *Medical Imaging, IEEE Transactions on*, 23(8):949–958, 2004.

[54] Steven Haker, Sigurd Angenent, Allen Tannenbaum, Ron Kikinis, Guillermo Sapiro, and Michael Halle. Conformal surface parameterization for texture mapping. *IEEE Transactions on Visualization & Computer Graphics*, (2):181–189, 2000.

[55] Steven Haker, Lei Zhu, Allen Tannenbaum, and Sigurd Angenent. Optimal mass transport for registration and warping. *International Journal of computer vision*, 60(3):225–240, 2004.

[56] M. A. Hall. *Correlation-based Feature Subset Selection for Machine Learning*. PhD thesis, University of Waikato, Hamilton, New Zealand, 1998.

[57] Chris Harris and Mike Stephens. A combined corner and edge detector. In *Alvey vision conference*, volume 15, page 50. Citeseer, 1988.

[58] Yong He, Zhang Chen, and Alan Evans. Structural insights into aberrant topological patterns of large-scale cortical networks in Alzheimer's disease. *The Journal of neuroscience*, 28(18):4756–4766, 2008.

[59] Oliver P Hinds, Niranjini Rajendran, Jonathan R Polimeni, Jean C Augustinack, Graham Wiggins, Lawrence L Wald, H Diana Rosas, Andreas Potthast, Eric L Schwartz, and Bruce Fischl. Accurate prediction of v1 location from cortical folds in a surface coordinate system. *Neuroimage*, 39(4):1585–1599, 2008.

[60] D. Huber, A. Kapuria, R.R. Donamukkala, and M. Hebert. Parts-based 3D object classification. In *CVPR*, pages II: 82–89, June 2004.

[61] Monica K Hurdal and Ken Stephenson. Cortical cartography using the discrete conformal approach of circle packings. *NeuroImage*, 23:S119–S128, 2004.

[62] Krista L Hyde, Fabienne Samson, Alan C Evans, and Laurent Mottron. Neuroanatomical differences in brain areas implicated in perceptual and other core features of autism revealed by cortical thickness analysis and voxel-based morphometry. *Human brain mapping*, 31(4):556–566, 2010.

[63] M. Jin, J. Kim, F. Luo, and X. Gu. Discrete surface Ricci flow. *IEEE TVCG*, 14(5):1030–1043, 2008.

[64] Hans J Johnson and Gary E Christensen. Consistent landmark and intensity-based image registration. *Medical Imaging, IEEE Transactions on*, 21(5):450–461, 2002.

[65] Anand A Joshi, Dimitrios Pantazis, Quanzheng Li, Hanna Damasio, David W Shattuck, Arthur W Toga, and Richard M Leahy. Sulcal set optimization for cortical surface registration. *Neuroimage*, 50(3):950–959, 2010.

[66] Anand A Joshi, David W Shattuck, Paul M Thompson, and Richard M Leahy. Cortical surface parameterization by p-harmonic energy minimization. In *Biomedical Imaging: Nano to Macro, 2004. IEEE International Symposium on*, pages 428–431. IEEE, 2004.

[67] Anand A Joshi, David W Shattuck, Paul M Thompson, and Richard M Leahy. A finite element method for elastic parameterization and alignment of cortical surfaces using sulcal constraints. In *Biomedical Imaging: From Nano to Macro, 2007. ISBI 2007. 4th IEEE International Symposium on*, pages 640–643. IEEE, 2007.

[68] Anand A Joshi, David W Shattuck, Paul M Thompson, and Richard M Leahy. Surface-constrained volumetric brain registration using harmonic mappings. *Medical Imaging, IEEE Transactions on*, 26(12):1657–1669, 2007.

[69] Lili Ju, Josh Stern, Kelly Rehm, Kirt Schaper, Monica Hurdal, and David Rottenberg. Cortical surface flattening using least square conformal mapping with minimal metric distortion. In *Biomedical Imaging: Nano to Macro, 2004. IEEE International Symposium on*, pages 77–80. IEEE, 2004.

[70] Arno Klein, Jesper Andersson, Babak A Ardekani, John Ashburner, Brian Avants, Ming-Chang Chiang, Gary E Christensen, D Louis Collins, James

Gee, Pierre Hellier, et al. Evaluation of 14 nonlinear deformation algorithms applied to human brain mri registration. *Neuroimage*, 46(3):786–802, 2009.

[71] Arno Klein, Satrajit S Ghosh, Brian Avants, BT Thomas Yeo, Bruce Fischl, Babak Ardekani, James C Gee, J John Mann, and Ramin V Parsey. Evaluation of volume-based and surface-based brain image registration methods. *NeuroImage*, 51(1):214–220, 2010.

[72] Arno Klein, Jason Tourville, et al. 101 labeled brain images and a consistent human cortical labeling protocol. *Front. Neurosci*, 6(171):10–3389, 2012.

[73] Ron Kohavi and George H John. Wrappers for feature subset selection. *Artificial intelligence*, 97(1-2):273–324, 1997.

[74] Sebastian Kurtek, Anuj Srivastava, Eric Klassen, and Hamid Laga. Landmark-guided elastic shape analysis of spherically-parameterized surfaces. In *Computer graphics forum*, volume 32, pages 429–438. Wiley Online Library, 2013.

[75] Sergei K Lando and Alexander K Zvonkin. *Graphs on surfaces and their applications*, volume 141. Springer Science & Business Media, 2013.

[76] Huu Le, Tat-Jun Chin, and David Suter. Conformal Surface Alignment with Optimal Möbius Search. pages 2507–2516, 2016.

[77] Tong-Yee Lee and Po-Hua Huang. Fast and intuitive metamorphosis of 3D polyhedral models using smcc mesh merging scheme. *IEEE Transactions on Visualization and Computer Graphics*, 9(1):85–98, 2003.

[78] Samuel JJ Leistedt, Nathalie Coumans, Martine Dumont, Jean-Pol Lanquart, Cornelis J Stam, and Paul Linkowski. Altered sleep brain functional connectivity in acutely depressed patients. *Human brain mapping*, 30(7):2207–2219, 2009.

[79] B. Levy, S. Petitjean, N. Ray, and J. Maillot. Least squares conformal maps for automatic texture atlas generation. In *SIGGRAPH02*, pages 362–371, 2002.

[80] Bruno Lévy, Sylvain Petitjean, Nicolas Ray, and Jérome Maillot. Least squares conformal maps for automatic texture atlas generation. In *ACM Transactions on Graphics (TOG)*, volume 21, pages 362–371. ACM, 2002.

[81] S. Li, S. Dragicevic, F. Anton, M. Sester, S. Winter, A. Coltekin, C. Pettit, B. Jiang, J. Haworth, A. Stein, and T. Cheng. Geospatial big data handling theory and methods: A review and research challenges. *ISPRS Journal of Photogrammetry and Remote Sensing*, 115:119–133, 2016.

[82] Jing Liao, Rodolfo S Lima, Diego Nehab, Hugues Hoppe, Pedro V Sander, and Jinhui Yu. Automating image morphing using structural similarity on a halfway domain. *ACM Transactions on Graphics (TOG)*, 33(5):168, 2014.

[83] Yaron Lipman. Bounded distortion mapping spaces for triangular meshes. *ACM Transactions on Graphics*, 31(4):108:1–108:13, 2012.

[84] Ligang Liu, Lei Zhang, Yin Xu, Craig Gotsman, and Steven J. Gortler. A local/global approach to mesh parameterization. In *Proceedings of the Symposium on Geometry Processing*, pages 1495–1504, 2008.

[85] Xiuwen Liu, Yonggang Shi, Ivo Dinov, and Washington Mio. A computational model of multidimensional shape. *International journal of computer vision*, 89(1):69–83, 2010.

[86] Ya-Shu Liu, Han-Bing Yan, and Ralph R Martin. As-rigid-as-possible surface morphing. *Journal of Computer Science and Technology*, 26(3):548–557, 2011.

[87] Yong Liu, Chunshui Yu, Xinqing Zhang, Jieqiong Liu, Yunyun Duan, Aaron F Alexander-Bloch, Bing Liu, Tianzi Jiang, and Ed Bullmore. Impaired long distance functional connectivity and weighted network architecture in alzheimer's disease. *Cerebral Cortex*, 24(6):1422–1435, 2014.

[88] Gabriele Lohmann, Daniel S Margulies, Annette Horstmann, Burkhard Pleger, Joeran Lepsien, Dirk Goldhahn, Haiko Schloegl, Michael Stumvoll, Arno Villringer, and Robert Turner. Eigenvector centrality mapping for analyzing connectivity patterns in fmri data of the human brain. *PloS one*, 5(4):e10232, 2010.

[89] Herve Lombaert, Michael Arcaro, and Nicholas Ayache. Brain transfer: Spectral analysis of cortical surfaces and functional maps. In *Information Processing in Medical Imaging*, pages 474–487. Springer, 2015.

[90] Herve Lombaert, Jon Sporring, and Kaleem Siddiqi. Diffeomorphic spectral matching of cortical surfaces. In *Information Processing in Medical Imaging*, pages 376–389. Springer, 2013.

[91] Lok Ming Lui, Ka Chun Lam, Shing-Tung Yau, and Xianfeng Gu. Teichmuller mapping (tmap) and its applications to landmark matching registrations. *SIAM Journal on Imaging Sciences*, 7(1):391–426, 2013.

[92] Lok Ming Lui, Tsz Wai Wong, Wei Zeng, Xianfeng Gu, Paul M. Thompson, Tony F. Chan, and Shing-Tung Yau. Optimization of Surface Registrations Using Beltrami Holomorphic Flow. *Journal of Scientific Computing*, 50(3):557–585, 2012.

[93] Jérôme Maillot, Hussein Yahia, and Anne Verroust. Interactive texture mapping. In *Proceedings of the 20th annual conference on Computer graphics and interactive techniques*, SIGGRAPH '93, pages 27–34, New York, NY, USA, 1993. ACM.

[94] Nikos Makris, Jill M Goldstein, David Kennedy, Steven M Hodge, Verne S Caviness, Stephen V Faraone, Ming T Tsuang, and Larry J Seidman. Decreased volume of left and total anterior insular lobule in schizophrenia. *Schizophrenia research*, 83(2):155–171, 2006.

[95] Daniel S Marcus, Tracy H Wang, Jamie Parker, John G Csernansky, John C Morris, and Randy L Buckner. Open access series of imaging studies (oasis): cross-sectional mri data in young, middle aged, nondemented, and demented older adults. *Journal of cognitive neuroscience*, 19(9):1498–1507, 2007.

[96] Patrick Mullen, Yiying Tong, Pierre Alliez, and Mathieu Desbrun. Spectral conformal parameterization. In *Computer Graphics Forum*, volume 27, pages 1487–1494. Wiley Online Library, 2008.

[97] Ashish Myles, Nico Pietroni, and Denis Zorin. Robust field-aligned global parametrization. *ACM Transactions on Graphics*, 33(4):135:1–135:14, 2014.

[98] Paul G Nestor, Toshiaki Onitsuka, Ronald J Gurrera, Margaret Niznikiewicz, Melissa Frumin, Martha E Shenton, and Robert W McCarley. Dissociable contributions of mri volume reductions of superior temporal and fusiform gyri to symptoms and neuropsychology in schizophrenia. *Schizophrenia research*, 91(1):103–106, 2007.

[99] Toshiaki Onitsuka, Paul G Nestor, Ronald J Gurrera, Martha E Shenton, Kiyoto Kasai, Melissa Frumin, Margaret A Niznikiewicz, and Robert W McCarley. Association between reduced extraversion and right posterior fusiform gyrus gray matter reduction in chronic schizophrenia. *American Journal of Psychiatry*, 2005.

[100] Dimitrios Pantazis, Anand Joshi, Jintao Jiang, David W Shattuck, Lynne E Bernstein, Hanna Damasio, and Richard M Leahy. Comparison of landmark-based and automatic methods for cortical surface registration. *Neuroimage*, 49(3):2479–2493, 2010.

[101] Federico Perazzi, Philipp Krähenbühl, Yael Pritch, and Alexander Hornung. Saliency filters: Contrast based filtering for salient region detection. In *Computer Vision and Pattern Recognition (CVPR), 2012 IEEE Conference on*, pages 733–740. IEEE, 2012.

[102] Rudolph Pienaar, Bruce Fischl, V Caviness, Nikos Makris, and P Ellen Grant. A methodology for analyzing curvature in the developing brain from preterm to adult. *International journal of imaging systems and technology*, 18(1):42–68, 2008.

[103] Chuchart Pintavirooj, Fernand S. Cohen, and Prasong Tosranon. 3D face alignment and registration in the presence of facial expression differences. *IEEE Transactions on Electrical and Electronic Engineering*, 8(4):395–407, 2013.

[104] Anqi Qiu and Michael I Miller. Multi-structure network shape analysis via normal surface momentum maps. *NeuroImage*, 42(4):1430–1438, 2008.

[105] J Rademacher, VS Caviness, H Steinmetz, and AM Galaburda. Topographical variation of the human primary cortices: implications for neuroimaging, brain mapping, and neurobiology. *Cerebral Cortex*, 3(4):313–329, 1993.

[106] A Raj, Susanne G Mueller, Karl Young, Kenneth D Laxer, and M Weiner. Network-level analysis of cortical thickness of the epileptic brain. *Neuroimage*, 52(4):1302–1313, 2010.

[107] Muhammad Razib, Zhong-Lin Lu, and Wei Zeng. Structural Brain Mapping. In *Medical Image Computing and Computer-Assisted Intervention–MICCAI 2015*, pages 760–767. Springer, 2015.

[108] Edward Rosten, Reid Porter, and Tom Drummond. Faster and better: A machine learning approach to corner detection. *IEEE transactions on pattern analysis and machine intelligence*, 32(1):105–119, 2010.

[109] Pedro V. Sander, John Snyder, Steven J. Gortler, and Hugues Hoppe. Locally injective mappings. In *Proceedings of the 28th annual conference on Computer graphics and interactive techniques*, pages 409–416, 2011.

[110] Christian Schller, Ladislav Kavan, Daniele Panozzo, and Olga Sorkine-Hornung. Locally injective mappings. In *Proceedings of the Symposium on Geometry Processing*, pages 125–135, 2013.

[111] Richard M Schoen and Shing-Tung Yau. *Lectures on harmonic maps*, volume 2. Amer Mathematical Society, 1997.

[112] E. Sharon and D. Mumford. 2D-shape analysis using conformal mapping. *International Journal of Computer Vision*, 70(1):55–75, 2006.

[113] David W Shattuck and Richard M Leahy. Brainsuite: an automated cortical surface identification tool. *Medical image analysis*, 6(2):129–142, 2002.

[114] David W Shattuck, Mubeena Mirza, Vitria Adisetiyo, Cornelius Hojatkashani, Georges Salamon, Katherine L Narr, Russell A Poldrack, Robert M Bilder, and Arthur W Toga. Construction of a 3D probabilistic atlas of human cortical structures. *Neuroimage*, 39(3):1064–1080, 2008.

[115] Eli Shechtman, Alex Rav-Acha, Michal Irani, and Steve Seitz. Regenerative morphing. In *Computer Vision and Pattern Recognition (CVPR), 2010 IEEE Conference on*, pages 615–622. IEEE, 2010.

[116] Alla Sheffer, Emil Praun, and Kenneth Rose. Mesh parameterization methods and their applications. In *Foundations and Trends in Computer Graphics and Vision*, page 2006. Now Publishers, 2006.

[117] Yvette I Sheline. 3D mri studies of neuroanatomic changes in unipolar major depression: the role of stress and medical comorbidity. *Biological psychiatry*, 48(8):791–800, 2000.

[118] Dinggang Shen and Christos Davatzikos. Very high-resolution morphometry using mass-preserving deformations and hammer elastic registration. *NeuroImage*, 18(1):28–41, 2003.

[119] Jonathan Richard Shewchuk. Delaunay refinement algorithms for triangular mesh generation. *Computational geometry*, 22(1):21–74, 2002.

[120] Jie Shi, Paul M Thompson, Boris Gutman, Yalin Wang, Alzheimer's Disease Neuroimaging Initiative, et al. Surface fluid registration of conformal representation: Application to detect disease burden and genetic influence on hippocampus. *Neuroimage*, 78:111–134, 2013.

[121] Rui Shi, Wei Zeng, Zhengyu Su, Hanna Damasio, Zhonglin Lu, Yalin Wang, Shing-Tung Yau, and Xianfeng Gu. Hyperbolic harmonic mapping for constrained brain surface registration. In *Proceedings of the IEEE Conference on Computer Vision and Pattern Recognition*, pages 2531–2538, 2013.

[122] Peng-Lang Shui and Wei-Chuan Zhang. Corner detection and classification using anisotropic directional derivative representations. *IEEE Transactions on Image Processing*, 22(8):3204–3218, 2013.

[123] Jasper Snoek, Hugo Larochelle, and Ryan P Adams. Practical bayesian optimization of machine learning algorithms. In *Advances in neural information processing systems*, pages 2951–2959, 2012.

[124] Boris Springborn, Peter Schröder, and Ulrich Pinkall. Conformal equivalence of triangle meshes. *ACM Transactions on Graphics*, 27(3):1–11, 2008.

[125] J. Starck and A. Hilton. Correspondence labelling for wide-timeframe free-form surface matching. In *ICCV*, 2007.

[126] Zhengyu Su, Wei Zeng, Rui Shi, Yalin Wang, Jian Sun, and Xianfeng Gu. Area preserving brain mapping. In *Proceedings of the IEEE Conference on Computer Vision and Pattern Recognition*, pages 2235–2242, 2013.

[127] Zhengyu Su, Wei Zeng, Yalin Wang, Zhong-Lin Lu, and Xianfeng Gu. Shape classification using wasserstein distance for brain morphometry analysis. In *International Conference on Information Processing in Medical Imaging*, pages 411–423. Springer, 2015.

[128] Jian Sun, Tianqi Wu, Xianfeng Gu, and Feng Luo. Discrete Conformal Deformation: Algorithm and Experiments. *SIAM J. Imaging Sciences*, 8(3):1421–1456, 2015.

[129] Y. Sun and M.A. Abidi. Surface Matching by 3D Point's Fingerprint. *ICCV01*, II:263–269, 2001.

[130] J Talairach and J Bancaud. Stereotaxic approach to epilepsy. 1973.

[131] Paul Thompson and Arthur W Toga. A surface-based technique for warping three-dimensional images of the brain. *Medical Imaging, IEEE Transactions on*, 15(4):402–417, 1996.

[132] Paul M Thompson, Jay N Giedd, Roger P Woods, David MacDonald, et al. Growth patterns in the developing brain detected by using continuum mechanical tensor maps. *Nature*, 404(6774):190, 2000.

[133] Duygu Tosun, Allan L Reiss, Agatha D Lee, Rebecca A Dutton, Kiralee M Hayashi, Ursula Bellugi, Albert M Galaburda, Julie R Korenberg, Debra L Mills, Arthur W Toga, et al. Use of 3-d cortical morphometry for mapping increased cortical gyrification and complexity in williams syndrome. In *Biomedical Imaging: Nano to Macro, 2006. 3rd IEEE International Symposium on*, pages 1172–1175. IEEE, 2006.

[134] Alain Trouvé and Laurent Younes. Metamorphoses through lie group action. *Foundations of Computational Mathematics*, 5(2):173–198, 2005.

[135] Alex Tsui, Devin Fenton, Phong Vuong, Joel Hass, Patrice Koehl, Nina Amenta, David Coeurjolly, Charles DeCarli, and Owen Carmichael. Globally optimal cortical surface matching with exact landmark correspondence. In *Information Processing in Medical Imaging*, pages 487–498. Springer, 2013.

[136] William Thomas Tutte. Convex representations of graphs. *Proceedings of the London Mathematical Society*, 3(1):304–320, 1960.

[137] William Thomas Tutte. How to draw a graph. *Proc. London Math. Soc*, 13(3):743–768, 1963.

[138] Edwin Van Dellen, Linda Douw, Johannes C Baayen, Jan J Heimans, Sophie C Ponten, W Peter Vandertop, Demetrios N Velis, Cornelis J Stam, and Jaap C Reijneveld. Long-term effects of temporal lobe epilepsy on local neural networks: a graph theoretical analysis of corticography recordings. *PLoS One*, 4(11):e8081, 2009.

[139] Tom Vercauteren, Xavier Pennec, Aymeric Perchant, and Nicholas Ayache. Diffeomorphic demons: Efficient non-parametric image registration. *NeuroImage*, 45(1):S61–S72, 2009.

[140] Pan Wang, Bo Zhou, Hongxiang Yao, Yafeng Zhan, Zengqiang Zhang, Yue Cui, Kaibin Xu, Jianhua Ma, Luning Wang, Ningyu An, et al. Aberrant intra-and inter-network connectivity architectures in Alzheimers disease and mild cognitive impairment. *Scientific reports*, 5, 2015.

[141] Yalin Wang, Xianfeng Gu, Tony F Chan, and Paul M Thompson. Shape analysis with conformal invariants for multiply connected domains and its

application to analyzing brain morphology. In *Computer Vision and Pattern Recognition, 2009. CVPR 2009. IEEE Conference on*, pages 202–209. IEEE, 2009.

[142] Yalin Wang, Xianfeng Gu, Tony F Chan, Paul M Thompson, and Shing-Tung Yau. Conformal slit mapping and its applications to brain surface parameterization. In *Medical Image Computing and Computer-Assisted Intervention–MICCAI 2008*, pages 585–593. Springer, 2008.

[143] Yalin Wang, Lok Ming Lui, Xianfeng Gu, Kiralee M Hayashi, Tony F Chan, Arthur W Toga, Paul M Thompson, and Shing-Tung Yau. Brain surface conformal parameterization using riemann surface structure. *Medical Imaging, IEEE Transactions on*, 26(6):853–865, 2007.

[144] Yalin Wang, Jie Shi, Xiaotian Yin, Xianfeng Gu, Tony F Chan, Shing-Tung Yau, Arthur W Toga, and Paul M Thompson. Brain surface conformal parameterization with the ricci flow. *Medical Imaging, IEEE Transactions on*, 31(2):251–264, 2012.

[145] O. Weber, A. Myles, and D. Zorin. Computing extremal quasiconformal maps. *Computer Graphics Forum*, 31(5):1679–1689, 2012.

[146] FG Woermann, SL Free, MJ Koepp, SM Sisodiya, and JS Duncan. Abnormal cerebral structure in juvenile myoclonic epilepsy demonstrated with voxel-based analysis of mri. *Brain*, 122(11):2101–2108, 1999.

[147] Friedrich G. Woermann, Samantha L. Free, Matthias J. Koepp, John Ashburner, and John S. Duncan. Voxel-by-voxel comparison of automatically segmented cerebral gray matterxa rater-independent comparison of structural MRI in patients with epilepsy. *NeuroImage*, 10(4):373 – 384, 1999.

[148] George Wolberg. Image morphing: a survey. *The visual computer*, 14(8):360–372, 1998.

[149] Roger P Woods, Scott T Grafton, Colin J Holmes, Simon R Cherry, and John C Mazziotta. Automated image registration: I. general methods and intrasubject, intramodality validation. *Journal of computer assisted tomography*, 22(1):139–152, 1998.

[150] J.V. Wyngaerd, L.V. Gool, R. Koch, and M. Proesmans. Invariant-based registration of surface patches. *ICCV99*, I:301–306, 1999.

[151] Zhijun Yao, Yuanchao Zhang, Lei Lin, Yuan Zhou, Cunlu Xu, Tianzi Jiang, Alzheimer's Disease Neuroimaging Initiative, et al. Abnormal cortical networks in mild cognitive impairment and alzheimer's disease. *PLoS Comput Biol*, 6(11):e1001006, 2010.

[152] Lijun Yin, Xiaozhou Wei, Yi Sun, Jun Wang, and Matthew J Rosato. A 3D facial expression database for facial behavior research. In *7th international conference on automatic face and gesture recognition (FGR06)*, pages 211–216. IEEE, 2006.

[153] A. Zaharescu, E. Boyer, and R. Horaud. Topology-Adaptive Mesh Deformation for Surface Evolution, Morphing, and Multiview Reconstruction. *IEEE Transactions on Pattern Analysis and Machine Intelligence*, 33(4):823–837, April 2011.

[154] W. Zeng, F. Luo, S.-T. Yau, and X. Gu. Surface Quasi-conformal Mapping by Solving Beltrami Equations. In *IMA International Conference on Mathematics of Surfaces XIII*, pages 391–408, 2009.

[155] W. Zeng and Y. J. Yang. Colon Flattening by Landmark-Driven Optimal Quasiconformal Mapping. In *The 17th International Conference on Medical Image Computing and Computer Assisted Intervention (MICCAI'14)*, Boston, MA, USA, September 14-18 2014.

[156] Wei Zeng and Xianfeng Gu. Registration for 3D Surfaces with Large Deformations Using Quasi-Conformal Curvature Flow. In *CVPR*, Colorado Springs, Colorado, USA, June 20-25 2011.

[157] Wei Zeng, Lok Ming Lui, and Xianfeng Gu. Surface Registration by Optimization in Constrained Diffeomorphism Space. In *CVPR*, Colorado Springs, Colorado, USA, June 20-25 2014.

[158] Wei Zeng, Lok Ming Lui, Feng Luo, Tony Chan, Shing-Tung Yau, and Xianfeng Gu. Computing Quasiconformal Maps Using an Auxiliary Metric with Discrete Curvature Flow. *Numeriche Mathematica*, 121(4):671–703, 2012.

[159] Wei Zeng, Lok Ming Lui, and Xianfeng Gu. Surface registration by optimization in constrained diffeomorphism space. In *Proceedings of the IEEE Conference on Computer Vision and Pattern Recognition*, pages 4169–4176, 2014.

[160] Wei Zeng, Muhammad Razib, and Abdur Bin Shahid. Diffeomorphism Spline. *Axioms*, 4(2):156–176, 2015.

[161] Wei Zeng, Rui Shi, Yalin Wang, Shing-Tung Yau, Xianfeng Gu, Alzheimers Disease Neuroimaging Initiative, et al. Teichmüller shape descriptor and its application to Alzheimers disease study. *International journal of computer vision*, 105(2):155–170, 2013.

[162] Wei Zeng and Yi-Jun Yang. Surface Matching and Registration by Landmark Curve-Driven Canonical Quasiconformal Mapping. pages 710–724, 2014.

[163] Wei Zeng, Yi-Jun Yang, and Muhammad Razib. Graph-Constrained Surface Registration Based on Tutte Embedding. In *The IEEE Conference on Computer Vision and Pattern Recognition (CVPR) Workshops*, June 2016.

[164] Lei Zhu, Yan Yang, Steven Haker, and Allen Tannenbaum. An image morphing technique based on optimal mass preserving mapping. *IEEE Transactions on Image Processing*, 16(6):1481–1495, 2007.

VITA

MUHAMMAD RAZIB

February 20, 1986	Born, Mymensingh, Bangladesh
2004–2009	B.Sc., Computer Science and Engineering Bangladesh University of Engineering and Technology Dhaka, Bangladesh
2013–2016	M.Sc., Computer Science Florida International University Miami, Florida
2013–2017	Doctoral Candidate, Computer Science Florida International University Miami, Florida

PUBLICATIONS

Wei Zeng, Yi-Jun Yang, and Muhammad Razib. Graph-Constrained Surface Registration Based on Tutte Embedding. In *The IEEE Conference on Computer Vision and Pattern Recognition (CVPR) Workshops*, June 2016.

Muhammad Razib, Zhong-Lin Lu, and Wei Zeng. Structural Brain Mapping. In *Medical Image Computing and Computer-Assisted Intervention–MICCAI 2015*, pages 760–767. Springer, 2015.

Wei Zeng, Muhammad Razib, and Abdur Bin Shahid. Diffeomorphism Spline. *Axioms*, 4(2):156–176, 2015.

Muhammad Razib, Yi-Jun Yang, Zhong-Lin Lu, and Wei Zeng. A Novel Brain Registration Framework by Atlas-Constrained Mappings. In *IEEE Conference on Computer Vision and Pattern Recognition (CVPR)*, 2018. (In Submission).

Muhammad Razib, Yi-Jun Yang, Zhong-Lin Lu, and Wei Zeng. Intrinsic Parameterization and Registration of Graph Constrained Surfaces. In *Graphical Models*, 2018. (In Submission).